ISSN 0038-531X

Russian Original Vol. 46, No. 2, February, 1979

August 1979

SATEAZ 46(2) 81-160 (1979)

FILE

SOVIET ATOMIC ENERGY

АТОМНАЯ ЭНЕРГИЯ
(ATOMNAYA ÉNERGIYA)

TRANSLATED FROM RUSSIAN

CONSULTANTS BUREAU, NEW YORK

SOVIET ATOMIC ENERGY

Soviet Atomic Energy is a cover-to-cover translation of *Atomnaya Énergiya*, a publication of the Academy of Sciences of the USSR.

An agreement with the Copyright Agency of the USSR (VAAP) makes available both advance copies of the Russian journal and original glossy photographs and artwork. This serves to decrease the necessary time lag between publication of the original and publication of the translation and helps to improve the quality of the latter. The translation began with the first issue of the Russian journal.

Consultants Bureau journals appear about six months after the publication of the original Russian issue. For bibliographic accuracy, the English issue published by Consultants Bureau carries the same number and date as the original Russian from which it was translated. For example, a Russian issue published in December will appear in a Consultants Bureau English translation about the following June, but the translation issue will carry the December date. When ordering any volume or particular issue of a Consultants Bureau journal, please specify the date and, where applicable, the volume and issue numbers of the original Russian. The material you will receive will be a translation of that Russian volume or issue.

Subscription (2 volumes per year)
Vols. 44 & 45: $130 per volume (6 Issues)
Vols. 46 & 47: $147.50 per volume (6 Issues)

Single Issue: $50
Single Article: $7.50

Prices somewhat higher outside the United States.

CONSULTANTS BUREAU, NEW YORK AND LONDON

227 West 17th Street
New York, New York 10011

Published monthly. Second-class postage paid at Jamaica, New York 11431.

Soviet Atomic Energy is abstracted or indexed in *Applied Mechanics Reviews, Chemical Abstracts, Engineering Index, INSPEC—Physics Abstracts and Electrical and Electronics Abstracts, Current Contents,* and *Nuclear Science Abstracts.*

SOVIET ATOMIC ENERGY

A translation of *Atomnaya Énergiya*

August, 1979

Volume 46, Number 2 February, 1979

CONTENTS

CONTENTS

(continued)

The Russian press date (podpisano k pechati) of this issue was 1/22/1979. Publication therefore did not occur prior to this date, but must be assumed to have taken place reasonably soon thereafter.

ARTICLES

EXPERIMENTAL MEASUREMENT OF THE GRAVITY COEFFICIENT OF COOLANT REACTIVITY FOR REACTORS AT THE BILIBINSK ATOMIC COMBINED ELECTRIC POWER AND HEAT-GENERATING PLANT

A. V. Bondarenko, A. A. Vaimugin,
P. G. Dushin, A. G. Kostromin,
G. V. Plotnikov, G. E. Soldatov,
V. N. Sharapov, and É. A. Yanovskii

UDC 621.039.524.2.034.44:621.039.519

The Bilibinsk atomic combined electric power and heat-generating plant (BATÉTs) consists of four identical units with channelized boiling water—graphite reactors whose heat is removed by naturally circulating coolant through six independent loops locked to a drum-separator [1, 2]. The first unit was placed in operation in January 1974; the fourth was put into service in January 1977.

All the reactors are of practically identical construction. The third and fourth reactors differ slightly from the first two in that four (out of 60) control and safety rod units are located in the active zone. The neutron-physical characteristics of the reactors are therefore the same for the same fuel burnup.

The electrical and thermal output of BATÉTs is regulated in accordance with a dispatching plot. During a 24-h period the output varies by a factor of 7-8. The daily variation of the load graph (ratio of minimum to maximum) reaches 0.59 on winter days and 0.68 on summer days. In relation to this, it is important to know the parameters which determine the controllability of the reactors, in particular the reactivity coefficients.

For rapid transitional processes, such as during sudden changes of output, the reactivity of the BATÉTs reactors varies mainly because of the changes in coolant density and fuel temperature. This is because the time constants of the changes in the other parameters which affect the reactivity (temperature of the graphite walling, xenon concentration) are considerably larger than the time constants of the variation in coolant density and fuel temperature. Of all of the reactivity coefficients, the ones which are therefore of greatest interest from the viewpoint of regulating these reactors are the gravity coefficient of the coolant and the temperature coefficient of the fuel. In calculations, the greatest error is associated with the gravity reactivity coefficient. It is therefore important to measure it experimentally in order to improve the accuracy of the neutron-physical reactor characteristics.

From March 1976 to January 1977 a series of measurements was carried out at the BATÉTs in order to determine the gravity coefficient of the coolant reactivity and to clarify how it varies during the course of an operating period in proportion to the fuel burnup. At that time none of the BATÉTs reactors had yet completely exhausted the reactivity established at the initial loading, which was the same for all the reactors. There were, however, wide differences among the reactors of the different units with respect to uranium burnup, since there was an interval of about a year which elapsed between the time each unit of the station was placed into service and the time the following one was placed into service. The measurements could be carried out in a rather short period thanks to the fact that several identical reactors with different amounts of uranium burnup were in simultaneous operation at the station. A total of seven measurements were made on the reactors of the first to the third units in a range of values of average uranium burnup of 0.2-5.5 MW-day/kg U. It should be noted that at the end of the first operating period (∿700 effective days) the average uranium burnup in the production channels loaded in the reactor equalled 6.1 MW-day/kg U. The measurements thus spanned practically the whole range of values of uranium burnup characteristic of the first operating period of the reactors.

The measurements were made as follows. At a certain time there was a change in the steam content and coolant density in the production channels of the reactors, which were

Translated from Atomnaya Énergiya, Vol. 46, No. 2, pp. 75-78, February, 1979. Original article submitted February 2, 1978.

0038-531X/79/4602-0081$07.50

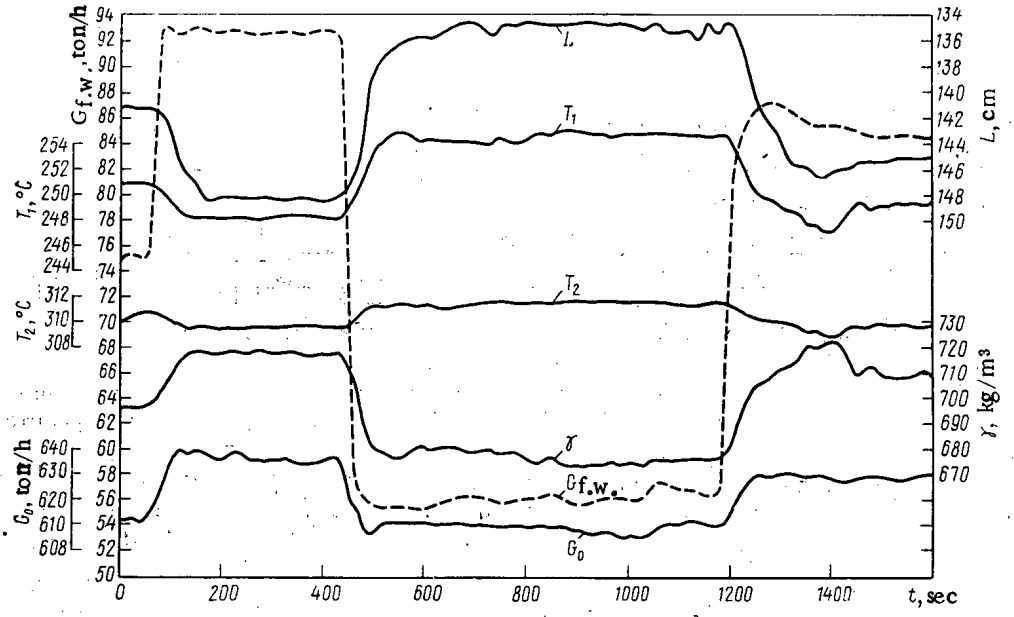

Fig. 1. Variation of the parameters of the second BATÉTs unit within a period of 290 effective days. T_1) water temperature at entrance to production channel; T_2) mean fuel temperature; γ) mean coolant density; L) depth of immersion into active zone of automatic regulator rods.

operating at 80% of nominal output; after the automatic regulator rods were finished off, the resulting change in reactor reactivity was recorded. The coolant density in the production channels was varied by changing the feed water flow rate. Due to the large volume of water in the drum-separator, the BATÉTs heat-flow circuit made it possible (by varying the feed water flow rate) to change the steam content in the production channels at a certain time without changing the thermal output of the reactor. The reactor operated in a regime of automatic power maintenance while the measurements were being taken. The change in reactivity was compensated for by adjustment of the automatic regulator rods. The pressure in the coolant loop was maintained at the constant value of 6.5 MPa. In order to exclude the effect of xenon concentration, measurements were made on reactors which had previously operated for a rather extended period (∿3 days) at constant output.

The variation of the feed water flow rate was carried out in a definite sequence. At first the rate was increased by 15-25% compared with its starting value corresponding to a stationary state of the reactor, and maintained at the higher value for a period of 6 min. The feed water flow rate was then decreased by 30-50% and maintained at the lower value while the reactor operated ∿7 min, after which the flow rate was increased to a level at or near its original value. The feed water flow rate varied from 55 to 95 ton/h for a total coolant flow rate in the circulation loop ∿600 ton/h. The decrease and increase of the feed water flow rate was carried out at a rate of 30-120 ton/h in 1 min.

The change in the coolant density averaged over the reactor was not measured directly in the experiments; it was found by calculating it from measured values of the fundamental reactor parameters. Along with the variation of reactor reactivity, the following reactor parameters were therefore recorded (with a frequency of 0.5 or 1 Hz) in making the measurements: feed water flow rate $G_{f.w.}$ and total flow rate G_0 of the coolant in the circulation loop, fuel temperature (of one of the elements), reactor output, and pressure in the circulation loop. A special apparatus developed for BATÉTs* was used to record the reactor parameters. Fourteen parameters were recorded simultaneously, with the information being written on punched tape in binary code for subsequent computer processing. The signals from the gauges of standard instruments were used to record the data. The apparatus is connected to the gauges in parallel with standard recorders, adding less than 1% error to the readings of the latter. The variation during the experiment of the fundamental reactor parameters is shown in Fig. 1.

*The apparatus was developed and produced by Yu. I. Gribanov, A. P. Gormatyuk, V. G. Gromov, and V. P. Scheslavskii.

TABLE 1. Measurements of the Gravity Reactivity Coefficient of Coolant in the Reactors of the First Three Units of BATÉTs

Reactor No., startup date	Date of meas.	Reactor av. ofuranium burnup, MW-day/kg U	$K_\gamma \cdot 10^5$, $kg^{-1} \cdot m^3$
III, 22.12.75	03.76	0,21	1,50±0,20
	10.76	1,25	1,10±0,15
	01.76	1,76	1,05±0,15
II, 30.12.74	03.76	2,56	0,90±0,15
	10.76	3,74	0,45±0,10
I, 12.01.74	03.76	4,41	0,25±0,10
	10.76	5,49	0,10±0,10

The feed water temperature of BATÉTs is about 170°C less than the temperature of the water in the drum-separator. As a consequence, a change in the feed water flow rate results in a change of the water temperature at the entrance to the production channels (°C), which for stable regimes is proportional to the change in the feed water flow rate:

$$\Delta T_1 = -0.21 \Delta G_{f.w} \text{ [ton/h]}. \quad (1)$$

The variation of the water temperature at the entrance to the production channels is associated with changes in their hydrodynamical resistance and the driving pressure of the natural circulation of coolant, which results in a change in the total coolant flow rate.

The changes in the total coolant flow rate and in the water temperature at the entrance to the production channels results in a change in the density of the coolant in them (see Fig. 1), mainly because of the change in the average steam content and to a certain change in the fuel temperature arising from changes in the length of the economizer section and the temperature of the coolant in it. Since the time constant of the circulating water temperature in a change of the feed water flow rate is much larger than the time constant of the changes in fuel temperature and coolant density, quasistationary equations are used to determine the coolant density. The distribution in the channel height of the heat content was determined as a function of the water temperature at the entrance to the channels, coolant flow rate, and reactor output for a given distribution in height of the active zone. The volumetric steam content in the boiling part of the channel was taken as proportional to the volumetric steam content expended, with a proportionality factor equal to 0.83. The coolant density was averaged over the whole volume of coolant in the channel including the volume of the central drop tube of the channel where the water does not boil but whose density varies with changes in the water temperature at the channel entrance. The distribution of the flux and value of the neutrons with respect to the height of the reactor was taken into account in calculating the mean coolant density in the fuel elements.

The reactivity of the reactor varied in the experiments only because of the changes in coolant density and fuel temperature, since all the other reactor parameters which affect the reactivity (xenon concentration, graphite temperature, etc.) stayed constant. During the experiment, the fluctuations in reactor reactivity $\rho = \Delta k/k$, coolant density γ, and fuel temperature T_2 were not large: $\Delta\rho_{max} \approx 1.5 \cdot 10^{-3}$, $\Delta\gamma_{max} \approx 70$ kg/m³, and $\Delta T_{2max} \approx 2$°C. One can therefore express the relation between these values over the whole interval of their variation by the linear function

$$\Delta\rho = \rho(t) - \rho(0) = K_\gamma[\gamma(t) - \gamma(0)] + K_T[T_2(t) - T_2(0)], \quad (2)$$

where time zero corresponds to the stationary state of the reactor prior to the start of the change in the feed water flow rate, $K_\gamma = \partial\rho/\partial\gamma$ is the gravity coefficient of coolant reactivity, and $K_T = \partial\rho/\partial T_2$ is the temperature coefficient of fuel reactivity.

After a further analysis (the calculation of γ, taking into account the values of G_0 and T_1), the results of each experiment can be expressed in the form of a large number (10^3-10^4) of values of $\rho(t)$ and the corresponding values of $\gamma(t)$ and $T_2(t)$.

The analysis of these data enabled the gravity coefficient of coolant reactivity $\partial\rho/\partial\gamma$ to be determined as an unknown parameter appearing in Eq. (2). The temperature coefficient of fuel reactivity K_T appearing in Eq. (2) was considered as a known quantity in the calculation,

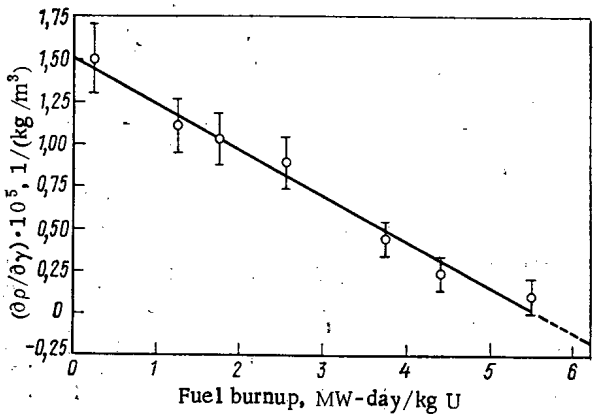

Fig. 2. The fuel burnup dependence of the gravity coefficient of coolant reactivity. ○) experiment; ——) calculated from Eq. (3).

with the value $2\cdot10^{-5}°C^{-1}$ (the design value). It should be noted that in the experiments, particularly in those for which the uranium burnup was fairly small, the effect on the reactivity due to the change in fuel temperature was considerably less than the effect associated with the change in the coolant density, since the fuel temperature varied only 1-2°C in the experiments. Therefore the possible errors which were allowed in the determination of K_T and T_2 did not contribute significant errors to the final result of the measurements. Changes in the reactor reactivity in the experiments were specified by the change in position of the automatic regulator rods and by the reactimeter readings. The motion of the automatic regulator rods was converted to absolute values of reactivity by taking into account the absolute values of their overall efficiency and the experimentally determined regulating characteristics of these rods.

There was little change in the efficiency of the automatic regulator rods during the experiments. According to estimates, the contribution of this change to the value of K_γ is equal to $0.03\cdot10^{-5}$, and it contributes to the error shown in Table 1 in the measurement of the reactivity coefficient.

It is clear from the data shown in Table 1 that the gravity coefficient of coolant reactivity K_γ is positive for an average uranium burnup of 0.2-5.5 MW-day/kg U. The value of K_γ drops considerably as the uranium burnup in the production channels increases. The dependence of K_γ on the uranium burnup is described fairly well by a linear equation (Fig. 2):

$$K_\gamma = 1.51\cdot10^{-5} - 2.70\cdot10^{-6}E, \qquad (3)$$

where E is the mean uranium burnup in the production channels situated in the reactor, MW-day/kg U.

The coefficients in Eq. (3) were found by analyzing the data of Table 1, using the least-squares method. According to this equation, K_γ must become zero at a uranium burnup of 5.6 MW-day/kg U, and at the very end of the first operating period (for E = 6.1 MW-day/kg U) must become negative and equal to $0.14\cdot10^{-5}$ $kg^{-1}\cdot m^{-3}$.

Although no calculated data are presented here for the gravity coefficient of reactivity, theoretical analysis indicates that the positive value of the gravity coefficient of coolant reactivity at the start of the operating period is mainly due to two effects. As the coolant density in the production channels increases, there is a drop in the efficiency of the absorbing rods located in the reactor, and a drop in the neutron leakage from the active zone. At the start of the operating period, the neutron multiplication factor in the channel lattice of the BATÉTs reactors (K_∞) is a slowly varying function of the water density, and therefore its change is not important for the reactivity balance.

The positive effect of the reactivity associated with the presence of absorbing rods in the reactor decreases in proportion to the operation of the reactor and emerges as a negative effect caused by the uranium burnup and the accumulation of plutonium. By the end of the first operating period, the effect from the control and safety rods decreases to practically zero, and the effect from the decrease of neutron leakage is compensated by the change in

the neutron multiplication factor K_∞ so that on the whole the gravity coefficient of coolant reactivity becomes nearly zero.

Although the data obtained refer only to the initial operating period of the reactor, they can be also used to estimate the gravity coefficient of coolant reactivity for reactor operation in a regime of partial reloading of the production channels. The plan for partially reloading the BATÉTs reactors in a steady-state regime calls for reloading ∿80 production channels roughly every 300 effective days. In this instance the mean uranium burnup in the production channels located in the reactor is equal to 3.5 MW-day/kg U immediately after reloading, and is 6.1 MW-day/kg U at the end of the run prior to the next reloading. It can be anticipated that K_γ will vary from $0.56 \cdot 10^{-5}$ to $-0.14 \cdot 10^{-5}$ $kg^{-1} \cdot m^3$ in a steady-state regime of partial reloadings. For these values, the reactor control and safety rods ensure the stability and safe operation of the reactor.

LITERATURE CITED

1. V. M. Abramov et al., At. Energ., 35, No. 5, 299 (1973).
2. A. A. Vaimugin et al., ibid., 39, No. 1, 3 (1975).

TRITIUM CONTENT IN THE COOLANT OF WATER-COOLED—WATER-MODERATED REACTORS

L. I. Golubev, V. M. Ilyasov,
A. I. Lur'e, R. N. Mekhedov,
L. N. Sukhotin, V. M. Arkhipkin,
and L. P. Kham'yanov

UDC 621.039.524.44

The considerable discharge of tritium into the atmosphere, and the difficulty of its removal in view of the wide distribution of its chemical analog, protium, together account for the recent upsurge of serious interest in the problem of tritium formation in atomic power stations.

The formation of tritium in the reactions $^{10}B(n, 2\alpha)^3H$ and $^{10}B(n, \alpha)^7Li(n, n\alpha)^3H$ was considered in [3, 4], where opposite conclusions were reached regarding the contribution of these processes to tritium accumulation. In [6], experimental results were given for the limiting values of the tritium concentration in the water-supply systems of Soviet atomic power stations.

The sources of tritium in atomic power stations are known to be the triple-fission reaction in the fuel, the ^{10}B reaction occurring in the coolant and the regulatory units, and also the reaction involving deuterium and impurity lithium entering the coolant with the chemical reagents KOH and H_3BO_3.

As there is boron regulation in the second to fourth units of the Novovoronezh atomic power station, the contribution of the ^{10}B reaction may be estimated and the effect of the water-transfer conditions in the first loop may be established; investigation of the behavior of tritium in the coolant of the first unit, which has only rod regulation, provides information on the migration of tritium from the fuel and boron steel and also on the contribution of the deuterium reaction.

In the present work, on the basis of information on the cross sections of the boron and lithium reactions [7], more complete than that in [3, 4], and of experimental data on the neutron spectrum in the active region of the water-cooled—water-moderated reactor at the Novovoronezh atomic power station [8] and the boron and lithium concentrations in the coolant [5], analytic dependences of the tritium concentration in the water of the first loop are found, taking account of filtering and purification, and are compared with experimental data.

The tritium concentration C_{3H} in the water of a reactor first loop of volume V_L, with boron regulation, is governed by the equation

Translated from Atomnaya Énergiya, Vol. 46, No. 2, pp. 79-82, February, 1979. Original article submitted January 30, 1978.

0038-531X/79/4602-0085$07.50

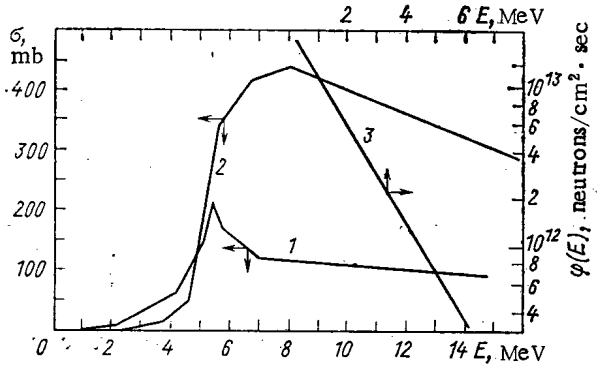

Fig. 1. Cross section of the reactions $^{10}B(n, 2\alpha)^3H$ (1) and $^7Li(n, n\alpha)^3H$ (2) as a function of neutron energy, and the neutron spectrum in the active region (3).

$$V_L \frac{dC_{^3H}}{dt} = P_{in} - [v_{fi}(1-\varepsilon_{fi}) + v_{pu}(1-\varepsilon_{pu}) + v_{gas} + \lambda] C_{^3H}, \quad (1)$$

where P_{in} is the rate of tritium input to the coolant from the boron reaction (P_B) and the lithium reaction (P_{Li}) in the coolant and the control units and from the triple-fission reaction in the fuel; v_{fi}, v_{pu}, and v_{gas} are the coolant flow rates in filtering, purification, and transition to the gas phase as a result of radiolysis; ε_{fi} and ε_{pu} are the efficiencies of "purification" from tritium (equal to the ratio of tritium concentrations in the recycled and initial water); λ is the decay constant.

The contribution of each source of tritium will be considered in turn.

Reaction $^{10}B(n, 2\alpha)^3H$

The rate of tritium formation may be found from the expression

$$P_B = \frac{4{,}18 \cdot 10^{-15} \varkappa \mu V_a C_B N_0}{A_B} \int_0^\infty \varphi(E)\sigma_B(E)\,dE \text{ Ci/day}, \quad (2)$$

where $\varkappa$, μ, N_0, and A_B are, respectively, the ^{10}B content in the element, the boron content in oxygen, Avogadro's number, and the atomic mass of boron; V_α is the volume of the active region of the reactor, liter; $\int_0^\infty \varphi(E)\sigma_B(E)dE$ is the activation integral, sec^{-1}; C_B is the boric-acid concentration, g/liter.

If the data on the cross section of the reaction $^{10}B(n, 2\alpha)^3H$ [7] and the fast-neutron spectrum in the active region of the reactors at the Novovoronezh atomic power station [8] shown in Fig. 1 are used, the total amount of tritium formed in a time t for a linear change in boron concentration with time

$$C_B = C_B^0 + v_B t \quad (3)$$

will be

$$a_{^3H} = 1.95 \cdot 10^{-4} W (C_B^0 t + v_B t^2/2) \text{ Ci}, \quad (4)$$

where W is the thermal power of the reactor, MW; v_B is the rate of change of boron concentration.

For example, in the 1975-1976 operating period, the total amount of tritium formed in the second, third, and fourth units was 130 ± 30, 134 ± 30, and 222 ± 50 Ci, respectively, with a mean electrical power of 361, 323, and 440 MW.

Reactions $^6Li(n, \alpha)^3H$ and $^7Li(n, n\alpha)^3H$

Natural lithium may enter the coolant as an impurity in the chemical reagents H_3BO_3 and KOH. According to spectral-analysis data, e.g., the lithium content in analytical-grade KOH is estimated at $(4 \pm 1) \cdot 10^{-4}$ mass %, while the figure for analytical-grade H_3BO_3 is $1 \cdot 10^{-4}$

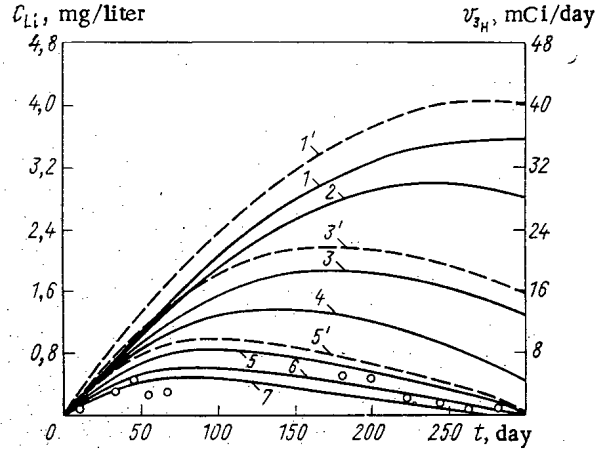

Fig. 2. Curves of the accumulation of ^7Li in the first-loop water (1-7) and the rate of formation of lithium in the reaction $^{10}B(n, \alpha)^7Li(n, n\alpha)^3H$ (1'-5') for purification coefficients from lithium $\beta_2 = 10^{-6}$, 10^{-3}, $5\cdot10^{-3}$, 10^{-2}, $2\cdot10^{-2}$, $3\cdot10^{-2}$, and $4\cdot10^{-2}$, respectively. The unfilled circles show the results of measurements of the lithium concentration according to the data of [5] in the second unit of the Novovoronezh atomic power station.

mass %; this corresponds to a lithium concentration in the second unit of the Novovoronezh power station at the beginning of the operating period of $(3 \pm 1)\cdot10^{-7}$ g/liter as a result of KOH and $4\cdot10^{-6}$ g/liter as a result of H_3BO_3.

A considerable amount of lithium is formed in the coolant as a result of the reaction $^{10}B(n, \alpha)^7Li$ ($\sigma'_{therm} = 3840$ b); e.g., calculation for the second unit of the Novovoronezh atomic power station gives 884 ± 80 g at the end of the operating period. However, sorption on the filters of the purification system [9] and dilution as a result of filtration leads to reduction in the lithium concentration in the first-loop water by a factor of approximately 10, to a level of $(4-5)\cdot10^{-4}$ g/liter. If the efficiencies of coolant purification from lithium as a result of sorption (ε'_{pu}) and filtering (ε'_{fi}) are introduced in the form of ratios of the lithium concentration in the recycled and initial water, the lithium concentration at time t (taking into account the coolant flow rate at filtration v_{fi} and purification v_{pu}) takes the form

$$C_{Li} = \frac{\int_0^\infty \varphi(E)\,\sigma'_B(E)\,dE\,\mu\varkappa N_0 V_a}{A_B V \beta_2}\left[v_B t + \left(C_B^0 - \frac{v_B}{\beta_2}\right)(1 - e^{-\beta_2 t})\right] \text{atom/liter}, \quad (5)$$

where β_2 is the purification coefficient from lithium

$$\beta_2 = [1 - (\varepsilon'_{pu})\,v_{pu} + (1 - \varepsilon''_{fi})\,v_{fi}\,]/V_L. \quad (6)$$

Then the rate of tritium formation is

$$P_{^3H} = \frac{4{,}18\cdot10^{-15}}{A_{Li}} \int_0^\infty \varphi(E)\sigma_{Li}(E)dE V_a N_a C_{Li} \text{ Ci/day}. \quad (7)$$

For example, for the second unit of the Novovoronezh atomic power station the total amount of tritium at the end of an operating period as a result of the reaction $^{10}B(n, \alpha)^7Li\cdot(n, n\alpha)^3H$ is found to be 7.4 and 2.4 Ci for purification coefficients of $\beta = 10^{-6}$ and $4\cdot10^{-2}$ day^{-1}, respectively, which is considerably less than the yield in the reaction $^{10}B(n, 2\alpha)^3H$. In Fig. 2, curves of the lithium concentration in the coolant calculated from Eq. (5) are shown, together with experimental data on the measured lithium concentrations [5] and the rate of formation of tritium in the reaction $^7Li(n, n\alpha)^3H$ for different values of β_2. It is evident from these data that curves 5-7, corresponding to purification coefficients $\beta_2 = (2-4)\cdot10^{-2}$ day^{-1}, are in the best agreement with the experimental results.

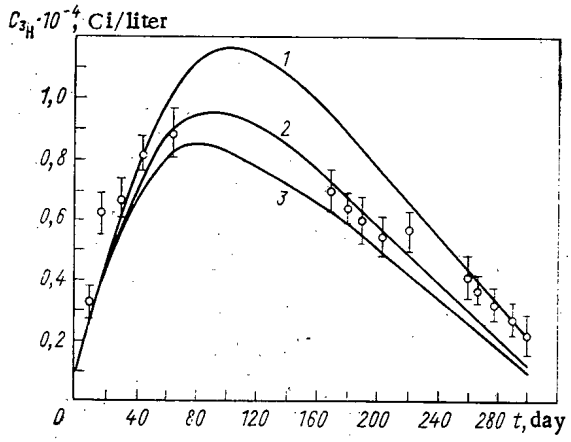

Fig. 3. Curves of the tritium concentration from the reaction $^{10}B(n, 2\alpha)^3H$ for purification coefficients $\beta_1 = 2.2 \cdot 10^{-2}$, $2.7 \cdot 10^{-2}$, and $3 \cdot 10^{-2}$ (1-3) in the first loop of the second unit at the Novovoronezh power station. The unfilled circles correspond to experiment.

The amount of lithium entering the coolant with the chemical reagents (KOH, H_3BO_3) is found to be considerably less than that formed in the ^{10}B reaction; however, the larger cross section (σ_{therm} = 943 b) of the reaction $^6Li(n, \alpha)^3H$ with thermal neutrons leads to a contribution of ^6Li to the rate of tritium formation at the beginning of the operating period comparable with that of ^7Li; the corresponding figures are $4.3 \cdot 10^{-4}$ Ci/day from KOH and less than $6 \cdot 10^{-3}$ Ci/day from H_3BO_3 for the natural concentration of ^6Li in lithium.

If the isotopic ratio of lithium is assumed to be constant in the course of the operating period, the upper limit on the total amount of tritium from the radiogenic and impurity lithium is 5 ± 2 Ci for $\beta_2 = 4 \cdot 10^{-2}$ day^{-1}. However, the amount of impurity in the chemical reagents may vary over a wide range, which must be taken into account in each specific case.

Reaction in the Fuel

According to the data of [4], which are confirmed by the results of the present calculations, the yield of tritium from the fuel as a result of the triple-fission reaction of ^{235}U is $1.2 \cdot 10^{-2}$ Ci/MW(thermal)·day, which corresponds to rates of formation of 9.1, 15.6, and 16.3 Ci/day for the second, third, and fourth units of the Novovoronezh atomic power station (thermal power of 760, 1320, and 1375 MW).

The yield of tritium in the coolant from the fuel elements is only ~0.1% of that accumulating in the fuel elements (according to [3]), which is a result of the high sorption capacity of the zirconium fuel shells for hydrogen. Experimental confirmation of this is found in the low [$(3-5) \cdot 10^{-6}$ Ci/liter] tritium concentration in the coolant of the first unit at the Novovoronezh atomic power station, in which there is no boron regulation. This also indicates that the tritium yield from the rods of the control and safety system is slight. The determining contribution to the tritium accumulation in the coolant is evidently that of the reaction $^{10}B(n, 2\alpha)^3H$ in boric acid.

In this case the solution of Eq. (1) takes the form

$$C_{^3H} = C^0_{^3H} e^{-(\lambda+\beta_1)t} + \frac{1.95 \cdot 10^{-4} W}{(\lambda+\beta_1) V} \left[v_B t + \left(C^0_B - \frac{v_B}{\lambda+\beta_1} \right) (1 - e^{-(\lambda+\beta_1)t}) \right] \text{Ci/liter}, \quad (8)$$

where $C^0_{^3H}$ is the tritium concentration in the coolant at the beginning of the operating period; and

$$\beta_1 = \frac{1}{V_L} [v_{fi} (1 - \varepsilon_{fi}) + v_{pu} (1 - \varepsilon_{pu}) + v_{gas}] \quad (9)$$

is the coefficient of "purification" from tritium. The tritium concentration in the first-loop water was measured by means of liquid scintillators, after purifying the initial samples by distillation.

Results obtained using Eq. (8), taking into account the change in reactor power at startup, and experimental data for the second unit are shown in Fig. 3, from which it is evident that the tritium concentration at first increases, then reaches $\sim 10^{-4}$ Ci/liter, and at the end of the operating period falls to the initial level of $(1.5\text{-}2)\cdot 10^{-5}$ Ci/liter. The value of the purification coefficient from tritium which gives the best fit is $2.7\cdot 10^{-2}$ day^{-1}, which is found to be in good agreement with data on the first-loop water transfer. The experimental results are rather higher than the calculated values at the end of the operating period, as a result of the rise in tritium concentration in the recycled water, which consists of a mixture of coolant distillate and debalanced water.

Thus, on the basis of the experimental and calculated results, the following conclusions may be drawn.

1. The main source of tritium accumulation in the coolant of reactors with boron regulation is the reaction $^{10}B(n, 2\alpha)^{3}H$ in boric acid, giving 90-140 and 170-240 Ci at the end of the operating period for the second and fourth units of the Novovoronezh atomic power station at the nominal power (at the 95% confidence level).

2. The contribution of the reactions involving ^{6}Li, ^{7}Li, triple fission, and ^{10}B (in the rods of the control and safety system) to the total tritium activity of the coolant is $15 \pm 8\%$ at the 95% confidence level. However, this contribution may be higher if the ^{6}Li impurity increases.

3. Investigation of the dynamics of tritium accumulation over time in the coolant shows that the maximum concentration $\sim 10^{-4}$ Ci/liter is reached three months after the beginning of the operating period. The change in tritium concentration in the coolant is satisfactorily described by equations taking account of the water transfer in the first loop. The purification coefficient from tritium as a result of dilution of the coolant of the second unit at the Novovoronezh atomic power station with recycled water is $(2.2\text{-}3.0)\cdot 10^{-2}$ day^{-1} at the 95% confidence level.

LITERATURE CITED

1. L. I. Gedeonov and A. G. Trusov, At. Tekh. Rub., No. 12, 22 (1973).
2. V. S. Yuzgin and B. E. Yavelov, At. Tekhn. Rub., No. 10, 22 (1973).
3. K. Langecker and H. Graupe, Kernenergie, 15, No. 5, 165 (1972).
4. I. Ray, Reactor Fuel Proc. Tech., 12, No. 1, 19 (1968).
5. Yu. P. Abolmasov, I. G. Golubchikova, and T. A. Samoilova, At. Energ., 43, No. 1, 52 (1977).
6. Yu. P. Abolmasov, At. Energ., 41, No. 3, 215 (1976).
7. K. Way and K. Kewer, At. Data Nucl. Data Tables, 12, No. 6, 585 (1973).
8. O. S. Lomakin et al., At. Energ., 31, No. 1, 34 (1971).
9. I. M. Plotnikov et al., in: Ten Years' Experience of Operating the Novovoronezh Atomic Power Station [in Russian], Novovoronezh (1974), p. 132.

NUCLEAR REACTOR CONTROL BY AN ASYMMETRIC REGULATING SYSTEM

I. Ya. Emel'yanov, L. N. Podlazov, N. N. Aleksakov, and V. M. Panin

UDC 621.039.562

One of the central problems of reactors with outputs ~1000 MW(electric) is that of suppressing nonstationary deformations and controlling the energy distribution [1]. The most widely used method for solving the problem of control is based on the principle of local regulation [2].

A theoretical study is made of control systems based on the changes in the spatial and dynamical properties of the energy distribution which are due to the introduction of so-called asymmetric external feedbacks [3-5]. Such a method is used to ensure the stability of the energy distribution, which is intrinsically unstable unless there are external feedbacks [4]. In the process, the necessary quantity of feedback is determined not by the degree of instability of the object, but by the spatial dimensions of the problem (e.g., one asymmetric feedback is sufficient to stabilize an unsteady one-dimensional model reactor). The main object of the present work is to study the practical aspects of the action of an asymmetric regulator and how it differs from the local principle of regulation.

Asymmetric Regulating System

The study is based on a one-dimensional model of spatial neutron kinetics with a single internal power feedback k_{fb} described by a first-order differential equation. The stationary energy distribution is given in the form

$$\Phi_0^*(x) = \text{const}, \quad 0 \leqslant x \leqslant 1.$$

In order to bring out the general laws and to simplify the problem, we consider the case in which the time constant of the feedback is much larger than the time constant of the delayed neutrons. The dynamical equation for the deviations of the variables is of the form

$$\frac{\partial^2 \varphi}{\partial x^2} + k_{fb} + k_r = 0; \tag{1}$$

$$\frac{\partial k_{fb}}{\partial t} = \varkappa_{fb}\varphi - k_{fb}, \tag{2}$$

where k_r takes the regulating effect into account. The time constant of the feedback is taken as the unit of time. The deviation of the neutron flux at a point other than the location of the control rod is taken as the controlling effect for the asymmetric regulator. Assuming that the time constant of the regulating system is negligible compared with the time during which the instability develops, we can write the equation for k_r in the form

$$k_r = -\alpha_1 \delta(x - x_1)\, \varphi|_{x=x_2}, \tag{3}$$

where $\alpha_1 > 0$ is the transfer constant of the regulator, x_1 is the point of application of the regulating effect, and x_2 is the location of the data unit of the system.

If we make use of a Laplace transform, and take into account Eqs. (2) and (3), we can write Eq. (1) in the form

$$\frac{\partial^2 \varphi}{\partial x^2} + \frac{\varkappa_{fb}}{s+1}\varphi - \alpha_1 \delta(x - x_1)\, \varphi|_{x=x_2} = 0. \tag{4}$$

Using the expansion $\varphi(x, s) = \sum_{i=1}^{\infty} \sqrt{2}\, A_i(s) \cos(i\pi x)$, we obtain the following system of equations:

$$\left[(i\pi)^2 - \frac{\varkappa_{fb}}{s+1}\right] A_i + \frac{2\alpha_1}{\gamma_i} \cos(i\pi x_1) \cdot \sum_{j=0}^{\infty} A_j \cos(j\pi x_2) = 0, \tag{5}$$

Translated from Atomnaya Énergiya, Vol. 46, No. 2, pp. 82-87, February, 1979. Original article submitted February 2, 1978.

 0038-531X/79/4602-0090$07.50

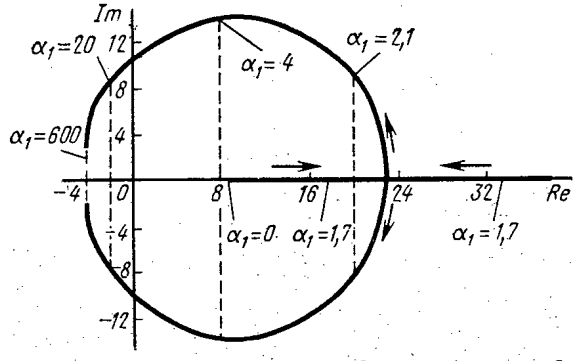

Fig. 1. Trajectories of the roots of the characteristic equation which for $\alpha_1 = 0$ correspond to the fundamental and first harmonic.

where $\gamma_k = \begin{cases} 2, & \text{if } k=0; \\ 1, & \text{if } k\neq 0. \end{cases}$

The analysis of the roots of the characteristic equation of system (5) can be made in practice with a finite number of harmonics. In order to estimate the number of harmonics sufficient to determine the roots with negligible error, we choose a large integer N. The characteristic equation then takes the form

$$A_N(s) = \begin{vmatrix} -2f(s)+a_{11} & a_{12} & a_{13}\ldots a_{1N} \\ a_{21} & \pi^2-f(s)+a_{22} & a_{23}\ldots a_{2N} \\ \ldots & \ldots & \ldots \\ a_{N1} & a_{N2} & a_{N3}\ldots((N-1)\pi)^2-f(s)+a_{NN} \end{vmatrix} = 0, \qquad (6)$$

where

$$a_{ij} = 2\alpha_1 \cos((i-1)\pi x_1)\cos((j-1)\pi x_2),$$

$$f(s) = \frac{\varkappa_{fb}}{s+1}.$$

We assume that $\cos((N-1)\pi x_1) \neq 0$; if this is not the case we make an expansion of the determinant in the N-th row. Multiplying each row of the determinant other than the N-th by $\cos((N-1)\pi x_1)$, multiplying the N-th row by $\cos((i-1)\pi x_1)$ and subtracting it from the i-th row (i = 1, 2, ..., N − 1), we can write the characteristic equation (6) as

$$\begin{vmatrix} -2f(s) & 0\ldots-[((N-1)\pi)^2-f(s)] \\ 0 & \pi^2-f(s)\ldots-[((N-1)\pi)^2-f(s)]\cos(\pi x_1) \\ \ldots & \ldots \\ 2\alpha_1 & 2\alpha_1\cos(\pi x_2)\ldots((N-1)\pi^2)-f(s)+2\alpha_1\cos((N-1)\pi x_1)\cos((N-1)\pi x_2) \end{vmatrix} = 0.$$

Let us consider the element of the determinant at the intersection of the N-th row and the N-th column. If $((N-1)\pi)^2/(2\alpha_1) \gg 1$, the third term in this element can be neglected. By multiplying the N-th row by $\cos((i-1)\pi x_1)$, adding it to the i-th row (i = 1, 2, ..., N − 1), and then expanding the resulting determinant in the N-th column, we get

$$\{[(N-1)\pi]^2-f(s)\}A_{N-1}(s) = 0.$$

In the limit as $N \to \infty$ the characteristic equation of system (5) takes the form

$$\ldots[((N+1)\pi)^2-f(s)][(N\pi)^2-f(s)][((N-1)\pi)^2-f(s)]\ldots[(n^*\pi)^2-f(s)]A_{n^*}(s) = 0, \qquad (7)$$

where n* is defined by the condition that

$$\frac{(n^*\pi)^2}{2\alpha_1} \gg 1.$$

By analyzing the roots of Eq. (7) for various values of x_1, x_2, and $\varkappa_{fb}$ one can easily show that maximum stabilizing effect for Φ_0 = const is achieved by conveying the measuring and regulating elements to the opposite ends of the reactor.

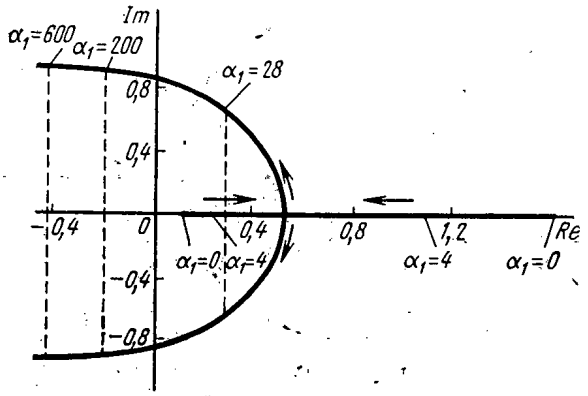

Fig. 2. Trajectories of the roots of the characteristic equation which for $\alpha_1 = 0$ correspond to the second and third harmonics.

The values

$$x_1 = 0;\ x_2 = 1;\ \varkappa_{fb} = 100 \tag{8}$$

are chosen for the parameters.

Without a regulating system, a reactor described by Eqs. (1) and (2) and having a given $\varkappa_{fb}$ is unstable at four harmonics. The following tendencies are seen in the behavior of the roots of the characteristic equation (7): the roots which at $\alpha_1 = 0$ correspond to 2i and 2i + 1 harmonics (i = 1, 2, ...) approach each other in proportion to the increase in α, become multiple, and then decay into two complex-conjugate roots. The trajectories of the roots which at $\alpha_1 = 0$ correspond to the fundamental and the first, second, and third harmonics are shown, respectively, in Figs. 1 and 2.

Starting with $\alpha_1 \approx 90$, the present model of a reactor with an asymmetric regulator becomes stable (all roots in the left half plane). Further increase in the amplification factor causes an increase in stability. In order to solve practical problems of control, it is necessary to study the quality of regulation. One of the main criteria of the quality is the speed of response of the regulating system, which in this case is characterized by the decay time of the transient disturbances in the energy distribution. An estimate of the speed of response was made on the basis of straightforward calculations of the transient processes, using a nodal model (51 nodes) of system of equations (1)-(3). In the model which was calculated, the value of k_{fd} was instantaneously increased at t = 0 by the amount Wk_{fd} at the point x_0. At the instant immediately after the indicated change, the profile of the neutron flux corresponding to this change is found from the equation

$$\frac{\partial^2 \varphi_0}{\partial x^2} + \Delta k_{fb}\,\delta(x - x_0) - \alpha_1 \delta(x)\,\varphi_0|_{x=1} = 0, \tag{9}$$

where

$$\varphi_0 = \varphi|_{t=0}.$$

By integrating Eq. (9) and taking into account the equations $\frac{\partial \varphi}{\partial x}\Big|_{x=0} = \frac{\partial \varphi}{\partial x}\Big|_{x=1} = 0$, it is easy to obtain the equation $\varphi_0 = (1 - \varepsilon)(x - x_0)\Delta k_{fb} + \Delta k_{fb}/\alpha_1$,

where $\varepsilon = \begin{cases} 1, & \text{if} \quad x_0 < x \leqslant 1 \\ 0, & \text{if} \quad 0 \leqslant x < x_0, \end{cases}$

i.e., the local perturbation at the initial instant results in a significant distortion of the neutron flux caused by the effect of the asymmetric regulator.

The transient process for the case $x_0 = 1$ and $\alpha_1 = 600$ is shown in Fig. 3.

The flow time t_f of the transient process can be taken as a measure of the speed of response. The former is a solution of the equation

$$\frac{\max\limits_{0 \leqslant x \leqslant 1} \varphi(t_f, x)}{\max\limits_{0 \leqslant x \leqslant 1} \varphi(0, x)} = \Delta, \tag{10}$$

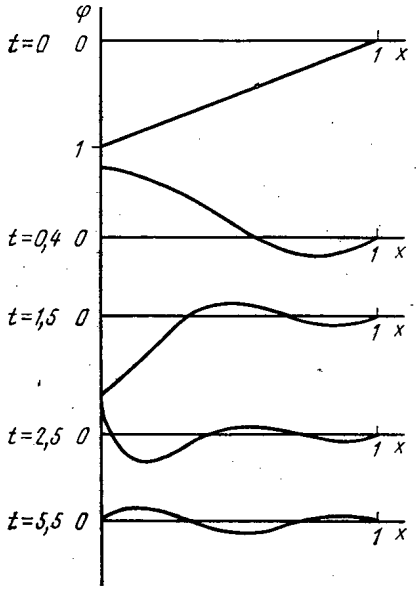

Fig. 3. The transient process of stabilization of a neutron flux profile by an asymmetric regulator.

where $\Delta = 0.01$–0.05.

For $\Delta = 0.05$, $t_f \approx 8.5$, and for $\alpha_1 \to \infty$, t_f is minimal. In order to obtain the limiting value, a calculation was made using various values of the transfer constant (up to $\alpha_1 = 10^6$). The result found was that t_f asymptotically approaches $t_f \approx 7$ as α_1 is increased.

The deformation of the neutron flux profile with an asymmetric regulator in operation thus continues for a time equal to seven time constants of the feedback. At the same time it should be kept in mind that xenon poisoning is very important in the nonstationary deformation of the energy distribution in real reactors. Xenon poisoning is characterized by more complicated dynamics and by longer time constants (up to 10 h).

Another characteristic peculiarity of the operation of an asymmetric regulating system is that such an important characteristic as the integral output is not controlled and varies during the whole transient process.

A Composite System of Regulation

A different regulator is needed to maintain the average output of the reactor during the operation of an asymmetric regulator. For this purpose we consider a system which includes a regulator of the integral output and an asymmetric regulator. In this case, the expression for k_r in Eq. (1) takes the form

$$k_r = -\alpha_1 \delta(x - x_1)\,\varphi|_{x=x_2} - \alpha_2 \delta(x - x_3) \int_0^1 \varphi\, dx,$$

where α_2 is the transfer constant of the integral output regulator; x_3 is the point of application of the regulating effect.

In order to satisfy the conditions for statistical stability of a combined regulating system, it is necessary to introduce positive feedback into the asymmetric regulator circuit, which by itself is undesirable because of the possibility of a breakdown or a cut-off of the integral output regulator. To keep the total output constant, we let the amplification factor $\alpha_2 = 1000$, leave the other parameters the same as in Eq. (8), and $\alpha_1 = -600$.

An analysis of the roots of the characteristic equation shows that the system being studied is stable when $0.1 \leq x_3 \leq 0.55$. We let $x_3 = 0.5$ and study the behavior of the roots of the characteristic equation as the amplification factor of the asymmetric regulator changes. For $\alpha_1 = 0$, the first, second, and third harmonics in the system being studied are unstable, and the instability in the fundamental is stabilized by the integral output regulator. The trajectories of the roots of the first and second harmonics are shown in Fig. 5.

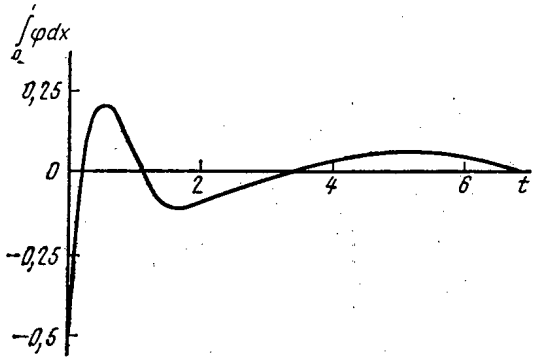

Fig. 4. Time variation of total reactor output.

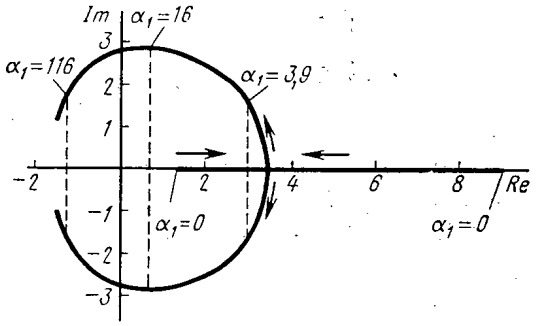

Fig. 5. Root hodograph for varying α_1.

The combined regulating system is stable for $\alpha_1 \leq -23.8$. The study of the roots of the characteristic equation was made for values of α_1 up to -1000. In this range of variation of α_1, an increase in the absolute value of the amplification factor of the asymmetric regulator increases the stability of the system.

The transient process for a perturbation at the point x = 1 ($\alpha_1 = -600$) is shown in Fig. 6. For $\Delta = 0.05$, its flow time $t_f \approx 3$. A comparison of the two systems shows that the regulation of the original system is qualitatively improved by the insertion of an integral output regulator and an appropriate choice of parameters, although the regulation time remains rather large.

The deformations of the energy distribution induced by the perturbation and specified by the algorithm of the asymmetric regulator action are also observed when the asymmetric regulator and the total output regulator operate together. In order to make a qualitative comparison of the characteristics, the present model was used to make a study of a local regulating system which is widely used in practice. The deviation of the neutron flux in the region surrounding the regulating element (a rod) was taken as the controlling effect for the local regulator. For a reactor that is unstable without a regulating system, stabilization to n harmonics requires at least n local regulators which are distributed uniformly in the reactor [6].

For the case considered here — instability to four harmonics — the expression for k_r in Eq. (1) is given in the form

$$k_r = -\sum_{i=1}^{n} \gamma_i \delta\,[x-(2i-1)/8]\cdot\varphi\,|_{x=(2i-1)/8}.$$

Choosing $\gamma_1 = 600$ and introducing a perturbation of the feedback at the point x = 1, we obtain a transient process whose decay, unlike the ones considered earlier, has a monotonic character, with the deviation of the neutron flux from a stationary profile being localized in a small region in the reactor.

A comparison of the regulating quality of local and combined systems for identical perturbations shows that if one assumes the condition that there be identical levels of neutron flux (the numerator in Eq. (10)) at the end of the transient process for both systems, the

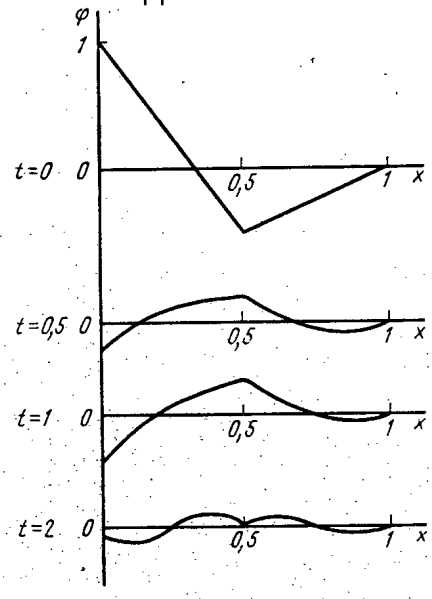

Fig. 6

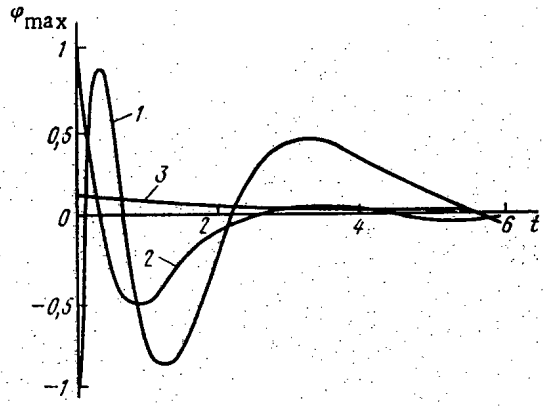

Fig. 7

Fig. 6. Stabilization of the neutron flux profile by a combined regulating system.

Fig. 7. Variation of neutron flux at a point with maximum amplitude.

time of the transient process is about 1.5 times as large for the latter system as it is for the former. For a local system, the maximal deviation of the neutron flux at the instant of introducing the perturbation is about an order of magnitude less than for a combined system.

Curves 1 and 2 in Fig. 7 correspond to asymmetric and combined regulating systems. The maximum amplitude of vibration in the present case corresponds to the point x = 0. For a local regulating system (curve 3) the maximum neutron flux is found at the point x = 1 at which the perturbation is introduced.

CONCLUSIONS

An asymmetric regulating system with scattered data units and regulating rods stabilizes an energy distribution which with no external feedback would be essentially unstable. However, with a system of reactor control constructed solely on the basis of an asymmetric regulator, the quality of the transient processes is unsatisfactory with regard to the regulating time, the character of the process, and the maintenance of the mean reactor output.

The quality of the transient processes is improved by the use of a combined regulating system which includes a mean output regulator and an asymmetric regulator with an appropriate choice of parameters. But the efficiency of such a system is noticeably inferior to that of a control system constructed on the principle of local regulation. For example, if the same perturbation applied to a combined system is applied to a system of local regulators, it is found that the perturbation is localized, the transient time of the process is one and a half times shorter, and the amplitude of the maximum deviation of the neutron flux is reduced by approximately an order of magnitude compared to that for the combined system. Another defect of the system is that when a breakdown of the mean output regulator occurs, the asymmetric regulator remaining in operation causes positive feedback, and under these conditions may induce an uncontrolled power excursion.

A subsequent search for optimal regulating systems evidently may be based on local regulators made partly asymmetric by choosing an appropriate distribution of data and regulating units.

LITERATURE CITED

1. D. Bauer and C. Poncelot, Nucl. Technol., 21, 165 (March, 1974).
2. I. Ya. Emel'yanov, P. A. Gavrilov, and B. N. Seliverstov, Control and Safety of Nuclear Power Reactors [in Russian], Atomizdat, Moscow (1975).

3. D. Wiberg, Nucl. Sci. Eng., 27, No. 3, 600 (1967).
4. P. S. Postnikov and E. F. Sabaev, At. Energ., 26, No. 1, 56 (1969).
5. A. M. Afanas'ev and B. Z. Torlin, ibid., 43, No. 4, 243 (1977).
6. A. Hitchcock, Nuclear Reactor Stability [Russian translation], Gosatomizdat, Moscow (1963).

THEORETICAL—EXPERIMENTAL MODEL OF THE NONSTEADY RADIATIONAL CREEP OF CERAMIC FUEL*

V. B. Malygin, Yu. V. Miloserdin, K. V. Naboichevko, N. S. Golovnin, and Yu. K. Bibilashvili

UDC 621.039.531

One of the most important characteristics required for the design of power-reactor fuel elements is the creep of the fuel. A great quantity of experimental data has now been accumulated on steady creep under steady conditions of irradiation. On the basis of the available information [1-3], it is thought that nonsteady creep plays the determining role in burnup of up to $(3-5)\cdot10^{19}$ fission/cm^3 and in some cases up to 10^{20} fission/cm^3. There is particular interest in the analysis of creep accompanying change in the fission density in the fuel and at reactor startup and shutdown, since these conditions considerably reduce the operational span of the fuel elements.

The model of the nonsteady radiational creep of ceramic fuel considered in the present work is a further development of the model of the annealing of material in the volume of a thermal peak which was proposed in [4] for the calculation of steady radiational creep.

Model of Nonsteady Radiational Creep

The thermal peak of fission, producing an elevated temperature over a certain volume, leads to annealing of part of the sample, which is then susceptible to deformation by nonsteady creep, as observed in the absence of irradiation. The development of creep in each annealed volume of the material begins at the moment at which the fission event occurs, i.e., is determined by the age of the peak.

Consider a sample of unit volume with fission density Φ. The accumulation of annealed regions in the sample is described by the equation

$$dV/dt = -V\Phi v_p + \Phi v_p V_{sam}, \quad (1)$$

where V is the proportion of the sample volume annealed by a thermal peak; v_p is the volume of the thermal peak; Φ is the fission density, which, in the general case, is a function of time; V_{sam} is the sample volume ($V_{sam} = 1$). The first term of this equation accounts for overlapping of the peaks and the second for the annealing of new regions. The solution of Eq. (1) when Φ = const may be written in the form

$$V(t) = 1 - \exp(-v_p \Phi t). \quad (2)$$

Since, after annealing, deformation develops as a result of nonsteady creep of the material in the absence of irradiation, the sections of the sample containing peaks of different ages correspond to different parts of the deformation curve. If the mechanism of creep in the absence of irradiation does not change with increase in deformation, the time dependence of the creep rate at constant temperature takes the form

$$\dot{\varepsilon}(t) = A(t)\sigma^n, \quad (3)$$

where A(t) is some function of the time; σ is the stress; n is a parameter characterizing the dependence of the creep rate on σ.

*This is an adaptation of the paper read to the Conference on Reactor Materials Science, Alushta, 1978.

Translated from Atomnaya Énergiya, Vol. 46, No. 2, pp. 87-91, February, 1979.

 0038-531X/79/4602-0096$07.50

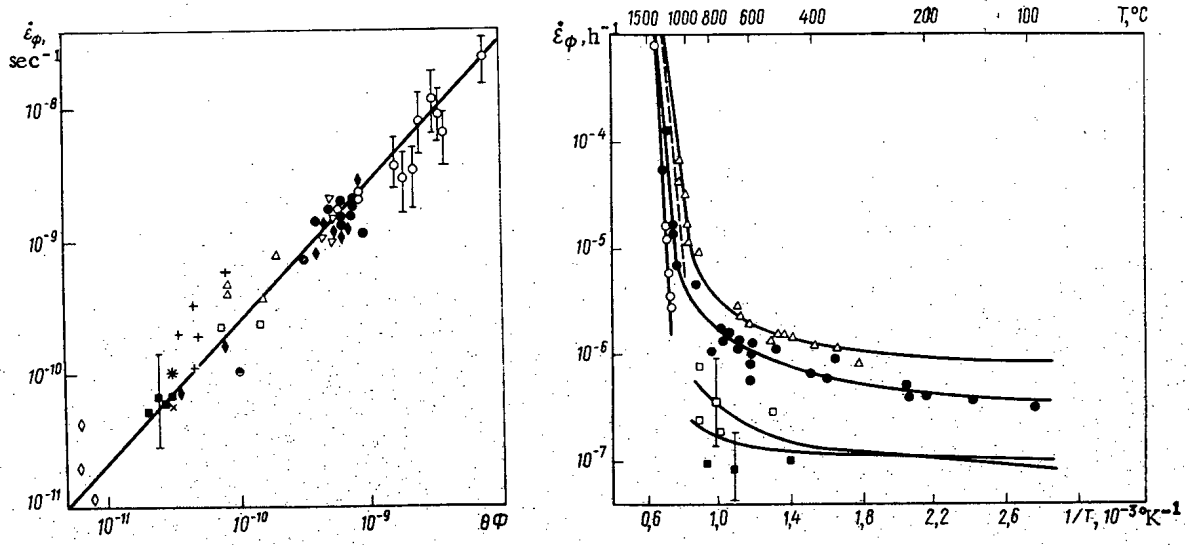

Fig. 1. Dependence of radiational-creep rate on $\theta\Phi$: ○) UO_2 [10]; ●) [11]; ■) [1]; □) [12]; Δ) [13]; ∇) [3]; ◆) $(UPu)O_2$ [14]; ◊) [15]; ▮) UC [17]; ◇) [2]; ⊖) UN [16]; ×) [17]; *) [17]; +) [18].

Fig. 2. Temperature dependence of the rate of steady radiational creep at $\Phi = 10^{13}$ fission/cm^3·sec and σ = 2 kgf/mm^2: ●) UO_2 in the channel [1, 3, 10-13, 18]; ○) UO_2 outside the channel [21]; Δ) $(UPu)O_2$ [3, 14, 15]; ---) $(UPu)O_2$ outside the channel [23]; □) UN [18]; ■) UC [12, 17].

Material in the volume of peaks of different ages is deformed at the same rate, but has a different creep resistance. Considering parallel coupling of the volumes containing peaks of different ages, the time dependence of the radiational-creep rate may be obtained, taking Eq. (3) into account, as follows

$$\dot{\varepsilon}_\Phi(t) = \left[\frac{\exp(-v_p\Phi t)}{\sqrt[n]{\dot{\varepsilon}(t}} + v_p\Phi\int_0^t \frac{\exp(-v_p\Phi t)}{\sqrt[n]{\dot{\varepsilon}(t)}}\right]^{-n}. \quad (4)$$

Equation (4) describes nonsteady radiational creep in the case when the loading sample occurs at the moment of reactor startup or later. In the case when the sample is stressed before reactor startup, the nonsteady radiational creep may again be described by Eq. (4) if $\dot{\varepsilon}(t)$ in the first term is replaced by $\dot{\varepsilon}(\tau)$, where τ is the time elapsed since the application of the load to the sample.

As is known, the time dependence of creep deformation is well described by the Li relation [5]. Substituting this relation into Eq. (4), and setting n = 1, the following result is obtained

$$\dot{\varepsilon}_\Phi(t) = \frac{\dot{\varepsilon}_y k(r+v_p\Phi)}{rk+v_p\Phi-r(k-1)\exp[-(r+v_p\Phi)t]}, \quad (5)$$

where $\dot{\varepsilon}_y$ is the steady rate of creep in the absence of irradiation; r is a coefficient characterizing the duration of the nonsteady-creep stage; k is the ratio of the initial creep rate to the steady rate.

For sufficiently large times, Eq. (5) transforms to the equation for steady radiational creep

$$\dot{\varepsilon}_\Phi = \frac{\dot{\varepsilon}_y k(r+v_p\Phi)}{rk+v_p\Phi}. \quad (6)$$

Equation (5) is valid for the whole temperature range, but for T < 900-1000°C the following relation is more convenient

$$\dot{\varepsilon}_\Phi(t) = \frac{\alpha v v\ \Phi}{v_p\Phi+v-v\exp(-v_p\Phi t)}, \quad (7)$$

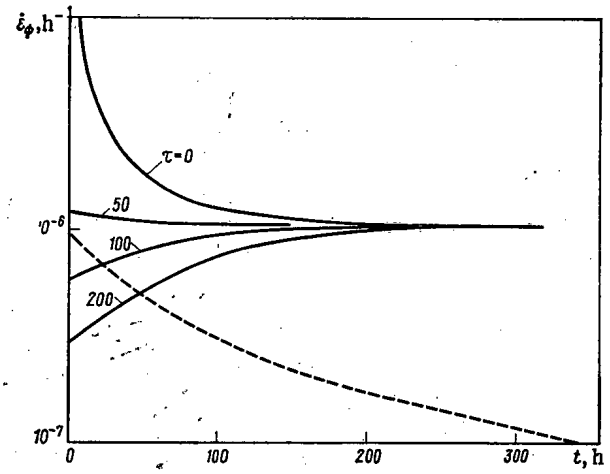

Fig. 3. Time dependence of rate of nonsteady radiational creep for UO_2: ——) instantaneous increase in fission density from zero to 10^{13} fission/cm^3•sec; – – –) instantaneous decrease in fission density from 10^{13} fission/cm^3·sec to zero.

where $\alpha = \dot{\varepsilon}_y/r$ and $\nu = kr$ are coefficients in the logarithmic equation of creep

$$\varepsilon(t) = \alpha \ln(1+\nu t). \tag{8}$$

Equation (7) is a particular case of Eq. (5) for low temperature, when $k \gg 0$ and $rt \ll 1$. For steady radiational creep at low temperatures when $v_p\Phi \ll \nu$, the following result is obtained

$$\dot{\varepsilon}_\Phi = \frac{\alpha\nu v_p\Phi}{v_p\Phi+\nu} \approx \alpha v_p\Phi. \tag{9}$$

As $\Phi \to \infty$, the radiational-creep rate does not exceed $k\dot{\varepsilon}_y$ at high temperatures and $\alpha\nu$ at low temperatures. At temperatures below 900-1000°C, the steady creep rate reaches saturation at a fission density $>10^{16}$-10^{17} fission/cm^3•sec, depending on the type of fuel [4].

The time dependence of the creep rate may be obtained from Eq. (5): for preliminary stress of the sample

$$\dot{\varepsilon}_\Phi(t) = \frac{\alpha\nu v_p\Phi}{v_p\Phi+\nu+\nu\exp(-v_p\Phi t)(v_p\Phi\tau-1)}, \tag{10}$$

where τ is the time elapsed at the onset of irradiation; and for drop in reactor power

$$\dot{\varepsilon}_\Phi(t) = \frac{\alpha v_p\Phi\nu}{v_p\Phi+\nu[1-\exp(-v_p\Phi\tau)]+t\nu v_p\Phi}, \tag{11}$$

where t is the time after the drop in power; τ is the total time of irradiation of the sample.

To evaluate the effect of irradiation on the creep rate of a material, the parameter θ was proposed in [4]:

$$\theta = \int_0^{t_{max}} v_p(t)\,dt = v_{p.E}t_E. \tag{12}$$

where $v_n(t)$ is the time dependence of the peak volume at a temperature $T \geq (0.5\text{-}0.7)T_{pl}$; t_{max} is the maximum time of existence of this peak; $v_{p.E.}$ is the effective peak volume; t_E is the effective time of existence of the peak.

The temperature dependence of θ given in [4] has now been corrected on the basis of data on the thermophysical properties [6-9]. From Eqs. (12) and (9) there follows a linear relation between the quantity $\theta\Phi$ and the radiational-creep rate (Fig. 1). Data on the radiational-creep rate of UO_2, $(UPu)O_2$, UC, and UN were given in [11] for a stress of 1 kgf/mm^2 and a density of 96% of the theoretical value. Thus, using Eqs. (9) and (12), Fig. 1, and the experimental value of α, the effective peak volume may be found for each fuel: $v_{p.E.} = (1.4\cdot10^5)\theta$.

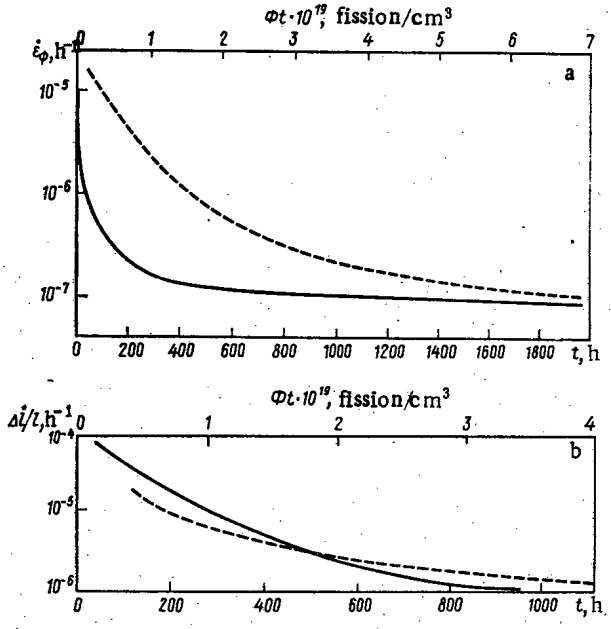

Fig. 4. The dependence of nonsteady radiational creep with σ = 2 kgf/mm^2 and $\Phi = 10^{13}$ fission/cm^3 sec for UC (a) and taking account of increase in fuel density for UO_2 (b): ——) calculation; ---) experiment [12].

Investigation of Nonsteady Creep outside the Reactor Radiation Field

If the relation given above is to be used for the calculation of the radiational creep, information is required on nonsteady creep in the absence of irradiation. To this end, the creep of UO_2 at a temperature of 293-1650°K and a stress of 1-5 kgf/mm^2 was determined. To predict the dependence of the radiational creep on the fuel density in the range 91-97% of the theoretical density and on the grain size (from 1-3 to 15-20 μm), the effect of these factors on the creep of UO_2 was studied on a special apparatus [19]. The experimental data were analyzed by the least-squares method by Eq. (8) for low temperatures and by the relation given in [5] for high temperatures (T > 1300°K).

The time dependence of UO_2 creep deformation at 1073°C obtained in [20] for spiral coils and recalculated for compressional deformation is satisfactorily approximated by Eq. (8). Investigation shows that, within the limits of measurement error, the coefficient α is independent both of the test temperature in the range 293-1073°K and of the grain size, and increases linearly with increase in stress up to 4 kgf/mm^2. The creep curve for a sample annealed at 1673°K for 10 min is the same as the initial curve for the "fresh" sample, and the value of α is approximately the same in these experiments. Investigation shows a practically linear increase in the coefficient ν, and hence in the rate of change of creep rate, with increase in stress. The dependence of the creep rate on the density of the samples has been associated with the change in α in Eq. (8), and approximated [11] by the relation

$$\alpha = \alpha_0 (1 + 0.125 p^2), \qquad (13)$$

where α_0 is the coefficient at zero porosity; p is the relative porosity, %.

In investigating creep at high temperatures, the dependence of the Li-equation coefficients [5] on the stress and temperature was found. In deriving Eq. (3), it was assumed that the creep mechanism does not change with change in the deformation, since it has been shown that the activation energy is independent of the deformation and the power index in the stress is constant. More reliable prediction of the radiational-creep rate would require investigation of the effect of burnup on the coefficients of the equations describing creep in the absence of irradiation.

Radiational Creep of Ceramic Fuel

Analysis of the equations of radiational creep and measurement of the creep in the absence of irradiation provides the basis for a number of conclusions on the effect of various factors on the radiational-creep rate.

The dependence of the radiational creep on the stress is analogous to the values obtained for the rate of steady creep in the absence of irradiation at high temperatures and for the parameter α in Eq. (8) at low temperatures. At a stress of less than 4 kgf/mm^2, the radiational creep of UO_2 and $(UPu)O_2$ is directly proportional to the stress, which is in agreement with experiment. The rate of radiational creep at low temperatures is independent of the grain size and at high temperatures varies analogously to the rate of steady creep.

Knowing the effect of stoichiometry on the rate of steady creep in the absence of irradiation, the rate of radiational creep at high temperature may be predicted. At low temperature, the rate of UO_2 radiational creep increases with deviations from stoichiometry, according to preliminary data. At low temperature, the radiational-creep rate depends only weakly on the temperature; with increase in temperature, the effect of irradiation on the creep of ceramic fuel decreases (Fig. 2).

Nonsteady radiational creep is calculated from Eqs. (5), (7), and (11) using the parameters obtained for Eq. (8). The time dependence of the radiational-creep rate is shown in Fig. 3 for the case when the calculated fission density is reached at the same time as the sample is loaded or earlier ($\tau = 0$) and for the case of preliminary loading of the sample ($\tau = 50$, 100, and 200); the parameters α and ν are assumed to be constant. Preliminary loading of the sample before constant fission density is reached may be identified with the preliminary deformational hardening of the material in the course of tablet preparation. This may be the explanation for the "nonstandard" time dependence of the creep rate observed in [1, 13]. The time dependence of the radiational-creep rate for UC is shown in Fig. 4a. The results of the calculations have been compared with the experimental data of [12]. The parameters α and ν used may be constant at high burnup, when the change in structure and density of the fuel has stabilized. Therefore, the curves in Figs. 3 and 4a are characteristic of transient processes at high burnup. It follows from Eqs. (5), (7), and (11) that it is more correct to take account of the variation in radiational-creep rate with fuel burnup.

Increase in density of the sample may affect radiational creep. On the one hand, increase in density decreases α, which leads to decrease in the calculated radiational-creep rate and increase in the time of the nonsteady process. On the other hand, increase in density results in decrease in size of the sample, and under compressional load this process sums with the radiational creep (Fig. 4b). The increase in density was calculated from the relationship obtained by analysis of the published data [11, 23, 25, 27]. The change in sample size due to nonsteady creep calculated from Eq. (7), taking account of the change in α with porosity, was summed with that arising as a result of increase in density. The results of the calculation are in satisfactory agreement with the experimental curve obtained for UO_2 [12]. This means that increase in density of the material under irradiation plays an important role in the deformation of fuel.

LITERATURE CITED

1. A. Soloman, J. Am. Ceram. Soc., 56, No. 3, 164 (1973).
2. D. Hough, J. Nucl. Mat., 52, 279 (1975).
3. D. Brucklacher, in: Proceedings of International CEBC Conference, Metals Society, London (1974), p. 118.
4. V. B. Malygin et al., At. Energ., 42, No. 1, 8 (1977).
5. J. Li, Acta Met., 11, 1269 (1963).
6. V. S. Chirkin, Thermophysical Properties of Atomic-Engineering Materials [in Russian], Atomizdat, Moscow (1968).
7. J. Leithaker and J. Godfrey, J. Nucl. Mat., 21, 175 (1967).
8. C. Affortit, J. Nucl. Mat., 34, 105 (1970).
9. H. Mikailoff, J. Cloude, and R. Lallement, in: Ceramic Nuclear Fuels, American Ceramic Society, New York (1968), p. 113.
10. D. Brucklacher and W. Dienst, J. Nucl. Mat., 36, 244 (1970).
11. D. Brucklacher and W. Dienst, J. Nucl. Mat., 42, 285 (1972).
12. D. Hough, J. Nucl. Mat., 65, 24 (1977).

13. E. Sykes and P. Sawbridge, Irradiation Creep of Uranium Dioxide, Report RD/B/M-1489 (1969).
14. W. Dienst, J. Nucl. Mat., 61, 185 (1976).
15. D. Brucklacher and W. Dienst, in: Proceedings of IAEA Symposium on Experimental Results on the Mechanical Interaction between Oxide Fuel and Cladding in Fuel and Fuel Elements for Fast Reactors, Vienna (1974), p. 147.
16. D. Brucklacher and W. Dienst, in: Proceedings of a Conference on the Physical Metallurgy of Reactor Fuel Elements, Berkeley (1973).
17. J. Routbort et al., J. Nucl. Mat., 58, 78 (1975).
18. P. Zeisser, G. Maraniello, and C. Merlini, J. Nucl. Mat., 65, 48 (1977).
19. L. I. Laveikin et al., in: Radiation-Experiment Techniques [in Russian], No. 5, Atomizdat, Moscow (1977), p. 24.
20. B. Burton and G. Reynolds, Acta Met., 21, 1073 (1973).
21. J. Perrin, J. Nucl. Mat., 39, 175 (1971).
22. J. Perrin, J. Nucl. Mat., 42, 101 (1972).
23. J. Routbort, N. Javed, J. Voglewede, J. Nucl. Mat., 44, 247 (1972).
24. N. Freshley et al., J. Nucl. Mat., 62, 138 (1976).
25. M. Marlowe, Trans. Am. Nucl. Soc., 18, 206 (1974).

EFFECT OF IRRADIATION CONDITIONS AND CHEMICAL COMPOSITION ON RADIATIONAL-DAMAGE DEVELOPMENT IN STEELS AND ALLOYS IRRADIATED BY NEUTRONS*

V. I. Shcherbak, V. N. Bykov,
V. D. Dmitriev, and S. I. Porollo

UDC 621.039.531

The development of fast reactors has stimulated intense investigation in the field of radiational materials science, as a result of which the main reatures of the development of vacancy porosity and radiational creep have been established. At the same time, a very broad range of questions remains unanswered, not least because the phenomena under investigation are very sensitive to a large number of factors.

The present work attempts the analysis and generalization of the effect of neutron irradiation on the properties of several experimental samples and also a number of steels and alloys used in active-region components of the BR-10 and BOR-60 reactors. Preliminary results of these investigations have already been published [1-7].

Vacancy Pores

The investigation of the effect of a flux Kt on the swelling kinetics of OKh18N9T, Kh18N9, 1Kh18N10T, and OKh16N15M3B steels has shown that in the initial period of vacancy-porosity development the mean pore diameter increases according to the law $(Kt)^{1/2}$, regardless of the composition of the material (Fig. 1). The rate of pore growth then falls, and at large fluxes the change in the mean pore diameter is slight. The pore concentration N_V, in contrast to the mean diameter, increases according to a power law up to approximately 100 dislocation/atom (TRN standard). Thus, for OKh18N9T steel, the relative pore volume at the initial stage increases according to a near-quadratic law, while after 30 dislocation/atom, $\Delta V/V$ increases in proportion to Kt.

Analysis of the experimental data shows that variable conditions of reactor operation affect the kinetics of vacancy-pore initiation and growth [6]. The radiational swelling of OKh16N15M3B steel used for fuel-element shells was less in the initial period of operation of a BOR-60 reactor than in the case of irradiation in a BR-5 reactor. The features of the irradiation of OKh16N15M3B steel in a BOR-60 reactor in this period include considerable oscillations of the temperature and rate of dislocation production. Nevertheless, in the

*This is an adaptation of a paper read to the Conference on Reactor Materials Science, Alushta, 1978.

Translated from Atomnaya Énergiya, Vol. 46, No. 2, pp. 91-96, February, 1979.

0038-531X/79/4602-0101$07.50

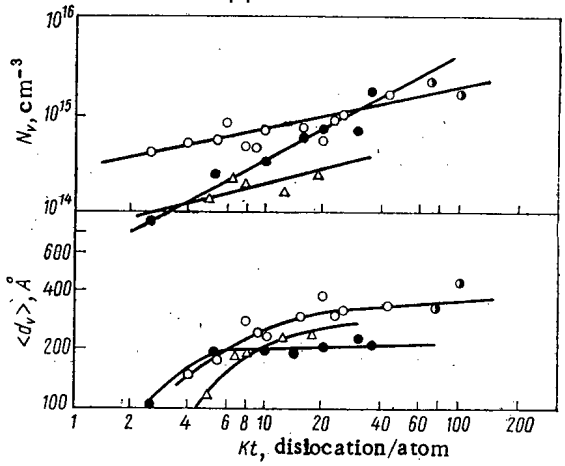

Fig. 1

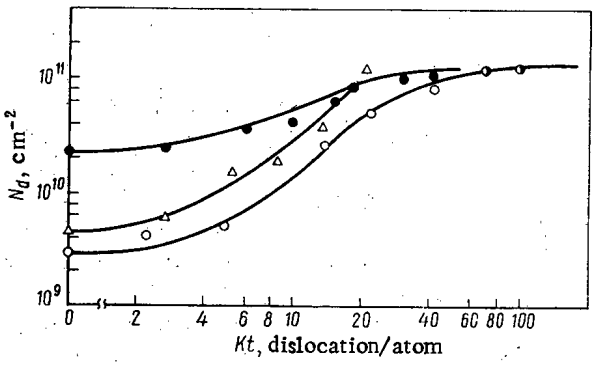

Fig. 2

Fig. 1. Effect of flux on N_V and $\langle d_V \rangle$ for pores in 0Kh18N9T (○), Kh18N9 (◑), 0Kh16N16M3B (●), and 1Kh18N10T (Δ) steels irradiated at 460-470°C.

Fig. 2. Dependence of the total dislocation density in 0Kh18N9T (○), Kh18N9 (◑), 0Kh16N15M3B (●), and 1Kh18N10T (Δ) steels on the flux (T_{rad} = 460-470°C).

complex changes in reactor conditions, it is possible to isolate characteristic values of the power at which the reactor has been operating for a predominant part of the time. The radiation-condition characteristics, results of investigation of this steel, and values of the swelling calculated from the empirical expression of [7] are given in Table 1. It follows from Table 1 that for a certain time (at a flux of ∿3-4 dislocation/atom) the material was irradiated at a temperature less than 360-370°C, as a result of which the development of vacancy porosity was considerably suppressed. In this case preliminary low-temperature irradiation has the same effect on the swelling as preliminary cold deformation. With increase in irradiation temperature, the annealing of the defects formed as a result of low-temperature irradiation becomes more rapid, and the effect of low-temperature is then less significant.

Dislocation Structure

The investigation of the dislocation structure is of exceptional interest, since the dislocation density determines the rate of initiation and growth not only of dislocation loops and vacancy power but also of inclusions of other phases. The evolution of the dislocation structure depends in a complex manner on the initial dislocation density N_d, the irradiation conditions, and the chemical composition of the steels and alloys. In the initial stage of irradiation, up to a flux of ∿10 dislocation/atom, the total dislocation density increases as a result of the development of dislocation loops, as follows from Fig. 2. Analysis of the experimental results and comparison with data on the development of porosity shows that the kinetics of dislocation-loop initiation and growth in steels irradiated by neutrons is less sensitive to the change in chemical composition of the material and the initial dislocation density. At relatively low temperature (∿360°C), Frank interstitial-type dislocation loops are observed in austenitic steels. With increase in irradiation temperature, prismatic loops are also observed. In samples irradiated at >550°C, only prismatic loops are found. Increase in nickel content in alloys of the system Fe—Cr—Ni leads to a sharp increase in the number of prismatic loops [3].

As in the case of vacancy pores, the dependence of the mean dislocation-loop diameter $\langle d_\zeta \rangle$ on the flux is characterized by two stages (Fig. 3). In the first stage, at small fluxes, accelerated loop growth is observed. At fluxes above 5 dislocation/atom, there is little change in the mean loop diameter.

The results of investigating the effect of the irradiation temperature on the kinetics of dislocation-loop growth in 0Kh16N15M3B steel indicate that with increase in temperature from 430 to 570°C the power-law index increases from 0.3 to 0.6 [6].

According to electron-microscope data, the increase in N_d at a flux of ∿10 dislocation/atom is associated with the appearance in the structure of the steel at this time of

TABLE 1. Irradiation Conditions and the Swelling of 0Kh16N15M3B Steel in a BOR-60 Reactor

Kt, dislocation/atom	T° C	Kt, dislocation/atom	T° C	Kt, dislocation/atom	T° C	Total flux, dislocation/atom	$\Delta V/V$,* %
3,1	334	6,3	395	31,6	425	41	0,05; 0,4
3,1	340	6,3	415	31,6	450	41	0,2; 1,0
2,9	360	5,9	450	29,6	490	38,5	1,0; 2,0
2,6	365	5,25	470	26.4	515	34	1,4; 1,9

*The first value is experimental and the second calculated.

high-density barriers in the form of loops and inclusions, which leads to a considerable distortion of the dislocation lines. It is for this reason that the dependence of the dislocation density on the flux for 1Kh18N10T is sharper than that observed for 0Kh18N9T steel. Further increase in the flux is accompanied by slowing of the growth of N_d and at large fluxes the difference in the values of N_d for the different steels becomes insignificant. The irradiation of material with an elevated initial dislocation density is a more complicated situation. In Fig. 4, the temperature dependence of the dislocation density is shown for 0Kh16N15M3B steel in which the value of N_d before irradiation was $4 \cdot 10^{10}$ cm^{-2}, which corresponds to 5-7% deformation. As is evident from Fig. 4, irradiation of steel at a temperature above 500°C led to a recovery process, as a result of which a drop in dislocation density was observed. On passing to large fluxes, the recovery processes was impeded by the development of an ensemble of inclusions and dislocation loops, and an increase in N_d was observed over the whole temperature range. Increasing the initial dislocation density to $3 \cdot 10^{11}$ cm^{-2} leads to the development of a recrystallization process, which becomes pronounced at temperatures above 500°C [4]. Further increase in N_d facilitates the acceleration of recrystallization.

Inclusions

Particles of inclusions of other phases are observed in the irradiation of steels even at a flux of $\sim 5 \cdot 10^{20}$ neutron/cm^2. Investigation of the dependence of the concentration and mean volume of a titanium carbide inclusion in 1Kh18N10T steel and of a niobium carbide inclusion in 0Kh16N15M3B steel on the flux has shown that the initial stage of irradiation is characterized by increase in the concentration and volume of the developing inclusions (Fig. 5). It follows from Fig. 5 that the formation and growth of niobium carbide in 0Kh16N15M3B steel is rather more rapid than the corresponding processes for titanium carbide in 1Kh18N9T steel. With increase in the flux, the concentration of the inclusions increases to a maximum and then falls according to the law $N_p \sim (Kt)^{-1}$. It is found that the coalescence of inclusions of titanium and niobium carbide and Laves phase has a different dependence on the flux. With increase in irradiation temperature from 430 to 570°C, the power-law index in the formula for niobium carbide varied from −0.4 to −0.95. The power-law index in the equation for the mean volume of these inclusions in the given temperature range increased from 0.6 to 1.2. The coalescence of Laves phase in this temperature range does not depend greatly on the temperature and the flux. As is known, the coalescence of the inclusions in steels may occur in two different ways. In particular, the inclusions forming as a result of irradiation may vanish as a result of the diffusion of individual impurity atoms from small to large inclusions through the matrix. According to the theory of diffusional coalescence [8], the kinetics of growth of particles of radius R_p is determined by the equations $R_p \sim t^{1/3}$, $N_p \sim 1/t$. If diffusion occurs over the dislocation lines, coalescence occurs more slowly than for volume diffusion, and the mean size and concentration of the inclusions must vary over time according the relations [9] $R_p \sim t^{1/7}$ and $N_p \sim t^{-3/7}$.

Turning to the experimental data, it is evident that the power-law index in the equations for the mean volume and concentraiton of niobium-carbide inclusions in 0Kh16N15M3B steel irradiated at 430°C is 3/7 and −3/7, respectively, as follows from the theory of coalescence with the diffusion of impurity atoms along dislocations. At higher irradiation temperature, the dependence of the concentration and mean volume of niobium-carbide particles on the flux takes a form similar to that predicted by the theory of diffusional coalescence.

Accordingly, it may be suggested that at low irradiation temperature the most probable mechanism of inclusion growth is particle coalescence by diffusion of impurity atoms along dislocation lines. In the case of irradiation at higher temperature and low dislocation

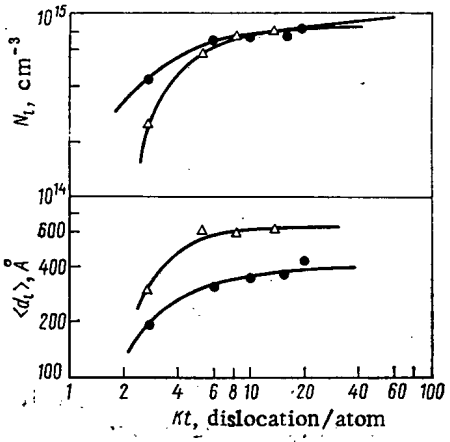

Fig. 3

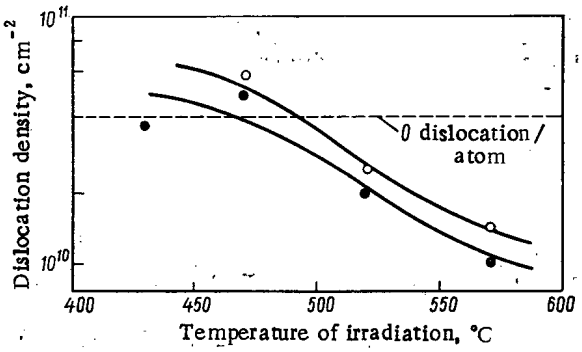

Fig. 4

Fig. 3. Dependence of N_l and $\langle d_l \rangle$ for dislocation loops in 0Kh16N15M3B (●) and 1Kh18N10T (Δ) steels on the flux (T_{rad} = 460-470°C).

Fig. 4. Temperature dependence of dislocation density in 0Kh16N15M3B at a flux of 5 (O) and 20 (O) dislocation/atom.

TABLE 2. Values of the Parameter (η − 1) for Some Steels and Alloys

Material	$(\eta-1)\cdot10^{-2}$	Material	$(\eta-1)\cdot10^{-2}$
1Kh12M2S2	0,3	0Kh16N15M3B	1,1
0Kh18N9T	0,8	0Kh16N40B	0,15
1Kh18N10T	1,0	0Kh16N80B	0,9
00Kh16N15M3B	0,75		

density, coalescence of inclusion particles as a result of volume diffusion is more probable. At intermediate irradiation temperatures and high dislocation density, both mechanisms may act simultaneously.

Effect of Chemical Composition

Electron-microscopic observation of radiational damage in 0Kh18N9T, 1Kh18N10T, 00Kh16N-16M3B, and 0Kh16N15M3B steels has shown that the effect of inclusions on pore initiation and growth depends on the irradiation temperature. In the investigation of samples irradiated at temperatures above 500°C, it is observed that some of the largest pores are associated with inclusion particles, while the relative proportion of such pores increases with increase in irradiation temperature. In addition, some of the larger incoherent inclusions, like grain boundaries, have regions that are free from pores. According to the results of [2], at temperatures above 500°C the inclusion particles affect the development of vacancy porosity indirectly, by increasing the dislocation density. This increase may be explained by the presence in the slip planes of scattered microdisperse inclusions, which lead, in conditions of supersaturation of the material with point defects, to considerable distortion of the dislocation lines.

The results of measurements of the swelling, dislocation density, and particle density of inclusions in steels and alloys irradiated at 460-500° by a flux of up to 14 inclusion/atom [2, 3] are shown in Fig. 6. According to these data, the development of pores and dislocation structure in 0Kh18N9T (1), 1Kh18N10T (5), 00Kh16N15M3B (4), and 0Kh16N15M3B (6) steel and 0Kh16N80B alloy (3) is determined to a considerable extent by the formation of inclusion particles. On the other hand, as noted above, the kinetics of inclusion-particle initiation and growth depend on the development of the dislocation structure. However, for 1Kh12M2S2 ferrite steel (7) and 0Kh16N40B alloy (2) no such correlation is observed. These results indicate that changes in the chemical composition of steels and alloys have a complex effect on the initiation and growth of point-defect aggregations. The effect of alloying elements on pore initiation and growth may be explained by a number of factors: an increase in

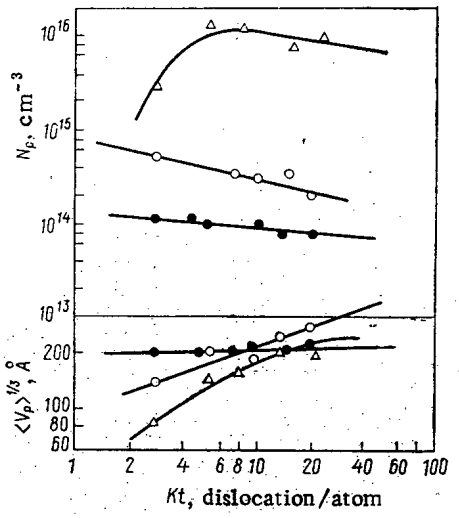

Fig. 5

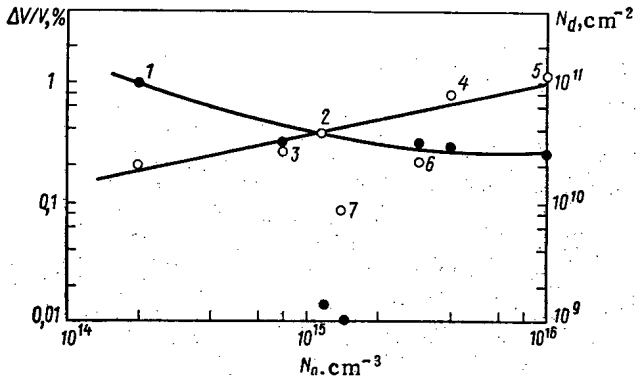

Fig. 6

Fig. 5. Concentration and mean volume of inclusions of titanium carbide (Δ), niobium carbide (○), and Laves phase (●) as a function of the flux (T_{rad} = 470°C; K = $2.2 \cdot 10^{-7}$ dislocation/atom·sec).

Fig. 6. The effect of the inclusion-particle concentration on the total dislocation density (○) and swelling (●) of some steels and alloys at T_{rad} = 460-500°C and Kt = 14 dislocation/atom (the steels and alloys corresponding to the numbers on the curves are identified in the text).

point-defect recombination rate [10]; anomalous changes in the partial diffusion coefficients of substituent atoms [11]; changes in the vacancy and interstitial-atom diffusion coefficients, in the defect packing energy, and in the surface energy; or changes in the concentration of inclusions able to act as neutral sinks [12] or to alter the dislocation density [2].

Analysis of results on the swelling of steels and alloys shows that none of these mechanisms can itself account for the whole set of experimental data. A more profound understanding of the role of certain alloying additives may be obtained if it is assumed that changes in the chemical composition significantly alter the capacity of the dislocations to capture point defects.

Table 2 gives values of the parameter $(\eta - 1)$ obtained in [2, 3]; η characterizes the ratio of the surface corresponding to capture by dislocations of interstitial atoms and vacancies. As follows from Table 2, the parameter $(\eta - 1)$ is approximately equal to 10^{-2} for most steels and is reduced to 10^{-3} only for ferrite steel and 0Kh16B40B alloy, which are characterized by very small swelling. Hence, the small swelling of these materials may be explained by the small difference in the surfaces corresponding to point-defect capture by dislocations.

Note that the effect of alloying elements on the swelling of a material is more clearly expressed at small fluxes and low irradiation temperature. One possible explanation for this is that irradiation of the material at large fluxes or high temperature leads to profound changes in the composition of the matrix as a result of the formation of inclusion particles. Many alloying elements, for example, Ti, Mo, Nb, C, and N, enter solid solution, and thus their role in pore initiation and growth becomes less significant.

CONCLUSIONS

The investigation of the initiation and growth kinetics of pores, dislocation structure, and particles of phase inclusions at fluxes of 1-100 dislocation/atom leads to the following conclusions.

1. The dependence of the pore concentration in steels on the flux is described by a power law; the power-law index depends strongly on the composition of the steel and the irradiation temperature. The mean pore diameter in the initial period of irradiation varies according to the law $(Kt)^{1/2}$; at large fluxes, it remains almost constant.

2. In all the steels investigated, at fluxes above 5 dislocation/atom, the total dislocation density increases according to a power law; the power-law index varies from 0.4 to 1 depending on the composition of the steel and the irradiation temperature.

3. In the initial period of irradiation, a stage of accelerated inclusion-particle initiation is observed, while at high fluxes they are seen to coalesce. The correlation of the kinetics of inclusion-particle initiation and growth with the dislocation density and the irradiation temperature has been established.

4. The effect of the chemical composition of the steel, which is particularly clearly expressed at low temperature and small fluxes, is evidently due to the action of the alloying elements either on the ability of the dislocations to capture interstitial atoms or on the mechanism of the formation of new-phase inclusions.

LITERATURE CITED

1. V. I. Shcherbak et al., in: Problems of Atomic Science and Engineering. Fuel and Constructional Materials Series [in Russian], No. 1(6), Izd. VNIINM, Moscow (1977), p. 14.
2. V. I. Shcherbak et al., in: Problems of Atomic Science and Engineering. Radiation-Damage Physics and Radiational Materials Science Series [in Russian], No. 1(4), Kharkov Physicotechnical Institute (1977), p. 83.
3. V. I. Shcherbak et al., in: Proceedings of an International Conference on Radiational Effects in Breeder Reactor Structural Materials, Met. Soc. AIME (1978), p. 773.
4. A. N. Vorob'ev et al., J. Nucl. Energ. Soc., 14, No. 2, 149 (1977).
5. S. I. Porollo et al., At. Energ., 43, No. 3, 207 (1977).
6. V. I. Shcherbak, V. N. Bykov, and V. D. Dmitriev, Fiz. Met. Metalloved., 43, No. 2, 419 (1977).
7. V. I. Shcherbak et al., J. Brit. Nucl. Energ. Soc., 14, No. 2, 145 (1975).
8. I. M. Lifshchits and V. V. Slezov, Zh. Eksp. Teor. Fiz., 35, 47 (1958).
9. A. Ardell, Acta Met., 20, 61 (1972).
10. F. Smidt and J. Sprague, Scripta Met., 7, No. 5, 495 (1973).
11. H. Venker and K. Ehrlich, J. Nucl. Mater., 60, 347 (1976).
12. R. Bullough and R. Perrin, in: Proceedings of a European Conference on Voids Formed by Irradiation of Reactor Materials, BNES, Reading (1971), p. 78.

MEASUREMENT OF NEUTRON SPECTRA IN CRITICAL ASSEMBLY BY ACTIVATION METHOD

K. I. Zolotarev, V. P. Koroleva,
Yu. F. Koleganov, and L. A. Chernov

UDC 621.039.51

Measurement of the energy spectra of neutrons is of great interest for both reactor construction and refinement of computational methods and choice of constants. Quite refined spectrum-measuring methods (time-of-flight, recoil-proton, etc.) could not displace an earlier method, the activation method [1] because of its considerable advantages. The main advantage for spectrometry is that it has small perturbations at the point of measurement and that it can be used in fields of mixed radiation and can encompass practically the entire energy range of the spectrum produced in the reactor. A serious drawback of the activation method is the lack of sufficient accuracy in the spectrum determined. The success of the application of the activation method to neutron spectrometry depends on the accuracy of determination of the reaction rate, the number of activated tracers with independent variation of the reaction cross section, the accuracy of the reaction cross sections used, and the method of reproducing the spectrum. In order to increase the accuracy of spectrum reproduction, therefore, it is desirable to refine both the experimental methods and the methods of reproducing the spectrum.

Translated from Atomnaya Énergiya, Vol. 46, No. 2, pp. 96-100, February, 1979. Original article submitted February 20, 1978.

 0038-531X/79/4602-0106$07.50

TABLE 1. Experimental Values of Reaction Rates

Reaction	Reaction rate, 10^{24} events/sec · nucleus	Cross-section data used
$^{23}Na\,(n,\gamma)\,^{24}Na$ *	$2{,}938\cdot10^{7}\pm4{,}6$†	[5]
$^{24}Mg\,(n,p)\,^{24}Na$	$1{,}196\cdot10^{6}\pm4{,}6$	[7]
$^{27}Al\,(n,p)\,^{27}Mg$	$2{,}891\cdot10^{6}\pm4{,}7$	[6]
$^{27}Al\,(n,\alpha)\,^{24}Na$	$5{,}810\cdot10^{5}\pm4{,}6$	[6]
$^{56}Fe\,(n,p)\,^{56}Mn$	$7{,}931\cdot10^{5}\pm4{,}6$	[6]
$^{58}Ni\,(n,p)\,^{58}Co$	$7{,}850\cdot10^{7}\pm4{,}7$	[6]
$^{115}In\,(n,n')\,^{115m}In$	$1{,}179\cdot10^{8}\pm5{,}5$	[6]
$^{233}U\,(n,f)$ *	$5{,}465\cdot10^{10}\pm9{,}6$	[5]
$^{235}U\,(n,f)$ *	$2{,}483\cdot10^{10}\pm8{,}8$	[5]
$^{238}U\,(n,f)$	$2{,}767\cdot10^{8}\pm8{,}9$	[6]
$^{239}Pu\,(n,f)$ *	$2{,}716\cdot10^{10}\pm8{,}8$	[5]

*Reaction-rate values given from cadmium limit.
†Error, %.

The objective of the present paper is that of using the activation method to measure the neutron spectrum in a methodological critical assembly development of a GIN program for unfolding the spectrum from activation data on the basis of methods presented in [2, 3], the application of the inductive approach to the process of spectrum reproduction, and comparison of the results with the spectrum measured by direct spectroscopic methods.

Experiment. The neutron spectrum was measured on a methodological critical assembly with a zirconium hydride moderator (the ratio of nuclear concentrations of hydrogen to ^{235}U is ∼25). In the center of the core we determined the absolute value of the reaction rates for $^{23}Na(n,\gamma)^{24}Na$, $^{24}Mg(n,p)^{24}Na$, $^{27}Al(n,p)^{27}Mg$, $^{27}Al(n,\alpha)^{24}Na$, $^{56}Fe(n,p)^{56}Mn$, $^{58}Ni(n,p)^{58}Co$, $^{115}In(n,n')^{115}In$, $^{235}U(n,f)$, $^{239}Pu(n,f)$ by the activation method and for $^{233}U(n,f)$ and $^{238}U(n,f)$ by an indirect method. The activation specimens had a diameter of 9-25 mm. They were irradiated in cadmium filters 0.5 mm thick. The induced activity was measured with a Ge(Li) semiconductor spectrometer (sensitive volume 5 cm^3, energy resolution 2.7 keV for ^{57}Co) by the photoabsorption of quanta of a particular characteristic energy for each reaction. After amplification, the pulses from the detector were analyzed with a 512-channel analog-to-digital converter (ADC) and stored in the magnetic immediate-access memory (MIAM) of the Reactor Measuring Center (RMC). The data accumulated in the MIAM were printed out by a BZ-15 digital printer or teletype. The measured amplitude γ-ray spectra were processed on a Nairi-1 computer. The procedure employed to calculate the area of the photopeak was described in [4].

Because of the lack of suitable specimens the $^{233}U(n,f)$ and $^{238}U(n,f)$ reaction rates were determined by an indirect method from the ratios $\sigma_f^{233}/\sigma_f^{235}$ and $\sigma_f^{238}/\sigma_f^{235}$ of the spectrum-averaged fission cross sections of the respective isotopes and the cadmium ratios R_{Cd}^{233} and R_{Cd}^{235} for ^{233}U and ^{235}U, measured by KNT-3, KNT-5, and KNT-8 ionization fission chambers.

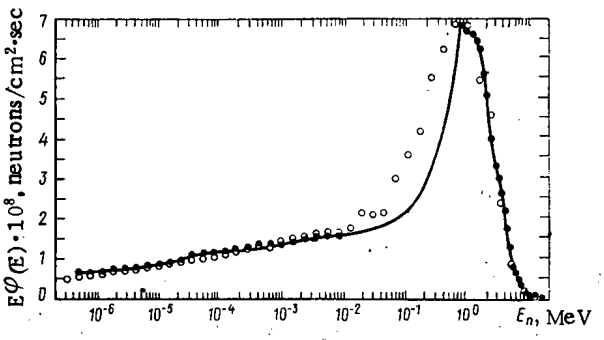

Fig. 1. Neutron energy spectrum unfolded by using the inductive approach: ●) unfolded spectrum; ○) experimental spectrum obtained by direct spectrometric methods of spectrometry.

The measured absolute values of the reaction rates are given in Table 1 along with the total error (in the experiment and in the constants used) for a confidence coefficient of 0.95-0.90.

The Spectrum-Unfolding Procedure and the GIN Program. The procedure employed in the present paper to unfold the neutron spectrum was based on the SPECTRA mathematical method first developed by Greer et al. [2] and improved by Fisher and Turi [3]. In the method described the sought differential neutron spectrum $\varphi(E)$ is presented in the form of a continuous piecewise-linear function $E\varphi(E)$ and the energy dependence of the microscopic cross sections for nuclear reactions is presented in the form of a continuous piecewise-linear function $\sigma(E)/E$. In this case the system of linear Fredholm integral equations of the first kind can be transformed into a matrix equation

$$a = Q\Phi, \tag{1}$$

where a is a column-vector of n elements which are measured values of the reaction rates A_i, Φ is a column-vector of m elements which are the values of the neutron flux density sought at given energy points, and Q is an $(n \times m)$ matrix whose elements are definite integrals of the reaction cross sections.

If the rows of matrix Q are separated into the corresponding elements of vector a and if the resulting matrix is denoted by C, then Eq. (1) can be rewritten as

$$C\Phi = (1_n), \tag{2}$$

where (1_n) is a column-vector of n elements, each of which is equal to unity.

Since the spectrum is usually determined at a larger number m of energy points than the number n of available activation data, the solution of Eq. (2) is mathematically indeterminate. Additional information is therefore necessary in order to obtain physically substantiated results. In this case, an initial spectrum $\varphi_0(E)$ is prescribed and among the spectra which satisfy Eq. (2) we find a spectrum $\varphi(E)$ for which the fundamentals

$$\int_{E_{min}}^{E_{max}} \left[\frac{\varphi(E)-\varphi_0(E)}{\varphi_0(E)}\right]^2 dE \text{ and } \sum_{i=1}^{n} (A_{B_i} - A_i)^2 \tag{3}$$

simultaneously assume a minimum value. Here, E_{max} and E_{min} are the upper and lower limits of the energy range in which the spectrum is determined, and A_{Bi} and A_i are the calculated and measured values reaction rates in the i-th isotope in the spectrum sought.

To derive an iteration formula with allowance for the condition (3) we set up the error function Δ_1 which characterizes the deviation between the calculated and measured reaction rates in the spectrum sought, on the one hand, and between the sought and initial spectra on the other:

$$\Delta_1 = [C\Phi_1 - (1n)]^T F^2 [C\Phi_1 - (1_n)] + (\Phi_1 - \Phi_0)^T G^2 (\Phi_1 - \Phi_0), \tag{4}$$

where G^2 and F^2 are the diagonal normalization matrices (det $G \neq 0$, det $F \neq 0$). Minimization of the function Δ_1 with respect to Φ_1 leads to

$$\Phi_1 = G^{-1}B[K^T F(1_n) + G\Phi_0],$$

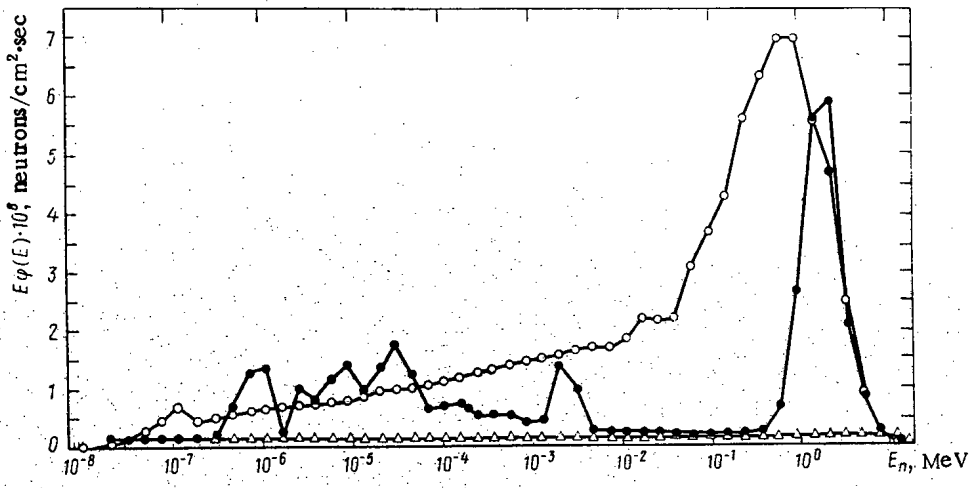

Fig. 2. Neutron energy spectrum, unfolded with initial 1/E spectrum prescribed at 50 energy points at once: Δ) initial 1/E spectrum; ●) unfolded spectrum; ○) experimental spectrum obtained by direct spectrometric methods.

where $B = (K^TK + I)^{-1}$, $K = FCG^{-1}$, and I is a unit matrix of order m.

A new function Δ_2 analogous to Eq. (4) can be constructed by replacing Φ_0 with Φ_1 and Φ_1 with Φ_2. Minimization is carried out with respect to the next approximation Φ_2 of the spectrum. If this process is repeated, the expression for the sought spectrum after k steps will be of the form

$$\Phi_k = G^{-1}B\,[K^TF\,(1_n) + G\Phi_{k-1}]. \qquad (5)$$

Equation (5) is the general formula of the iterative process which is continued until the rms deviation between the calculated and measured values of the reaction rates reaches a given value. The iterative process is also halted when the deviations between the calculation and measured values of the reaction rates reaches a given value. The iterative process is also halted when the deviations between the calculated and measured reaction rates become smaller than the relevant errors in the experimental data on the reaction rates.

The algorithms described here, including the method of controlling the rate of convergence of the iterative process [3], was executed in the GIN program. The GIN program is written in FORTRAN IV which is suitable for the translator of the ES-1030 computer and makes it possible to reproduce the values of the neutron flux density at 50 energy points. The maximum number of reactions used cannot exceed 30. The data on the reaction cross sections are fed in from magnetic tape whereas the other data are fed in from punched cards. The length of the objective module of the GIN program is ∿32K.

Spectrum Unfolding and Results. The inductive approach to the solution of the problem is proposed with a view to enhancing the reliability of the unfolding of the energy spectrum and reducing the influence of the choice of the initial information on the results of the algorithm. As already mentioned, the linear Fredholm integral equations of the first kind are approximated by a system of algebraic equations in matrix form (1). The proposed inductive method makes use of the fact that the solution of Eq. (1) can be unique only if the number of points of the spectrum sought coincides with the number of activation data available, i.e., if m = n. The principle of the inductive approach lies in the stage-by-stage unfolding of the spectrum. In the initial stage the spectrum is determined at points which correspond in number to number of experimental data. Each subsequent stage in the reproduction of the spectrum is accompanied by a gradual increase in the number of subdivisions of the energy scale. In any case, the results of the preceding calculation are used as the initial spectrum. In the problem of the initial spectrum at intermediate points account was taken of the assumption of the piecewise-linear dependence of the function E (E). The process of spectrum unfolding is continued until the resulting spectrum begins to repeat the spectrum of the preceding stage or until the number of points on the energy scale does not reach the maximum value predicted by the program.

It is known that the initial a priori spectrum is most expediently prescribed from mathematical calculation of the medium studied. However, in order to verify the capabilities

of the inductive method in unfolding the neutron spectrum of U—ZrH of a critical assembly, we deliberately used a 1/E spectrum differing substantially from the real spectrum, as the initial spectrum. The spectrum unfolding was carried out in five stages. In the first stage the 1/E spectrum was prescribed at 11 points on the energy scale (in accordance with the available activation data) in the range from 0.01 eV to 18 MeV with approximately the same step on the logarithmic scale, apart from the interval 8-800 keV. When the number of subdivisions of the energy scale was increased further the results of the fourth and fifth stages already practically did not differ from each other. Therefore, the spectrum after the fifth stage of unfolding, which is shown in Fig. 1, should be considered final. For comparison, we show the spectrum measured by direct methods [8] (using the time-of-flight and recoil-proton methods). Both spectra were normalized with respect to the absolute values of the reaction rates. The values of the normalization factor X was found from the condition that the expression $\sum_{i=1}^{n}(XA_{i-1})$ have a maximum. It is seen from Fig. 1 that in the energy ranges 0.5 eV-8 keV and 800 keV-18 MeV the spectra are in satisfactory agreement with each other (the maximum difference is no more than 15%). Because of the inadequacy of the experimental information no points were prescribed during the unfolding of the spectrum in the energy range 8-800 keV. The curve was drawn with the assumption of the linear dependence of the function $E\varphi(E)$ inside this range; it is meaningless, therefore, to speak of the accuracy of the reproduction of the spectrum.

To get a graphic picture of the advantages of the inductive method over the traditional approach to the reproduction of a spectrum (when the subdivisions of the energy scale far outnumber the experimental data) we made a calculation of the spectrum with the initial spectrum prescribed at 50 points at once. The results of the spectrum unfolding are shown in Fig. 2, from which it follows that the spectrum obtained does not give satisfactory results if the initial spectrum differs substantially from the real spectrum. Thus, in the range of intermediate energies the unfolded spectrum displays considerable oscillations whereas the time-of-flight measurements yield a smooth curve which obeys the $E^{-0.88}$ law. The most pronounced difference between the unfolded spectrum and the real spectrum is observed in the energy range 6-400 keV in which the resulting spectrum essentially repeats the initial spectrum, this being explained by the lack of sufficient experimental data in this range. Comparison of Figs. 1 and 2 confirms the effectiveness of using the inductive approach in the process of spectrum unfolding.

In conclusion, it should be added that for qualitative unfolding of a neutron energy spectrum in the range 8-800 keV it is necessary to employ additional reactions, e.g., $^{37}Cl\cdot(n, \gamma)$, $^{103}Rh(n, n')$, and $^{237}Np(n, f)$, as well as $^{6}Li(n, \alpha)$, $^{10}B(n, \alpha)$, $^{235}U(n, f)$, and $^{239}Pu(n, f)$ with irradiation in boron filters.

LITERATURE CITED

1. E. A. Kramer-Ageev, E. G. Tikhonov, and V. S. Troshin, Activation Methods of Neutron Spectrometry [in Russian], Atomizdat, Moscow (1976).
2. C. Greer et al., A Technique for Unfolding Neutron Spectrum from Activation Measurements, SC-RR-67-746 (1967).
3. A. Fisher and L. Turi, KFKI-71-22, Budapest (1971).
4. F. Rossitto and M. Terrani, Nucl. Instr. Methods, 79, 341 (1970).
5. J. Schmidt, KFK-120, Karlsruhe (1966).
6. B. Magurno, ENDF/B-IV Dosimetry File, BNL-NCS-50446 (1975).
7. A. A. Lapenas, in: Measurement of Neutron Spectra by the Activation Method [in Russian], Zinatne, Riga (1975), p. 35.
8. M. Ya. Bankrashkova et al., At. Energ., 44, No. 3, 260 (1978).

KAL'MAR-1 PULSED ELECTRON ACCELERATOR WITH RELATIVISTIC ELECTRON BEAM POWER OF UP TO $5 \cdot 10^{12}$ W/cm^2

B. A. Demidov, M. V. Ivkin,
V. A. Petrov, and S. D. Fanchenko

UDC 621.384.659

The possibility of achieving controlled thermonuclear fusion by using relativistic electron beams (REB), first pointed out by Zavoiskii [1], is arousing ever-increasing interest. As shown by Rudakov [2, 3], REB with a current of the order of 10^7 A and a power density of the order of 10^{13} W/cm^2 are required to accomplish this. The present paper describes the Kal'mar 1 accelerator producing REB with a power density of $5 \cdot 10^{11}$-$5 \cdot 10^{12}$ W/cm^2. We give the results of investigations on REB focusing in a high-voltage diode as a function of the electrode geometry and the magnitude of the voltage prepulse.

Accelerator Design. The design of the accelerator was chosen by proceeding from the following concepts. The accelerator should have these parameters: electron energy 1 MeV, impedance of high-voltage diode 1.5 Ω, pulse duration 70-100 nsec. For normal operation of the high-voltage diode the prepulse should not exceed 1-2% of the operating voltage. The circuit of the accelerator should be as simple and reliable as possible. It was decided to use a duplex shaping line (DSL) with water dielectric and one switching device (spark gap in water). The 4-Ω output resistance of the DSL was matched to the impedance of the high-voltage diode by using a coaxial tranformer with an output resistance of 1.5 Ω. One end of the central electrode was electrically (and mechanically) connected directly to the central cylinder of the DSL and the other end to the high-voltage diode (Fig. 1). The DSL (electrical length 70 nsec) is charged from a voltage-pulse (Arkad'ev—Marx) generator with an output voltage of 2 MV and a stored energy of 70 kJ. The generator, built of IMP-100-0,1 capacitors, consists of 20 multiplier stages. The first stage uses a pressurized-gas trigatron-type spark gap whereas the others have untriggered, open air spark gaps. Thanks to the insertion of an inductance shunting the second-stage output to the ground, the scatter of the generator triggering delay does not exceed $\Delta\tau_t$ = 10-20 nsec when τ_t = 250 nsec and the output voltage is more than 80% of the breakdown voltage [8]. The DSL, the coaxial transformer 5 with an output resistance of 1.5 Ω, and the high-voltage diode 7 are placed in a stainless steel case (see Fig. 1) of diameter 1 m and length 4.2 m in which a forevacuum is set up during filling with distilled water. The middle cylinder 3 of the DSL is mounted on stand-off insulators with elastic elements to dampen pressure surge; these elements allow the cylinder to move axially 3-5 mm.

The spark gap can operate in the spontaneous breakdown mode (the experimental data given below were obtained with this mode) as well as in a laser-ignition mode. For laser ignition of the water spark gap [5] the rod 2 was provided with a lens 12 to focus the laser radiation onto the surface of electrode 3 and a protective Plexiglas window 11. The neodymium—glass laser (pulse energy ∿2 J, duration 20 nsec) consists of a driving oscillator 13 with a modulated Q-factor and two amplifier stages 14.

The DSL charging circuit (Fig. 2) was chosen so that the prepulse amplitude could be regulated over wide limits to within 1-2% of the amplitude of the main voltage pulse U without an additional spark gap in the DSL—diode circuit. The capacitance of the generator (35 nF) was chosen to be close to that of the DSL (capacitance of DSL branches: C_2 = 14 nF, C_3 = 12.5 nF), thus ensuring a high efficiency of resonant charging of the DSL (the charging period corresponds to the cyclic frequency $\omega = 1.7 \cdot 10^6$ sec^{-1}). Since the resonant charging period exceeds the pulse duration by an order of magnitude, if account is taken of the relations between the values of the parameters of the electrical circuits, the prepulse amplitude can be given by the approximate formula

$$\Delta U = U L_0 C_3 \omega^2, \quad (1)$$

Translated from Atomnaya Énergiya, Vol. 46, No. 2, pp. 100-104, February, 1979. Original article submitted November 29, 1977.

0038-531X/79/4602-0111$07.50

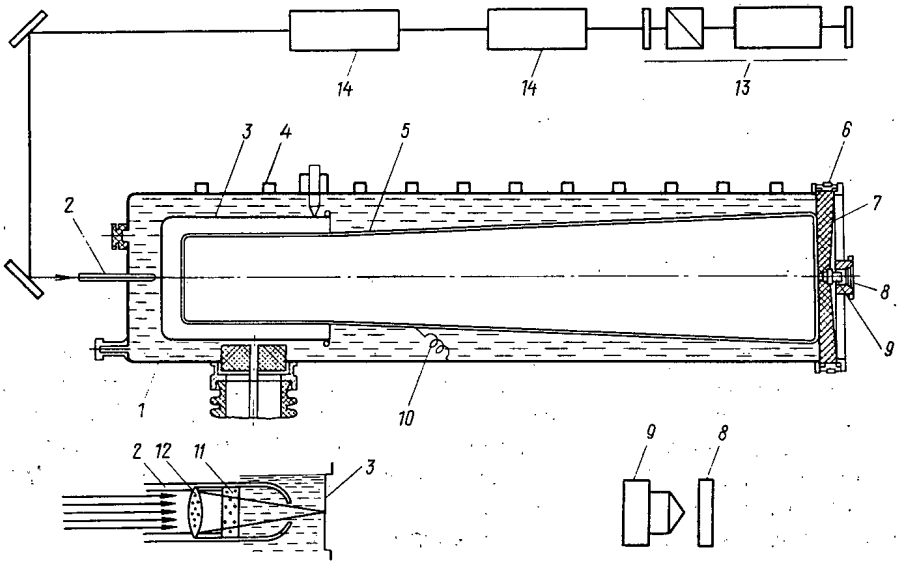

Fig. 1. Diagram of the apparatus.

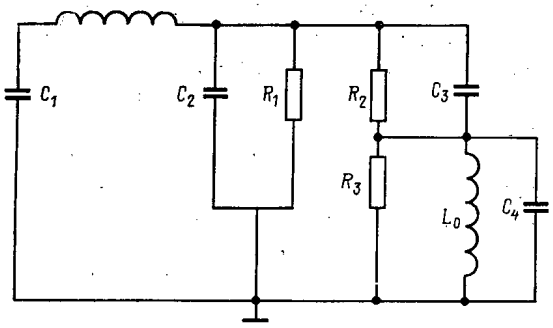

Fig. 2

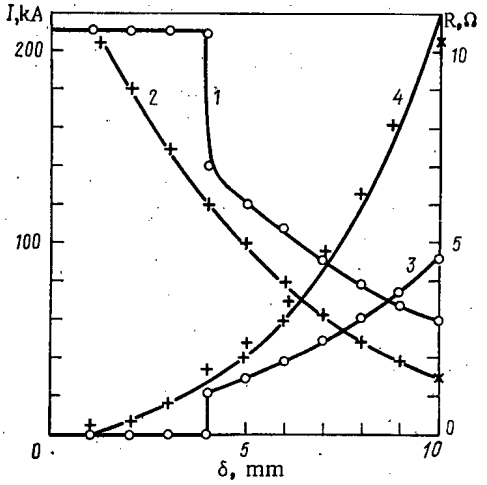

Fig. 3

Fig. 2. Equivalent circuit of apparatus in a charging mode: C_1, C_2, C_3, C_4) capacitances of voltage-pulse generator, branch of DSL, and coaxial transformer, respectively; L) inductance of generator and charging circuit; L_0) decoupling inductance; R_1, R_2, R_3) resistance of leaks through water.

Fig. 3. Diode current (1, 2) and diode impedance (3, 4) as function of cathode–anode gap: ○) prepulse amplitude 0.1 U; +) prepulse amplitude 0.01 U.

where L_0 is the inductance of the high-voltage decoupling 10 (see Fig. 1) ensuring symmetric charging of the DSL. When L_0 = 2.2 μH the prepulse $\Delta U \approx 0.1$ U, whereas with L_0 = 0.4 μH, the prepulse $\Delta U \approx 0.01$ U. In experiments without the laser the water spark gap operated in the spontaneous breakdown mode. A nonlinear Willite resistance was introduced into the DSL charging circuit to suppress postpulses in the generator-DSL circuit in cases when the spark gap failed to operate or did so imperfectly [6]. The high-voltage diode was provided with a plane anode 8 of diameter 80 mm and cathodes of different configurations were tried: plane, needle, ring, convex cone, and hollow cone.

The current was measured with a noninductive resistance 6 and a Faraday cylinder. The voltage across the DSL, across the input and output of the coaxial transformer, as well as across the diode was measured with the voltage divider 4 described in [7]. In order to study the REB self-focusing we used an x-ray camera obscura with a resolution of no worse than 0.1 mm. The Kal'mar-1 accelerator was equipped with an ion-exchange unit for desalinating water (the total volume of distilled water was 3 m^3 and the resistivity was $2 \cdot 10^6$ Ω•cm).

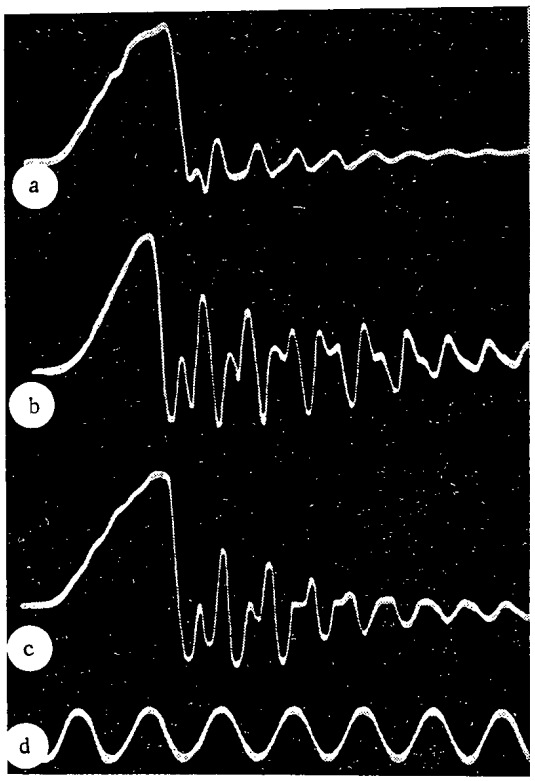

Fig. 4

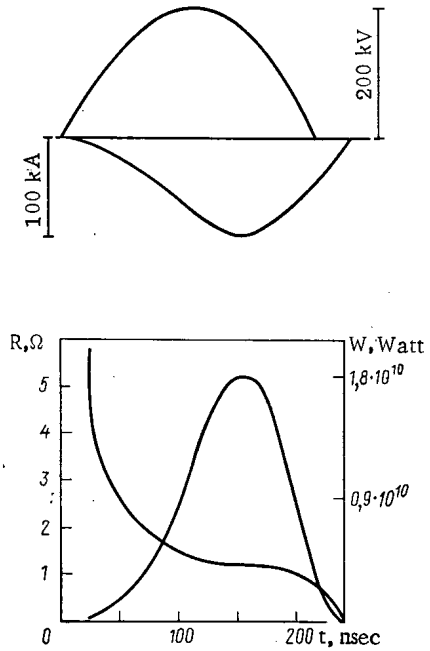

Fig. 5

Fig. 4. DSL voltage amplitude at various cathode-anode gaps in diode: a) $\delta = \delta^*$; b) $\delta < \delta^*$; c) $\delta > \delta^*$; d) calibration f = 1 MHz.

Fig. 5. Current and voltage oscillograms and dependence of diode resistance and electron beam power on time and plane cathode geometry.

Experimental Results. The first series of experiments on the Kal'mar-1 was carried out with a plane stainless steel cathode of diameter 70 mm. The experimental results are shown in Fig. 3. The DSL voltage under these conditions was 0.5 MV. It is seen that in the case of a large prepulse with gaps $\delta \leq 4$ mm breakdown occurred in the diode so that the measured current I differed little from the short-circuit current $I_{s.c.}$. It was possible, however, (with both a small and a large prepulse) to choose a gap δ^* at which the current I was roughly one-half $I_{s.c.}$, as should be the case with impedance matching of line and diode. The fact that the line and diode impedances are matched is confirmed by the data from DSL voltage measurements (Fig. 4), according to which the amplitude of the reflected voltage wave is a minimum when $\delta = \delta^*$. Figure 5 gives the experimental data on the current and voltage as well as on the time dependence of the diode impedance and the output power of the accelerator for a diode with a plane cathode. Under the operating conditions indicated, with the aid of an x-ray camera obscura and by cleavages of material from the anode in some cases we observed self-focusing of REB with a diameter of up to 2 mm.

Further experiments on the Kal'mar-1 accelerator were devoted to finding the conditions for stable REB self-focusing at a given point on the anode. Different authors [8-10] suggested that for this purpose use be made of a partially evaporating Plexiglas cathode at a given moment by means of a laser or plasma injector. The search for the solution to the problem of stable REB focusing was carried out on the Kal'mar-1 on the basis of changes in the configuration of the metallic cathode. All of the cathode configurations enumerated above were tried. The best REB focusing (focal point no greater than 1 mm in diameter) was achieved by using a cathode in the form of a convex metallic cone with a base diameter of 70 mm and an angle of 135° (Fig. 6). X-ray camera-obscura photographs and cleavages of anode material showed that such a cathode ensures REB focusing exactly in the center of the anode with 100% duplication. The current density reaches reaches 10^7 A/cm^2 and the power density, $5 \cdot 10^{12}$ W/cm^2. Good focusing is attained with a prepulse of both 0.01 U and 0.1 U. But because of the high impedance of the diode with a cathode in the form of a convex cone it was

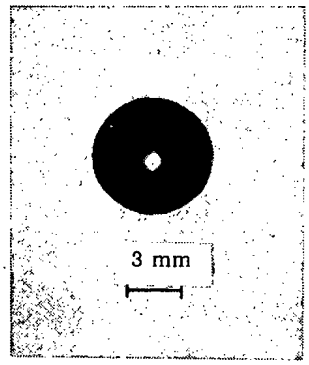

Fig. 6. X-ray camera-obscura photograph.

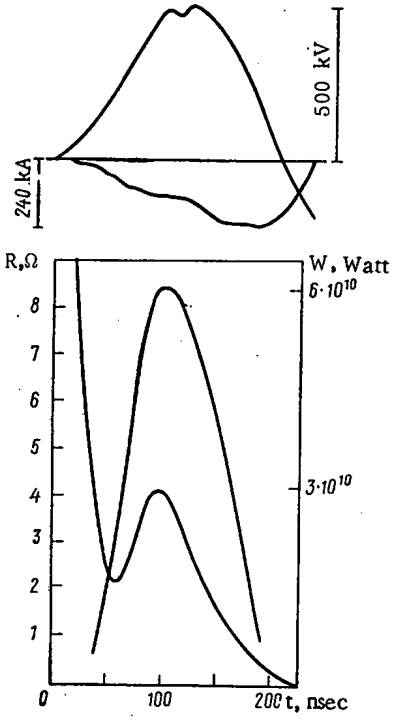

Fig. 7. Current and voltage oscillograms and time dependence of diode resistance and electron beam power under conditions of beam self-focusing.

not possible to achieve matching with the 1.5-Ω output resistance of the line; as a result, the absolute value of the energy contribution to the beam focus did not exceed 1 kJ.

The greatest energy contribution to the REB focal point was attained with a cathode in the form of a hollow metallic cone of diameter 8 mm, first employed in the Angara-1 accelerator [11]. Under these conditions the REB in the Kal'mar-1 was focused at the center of the anode, the current of the focused beam reached 200 kA, and the diameter of the focal point was 2-3 mm. In addition to cleavages from the outside of the anode, formed in one pulse, the REB formed a hemispherical crater of 5 to 5.5 mm deep on the inner surface of the aluminum anode and in some cases pierced an anode made of 6-mm aluminum. According to computer calculations [12], this corresponds to an energy of 3-4 kJ at the REB focal point. It must be emphasized that such an energy contribution to the focal point is attained only under the conditions of a small prepulse (0.01 U) at cathode—anode gaps of 1.5-3.5 mm in the diode for voltages of 500 kV. The current and voltage oscillograms under the conditions of a large energy contribution to the beam at the focal point (small prepulse) as well as the time dependence of the diode impedance and the output power of the accelerator are shown in Fig. 7.

Discussion of Results. The principal result is that the relatively simple circuit design of an electronic accelerator based on a DSL without peaking spark gaps makes it possible to obtain REB with parameters which meet the requirements for performing experiments on the construction of an electronic thermonuclear reactor. According to [13], a REB is absorbed in heavy metals in a layer 5 to 10 μm thick, so that the energy release of 4 kJ at the focal point of the beam in the Kal'mar-1 accelerator corresponds to an "instantaneous" energy release of ∿1 keV per atom of the material, just as in the proposed electronic thermonuclear reactor.

The results of the measurements of the impedance R of the high-voltage diode with large and small prepulses as well as with different cathode configurations are of interest in themselves. It is seen from Fig. 3 that the diode impedance is determined by two factors: the concentration of the preliminary plasma and the length of the cathode–anode gap. With a large prepulse and a given quantity δ the diode impedance is almost twice as small as with a small prepulse. The shape of curves 3 and 4 in Fig. 3 representing the cases of a small and large prepulse in a plane-cathode diode are in good agreement with the relation $R \approx \delta^2$ stemming from the three-halves power law. In both cases, however, the absolute value of R, as in [14], differ from the value calculated from this law by a factor of several and depends on the density of the preliminary plasma. It should be noted that with a large prepulse and gaps of less than 5 mm the diode is quickly short-circuited by the plasma and short-circuit conditions arise. In view of this, it is more convenient to operate with a small prepulse admitting the use of small δ, thus making it possible to obtain high REB currents. When a hollow-cone cathode was used with a small prepulse, we managed to reduce δ to 2-3 mm and to obtain a focused REB current of up to 200 kA. In this case the REB energy calculated by integrating the product of the measured diode current and voltage was 8 kJ, which is in satisfactory agreement with the estimate of an energy contribution of 3-4 kJ from the damage of the anode material.

Finally, it is of interest to note the time dependence of the diode resistance. It is seen from the curves in Fig. 5 that the impedance of a plane-cathode diode changes insignificantly in ∿100 nsec, as a result of which the diode impedance can be matched to the output resistance of the coaxial transformer for a long period. In the focused-beam mode there is some increase in the diode resistance with time (Fig. 7). This effect can apparently be attributed to the anomalous resistance of plasma in turbulent processes associated with the contraction of the beam into a narrow filament. The focused REB current of 200 kA at a voltage of 0.5 MV is in good agreement with the estimate from the formula proposed by Rudakov for a relativistic beam [11],

$$I = 0.3\sqrt{U},$$

where I is the current in MA and U is the diode voltage in MV.

LITERATURE CITED

1. M. V. Babykin and E. K. Zaimovskyi, in: Plasma Physics and Controlled Nuclear Fusion Research, IAEA, Vienna, Vol. 1 (1971), p. 635.
2. L. I. Rudakov and A. A. Samarskii, in: Proceedings of the Sixth European Conference on Controlled Nuclear Fusion and Plasma Physics, Moscow, Vol. 1 (1973), p. 487.
3. I. P. Afonin et al., in: Proceedings of the Seventh Symposium on Engineering Problems of Fusion Research, Knoxville (1973), p. 269.
4. B. A. Demidov and M. V. Ivkin, Prib. Tekh. Eksp., No. 3, 120 (1975).
5. B. A. Demidov et al., Prib. Tekh. Eksp., No. 1, 120 (1974).
6. B. A. Demidov et al., Prib. Tekh. Eksp., No. 3, 37 (1975).
7. B. A. Demidov and M. V. Ivkin, Prib. Tekh. Eksp., No. 2, 115 (1977).
8. V. I. Liksonov, Yu. L. Sidorov, and V. P. Smirnov, Pis'ma Zh. Eksp. Teor. Fiz., 19, 516 (1974).
9. Yu. V. Koba et al., in: Proceedings of the Fifth International Conference on Plasma Physics and Controlled Nuclear Fusion, IAEA, Vienna, Vol. 2 (1975), p. 337.
10. P. Miller et al., Phys. Rev. Lett., 35, No. 14, 940 (1975).
11. M. V. Babykin et al., in: Technology of Intertial Confinement Experiments, IAEA, Vienna (1977), p. 41 (Proc. IAEA Advisory Group Meeting, Dubna (1976)).
12. M. Widner and S. Thomson, Calculations of Anode Witness Plate Damage due to Pinched REB, Sandia Lab. Report Sand-74-351 (1979).

13. S. L. Bogolyubskii et al., Pis'ma Zh. Eksp. Teor. Fiz., 24, 203 (1976).
14. G. A. Mesyats, Generation of High-Power Nanosecond Pulses [in Russian], Sovetskoe Radio, Moscow (1974).

MEASUREMENTS OF DOSE EQUIVALENT OF MIXED RADIATION OUTSIDE THE SERPUKHOV PROTON SYNCHROTRON SHIELD

A. V. Antipov, I. S. Baishev
V. T. Golovachik, G. I. Krupnyi,
V. N. Kustarev, V. N. Lebedev,
and M. Khefert

UDC 539.12.08

A comparison of the readings of radiation monitoring systems, in particular systems employed at various high-energy accelerators, is of practical interest both for the justification of one or another method of measurement, and for further understanding and improvement of the methods.

Comparative measurements of radiation doses outside the Serpukhov proton synchrotron shield were made with the component method (CM) [1] and the "Cerberus" instrument [2, 3] used at the Institute of High Energy Physics (IHEP) and CERN as radiation monitors, and also with the "Sukhona-2" recombination dosimeter described in [4], a linear energy transfer (LET) radiation spectrometer based on a tissue equivalent (TE) proportional counter and a TE ionization chamber, employed at the IHEP for the direct measurements of doses and for calibrating monitoring devices used in radiation fields having an unknown composition and spectrum.

In the CM the dose equivalent is determined by using a rem-meter for neutrons with $E_n <$ 20 MeV [5], a carbon activation $^{12}C(x, xn)^{11}C$ plastic scintillator detector to measure the fluence of particles with E > 20 MeV, and an air-filled ionization chamber with aluminum walls to determine the contribution of gamma rays and charged particles to the total dose. A thermal-neutron detector in a moderator is used as a rem-meter for neutrons with $E_n <$ 20 MeV [1].

The "Cerberus" instrument used as a radiation monitor at CERN in combination with a $^{12}C(x, xn)^{11}C$ detector embodies another variant of the component method (Table 1). The instrument consists of a boron ionization chamber RIC in a cylindrical polyethylene moderator [6], an aluminum ionization chamber AIR with a nonhydrogenous filler, and a tissue equivalent ionization chamber TE.

Two algorithms are indicated for processing the results of the CM (IHEP): the standard [1] and one based on the response matrix [7], taking account of the depth distribution factors. The interpretation of measurements made by the CM (CERN) are described in detail in [8]. All the instruments were calibrated with the same neutron and gamma sources under identical radiation geometry. The factor $35 \cdot 10^{-9}$ rem·cm² [9] was used to transform the fluence of neutrons from a Pu—Be source to the dose equivalent.

Measurements were performed at three points outside the Serpukhov proton synchrotron shield in the experimental room. Outside the upper accelerator shield the main contribution to the dose was from hadrons with $E_h >$ 20 MeV; in the vicinity of channel 11 neutrons with $E_n <$ 20 MeV predominated; near channel 2 high-energy muons made the main contribution.

To interpret the detector readings in terms of the maximum dose equivalent (MADE) [10] the absorbed dose distribution in a phantom and the separate contributions to the dose made by neutrons with energies up to 20 MeV and those above 20 MeV were studied. Figure 1 shows measured absorbed doses and values calculated by integrating the dose distribution [11, 12] over the neutron spectrum [13] in a cubical water phantom 30 cm on an edge irradiated at the point of measurement outside the upper shield of the accelerator. The value of the dose in the absence of the phantom at the point where its center is later located (the open circles in Fig. 1) is taken as a unit. Figure 1 shows that the maximum dose in the phantom is 1.3

Translated from Atomnaya Énergiya, Vol. 46, No. 2, pp. 105-108, February, 1979. Original article submitted February 20, 1978.

 0038-531X/79/4602-0116$07.50

TABLE 1. Configuration of IHEP and CERN Component Methods; Algorithms for Interpreting Their Readings to Determine the Dose Equivalent

IHEP					CERN			
BF_3 (SNMO-5), moderator diam. 30 cm	BF_3 (SNM-3), moderator diam. 25.4 cm	^{103}Rh, moderator diam. 25.4 cm	Al ionization chamber	^{12}C (x, xn) ^{11}C	RIC	AIR	TE	^{12}C (x, xn) ^{11}C
neutron rem-meter					"Cerberus" [8]			
CM-1 [1]: $H=\frac{A_1}{\varepsilon_1}+\frac{A_2}{\varepsilon_{22}}+\frac{A_3}{\varepsilon_{33}}$; CM-2 [7]: $H=\alpha_1 H_1^m+\alpha_2 H_2^m+\alpha_3 H_3^m$; $A_1=\varepsilon_{11}H_1^m+\varepsilon_{12}H_2^m+\varepsilon_{13}H_3^m$; $A_2=\varepsilon_{21}H_1^m+\varepsilon_{22}H_2^m+\varepsilon_{23}H_3^m$; $A_3=\varepsilon_{31}H_1^m+\varepsilon_{32}H_2^m+\varepsilon_{33}H_3^m$					$H=H_n+D_\gamma+H_h$; $A^{RIC}=\varepsilon_\gamma^R D_\gamma+\varepsilon_n^R H_n$; $A^{AIR}=\varepsilon_\gamma^A D_\gamma+\varepsilon_n^A D_n$; $A^{TE}=\varepsilon_\gamma^T D_\gamma+\varepsilon_n^T D_n$; $H_h=C_{hn}F_h$			

Note: H, max. dose equiv. (MADE) of mixed radiation; A, readings of detectors; ε, factors taking account of sensitivity of detectors to various kinds of radiation; H_j^m, MADE of j-th component of radiation; α, depth distribution factors; H_n, D_γ, H_h, D_n, doses of radiation components; F_h, fluence of particles with energies above 20 MeV; C_{hn}, factor to convert fluence of neutrons with energies above 20 MeV to dose equivalent.

times as large as the dose measured at this point without the phantom. This emphasizes the importance of performing phantom measurements for the correct transformation to the MADE. The difference between the experimental data and the calculated results arises from the failure to take complete account of the irradiation conditions in the calculational model: in the first place the contribution to the dose from charged particles and gamma rays was not taken into account, and secondly only the case of an infinite layer irradiated normally from one or both sides was considered. Figure 2 shows the results of calculating the depth distribution of dose equivalents of neutrons with energies up to 20 MeV and those above, performed for these same conditions and under the same assumptions.

Analysis of the phantom distributions of doses shows the importance of taking account of their shapes in interpreting the results of the measurements. At the measuring point outside the upper shield of the accelerator a correction factor of 1.3 must be applied to the readings of the TE ionization chamber; the depth distribution factors for the MADE of neutrons with energies up to 20 MeV and those above are 0.80 and 0.93, respectively.

Table 2 compares the measurements normalized to the same value of the absorbed dose. The factor to convert the carbon detector readings to the equivalent neutron dose with $E_n > 20$ MeV was taken as $2.8 \cdot 10^{-8}$ rem·cm^2 for all methods [14, 15]. The experimental results were processed in the following way: CM-1 by the method of [1] (cf. Table 1); CM-2 by the method in [7] using the response matrix; "Cerberus" by the method in [8]. At the point outside the upper shield the depth penetration factors $\alpha_1 = 0.80$, $\alpha_2 = 0.93$, $\alpha_3 = 1$ were taken into account; the LET spectrometer readings were corrected by a factor of 1.3 to take account of the absorbed dose distribution in the phantom (cf. Fig. 1).

Outside the upper shield of the accelerator where the information on the radiation field is most complete and the MADE is most correctly determined from the point of view of the

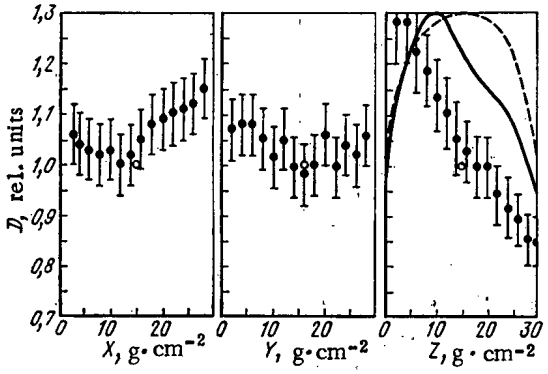

Fig. 1

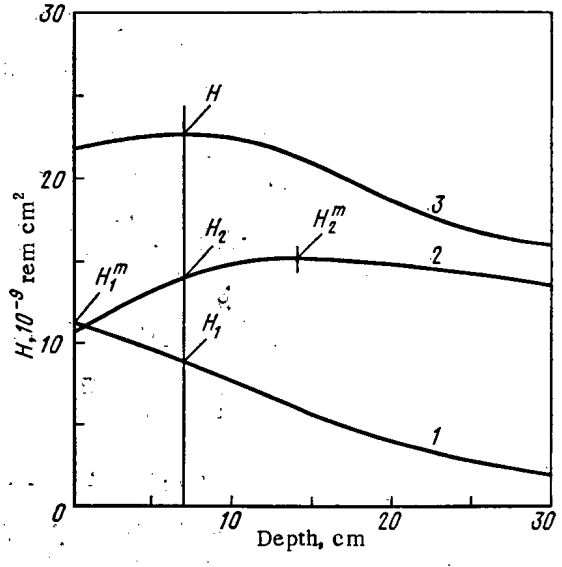

Fig. 2

Fig. 1. Distribution of absorbed dose along the axes of a water phantom 30 × 30 × 30 cm irradiated at the point of measurement outside the upper shield of the accelerator above the axis of the beam (0). The X axis coincides with the direction of the beam and the Z axis is directed upward: 0, absorbed dose in the absence of phantom at the intersection of XYZ axes (taken as a unit). When the phantom is in position its center is at this point; ——) calculated for normal incidence of a broad beam of neutrons with the spectrum given in [13] on a layer of tissue 30 cm thick; ---) the same for irradiation from both sides.

Fig. 2. Distribution of dose equivalent in a layer of tissue 30 cm thick irradiated by a normally incident broad beam of neutrons with an energy spectrum from [13]: 1, 2) Contribution of portions of spectrum with $E_n < 20$ and $E_n > 20$ MeV respectively; 3) total distribution; $H_1^m + H_2^m$, MADE for portions of spectrum; H_1 and H_2, contributions of portions of spectrum to total MADE (H).

recommendations in [10] by using the LET spectrometer, the results obtained are of considerable interest for the analysis of the divergences. It is clear that the use of the standard algorithm CM-1 to interpret the CM at the IHEP leads to overestimates of the MADE reaching 70% for a rem-meter with an SNMO-5 counter in a 30-cm diameter moderator. The CM-2 component method using the response matrix to interpret the detector readings and taking account of the depth distribution factors of the separately detected radiation components at this point gives a result very close to the MADE value of the dose equivalent. The results obtained with "Cerberus" are in somewhat worse agreement with the MADE. This results from the fact that the algorithm for interpreting the detector readings [8] does not take account of all the corrections introduced in the case of CM-2, for example the contribution of particles with energies above 20 MeV to the ionization chamber readings [5, 8]. Analysis of the recombination dosimeter and LET spectrometer differences is complicated by the large differences in detector geometries.

For measurements in the channel 11 area the recombination dosimeter readings were taken as a unit, since in the 0.2-20-MeV range the mean energy of the spectrum of neutrons which make the predominant contribution to the dose was estimated as 0.5 MeV by using the method in [16]. It is improper to use the LET spectrometer in such a neutron spectrum since in this case the particles do not produce a triangular pulse spectrum in the volume of the counter [18-20]. These differences in the values of the total dose are accounted for by the behavior of the response functions of the neutron rem-meters for $E_n < 20$ MeV in the energy range below 0.5 MeV [3, 21, 22] where the functions are considerably above the MADE curve for neutrons recommended by the ICRP [23].

TABLE 2. Comparison of Measurements Outside Shield of Serpukhov Proton Synchrotron

Place of measurement	E_n*, MeV	Methods	H, 10^{-6} rem	D, 10^{-6} rad	$\bar{Q}$	H_1^m	H_2^m	H_3^m	H/H_{LET}
						10^{-6} rem			
Upper shield (hadrons)	5	CM-1 (SNMO-5)	33,6±2,0	10,5±0,7	3,2±0,6	13,2±1,3	15,4±1,5	5,0±0,5	1,71±0,20
		CM-1 (SNM-3)	29,5±1,8	10,0±0,7	3,0±0,3	9,1±0,9	15,4±1,5	5,0±0,5	1,51±0,18
		CM-2 (SNM-3)	24,0±2,0	7,0±0,4	3,4±0,4	9,6±1,0	14,0±1,6	3,3±0,8	1,22±0,16
		"Cerberus"	26,9±1,6	6,4±0,3	4,2±0,3	9,2±0,6	15,2±1,5	2,5±0,3	1,37±0,16
		"Sukhona-2"	28,6±3,0	6,8±0,3	4,2±0,4				1,46±0,21
		LET spectrometer	19,6±2,0	7,0±0,4	2,8±0,3				1
Channel 11 (neutrons)	0,5	CM-1 (SNMO-5)	38,7±3,1	9,9±0,7	3,9±0,3	26,0±3,0	8,2±0,8	4,5±0,5	2,15±0,32
		CM-1 (SNM-3)	21,1±1,2	7,6±0,6	2,8±0,3	8,4±0,8	8,2±0,8	4,5±0,5	1,17±0,16
		CM-2 (SNM-3)	19,1±1,4	5,4±0,3	3,5±0,4	8,0±0,8	6,9±0,9	4,2±0,8	1,06±0,16
		"Cerberus"	29,3±1,5	4,8±0,3	6,1±0,5	17,5±1,1	8,2±0,8	3,6±0,4	1,63±0,22
		"Sukhona-2"	18,0±2,3	5,0±0,3	3,6±0.4				1
		LET spectrometer	10,8±1,1	5,4±0,3	2,0±0,2				0,60±0,10
Channel 2 (muons)	1	CM-1 (^{103}Rh)	6,7±0,6	5,9±0,6	1,1±0,2	0,6±0,1	0,43±0,04	5,7±0,6	1,03±0,13
		CM-2† (^{103}Rh)	6,6±0,9	5,4±0,3	1,2±0,2	0,6±0,1	0,20±0,30	5,9±0,9	1,02±0,17
		"Cerberus"	5,3±0,3	5,2±0,3	1,0±0,1	0,43±0,10	0,43±0,04	4,4±0,3	0,82±0,09
		"Sukhona-2"		6,3±0,3					
		LET spectrometer	6,5±0,6	5,4±0,3	1,2±0,1				

Note: H, total dose equivalent; D^m, absorbed dose; $\bar{Q}$, average quality factor of mixed radiation; H_1^m, H_2^m, MADE of neutrons with E_n < 20 and > 20 MeV respectively; H_3^m, MADE of gamma rays and charged particles. The relative errors of the measurements are indicated everywhere.
*E_n, average energy of fast neutrons (0.2-20 MeV) estimated by method in [16].
†Using the response matrix at this point in the processing, the contribution to the dose from high-energy muons was determined from the charged-particle counter [17] and the dose characteristics of muons from [12].

At channel 2 where more than 90% of the dose is due to high-energy muons, the results of all methods agree within the limits of error of the measurements. The differences in the values of the gamma and charged-particle doses obtained by using the CM-1 and "Cerberus" are accounted for by the difference in thickness of the walls of the aluminum chambers used.

Analysis shows that the main reasons for the divergences of the results in determining the dose equivalent by component methods in radiation fields with a preponderance of high-energy hadrons are the differences in interpretation algorithms; in radiation fields with a soft neutron spectrum the divergences result mainly from differences in the response functions of the rem-meters used. In both cases it is important to take account of the shape of the depth dose distributions of the separately detected radiation components and the differences in radiation spectra and depth dose distributions in calibration and in measurements. Values obtained by the CM may differ from the results of TE detectors because of differences in the principles of operation; the response functions of TE detectors model the dependence of the quality factor on the LET of the radiation, while the response functions of the component method detectors model the dependence of the MADE of particles of a definite type and energy range on their energy.

Thus, by the example of the interpretation of readings of component method detectors using the response matrix it has been shown possible to eliminate the main systematic errors without changing the instrumental part of the method. By using the matrix it is possible to determine the MADE of mixed radiation with an error of no more than 30% in radiation fields with a preponderance of hadrons with E_h > 20 MeV, 10% with a preponderance of neutrons with energies E_n < 20 MeV, and 5% with a preponderance of high-energy muons, which corresponds to the recommendations of the ICRU for practical radiation monitoring, and ensures agreement of the results of monitoring at various accelerator complexes.

In conclusion, the authors thank M. N. Chimankov for help in performing the measurements, and all the co-workers of the Department of Radiation Research of the IHEP for taking part in the discussion of this work and for their remarks and helpful advice.

LITERATURE CITED

1. V. E. Borodin et al., Preprint IHEP 74-131, Serpukhov (1974).
2. M. Höfert, Preprint CERN DI/HP/187, Geneva (1975).
3. M. Höfert, Preprint CERN DI/HP/177, Geneva (1974).
4. V. T. Golovachik et al., in: Proceedings of the International Congress on Protection against Accelerator and Space Radiation, CERN, Geneva, Apr. 26-30, 1971. CERN 71-16, Vol. 1, p. 431.
5. I. S. Baishev et al., in: Proceedings of the Fifth All-Union Conference on Charged Particle Accelerators [in Russian], Vol. 1, Nauka, Moscow (1977), p. 224; Preprint CERN HS-RP/104, Geneva (1977).
6. I. Anderson and J. Brown, Nucleonics, 6, 237 (1964).
7. V. T. Golovachik et al., Preprint IHEP 77-114, Serpukhov (1977).
8. M. Höfert and M. Nielsen, Preprint CERN HP-75-142, Geneva (1975).
9. D. Nachtigall, Health Physics, 13, 213 (1967).
10. E. B. Keirim-Markus (Ed.), Radiation Safety. Papers 19 and 20 ICRU. Atomizdat, Moscow (1974).
11. K. Shaw, G. Stevenson, and R. Thomas, Preprint RHEL/M149, Chilton (1968).
12. V. T. Golovachik et al., in: Proceedings of the Fourth All-Union Conference on Charged Particle Accelerators [in Russian], Vol. 2, Nauka, Moscow (1975), p. 212.
13. E. A. Belogorlov and V. S. Lukanin, ibid., p. 236.
14. M. Höfert and J. Baarli, ibid., p. 207.
15. V. T. Golovachik, V. N. Kustarëv, and V. N. Lebedev, Preprint IHEP 77-91, Serpukhov (1977).
16. D. Hankins, in: Proceedings of the IAEA Symposium on Neutron Detection and Standardization, Vol. 2, IAEA, Vienna (1963), p. 123.
17. A. M. Biskupchuk, S. A. Drugachenok, and G. I. Krupnyi, Preprint IHEP 76-120, Serpukhov (1976).
18. R. Dvorak, Health Phys., 17, 279 (1969).
19. H. Rossi and W. Rosenzweig, Radiology, 64, No. 3, 404 (1955).
20. M. M. Komochkov, Soobshchenie OIYaI R16-10647, Dubna (1977).
21. Robert S. Sanna, Preprint HASL-267, N. Y. (1973).
22. E. A. Kramer-Ageev, in: Problems of Dosimetry and Radiation Shielding [in Russian], No. 6, Atomizdat, Moscow (1967), p. 3.
23. ICRP Publication 21. Data for Protection against Ionizating Radiation from External Sources: Supplement to ICRP Publication 15. Pergamon, Oxford (1973).

OBITUARY

VIKTOR MIKHAILOVICH GUSEV

B. B. Kadomtsev, V. V. Orlov,
M. S. Ioffe, Yu. V. Martynenko,
V. V. Titov, and O. B. Firsov

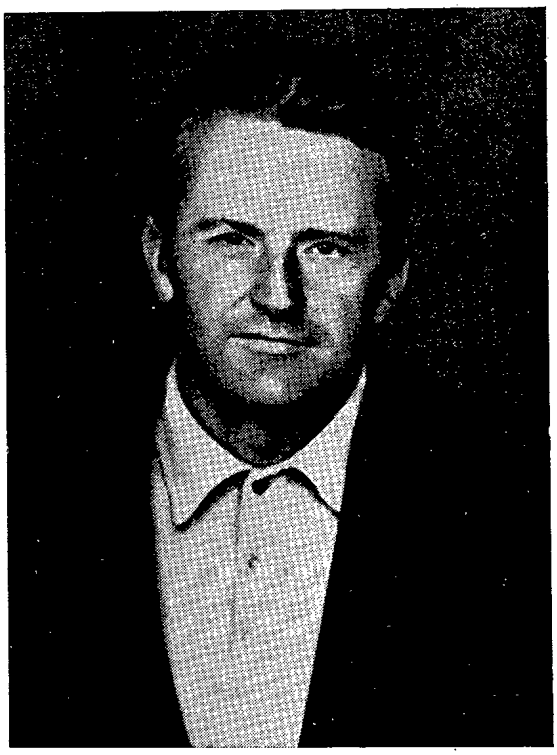

Viktor Mikhailovich Gusev, one of the leading workers of the I. V. Kurchatov Institute of Atomic Energy, an eminent specialist in atomic physics and solid-state physics, and head of the laboratory of the Plasma Physics Division, died on Oct. 6, 1978.

V. M. Gusev was born in 1919. In October 1941 he volunteered for the front while a third-year student in the physics department of Moscow State University. Before going into action, he joined the Communist Party of the Soviet Union. He was seriously wounded during fighting near Leningrad but after a long convalescence he returned to duty and fought until victory. He was decorated with the Order of the Great Patriotic War and many medals. When the war ended he returned to Moscow State University and graduated.

Over the more than 30 years of his scientific career, Viktor Mikhailovich Gusev made a significant contribution to a number of areas of physics. In the early years of his career he participated actively in the solution of the problems of creating atomic engineering in the country. He was awarded a State Prize for this work. A cycle of studies was done under his leadership in 1958-1960 on the implantation of deuterium ions in metals (by means of the $D(d, n)^3He$ reaction) as well as on measurement of the coefficients of metal sputtering by deuterium ions. These investigations served as the beginning of the study of the influence of wall material on the processes of obtaining and confining high-temperature plasma.

V. M. Gusev began working in the I. V. Kurchatov Institute of Atomic Energy in 1960. In 1961 he came out with the initiative for the creation of a new field of science and engineering, viz., ion implantation of semiconductors. Under his leadership and with his direct participation this field underwent an extensive development. He did a large complex of work, ranging from formulation of problems and elaboration of the physical foundations of the

Translated from Atomnaya Énergiya, Vol. 46, No. 2, pp. 109-110, February, 1979.

0038-531X/79/4602-0121$07.50

method of ion implantation to the practical realization of scientific and technological developments. His scheme and design were used to construct the small ILU high-current ion accelerator with mass separation of ions, making it possible to obtain currents of 300-keV doubly and triply charged ions of sufficient magnitude for practical use. Commercial production of ILU units was started in 1966. These accelerators have been set up in many scientific and industrial organizations of our country as well as in Hungary, the German Democratic Republic, and Bulgaria. Initially, this ensured the broad development of work on ion implantation, the introduction of a new progressive method into the fabrication of semiconductor devices based on silicon, especially photoelectric solar energy converters, p—i—n commutation diodes, diodes with various purposes, MOS and bipolar transistors, and integrated circuits. Along with his co-workers, V. M. Gusev was the first to obtain a p—n structure with ion beams in an ILU accelerator; this structure is characterized by high injection properties and a record-breaking intensity of radiation in the visible region of the spectrum.

V. M. Gusev made a great contribution to the development of the physical foundations of ion implantation: he studied the spatial distributions of implanted ions in amorphous and crystalline targets, the law of the generation and annealing of defects in implantation layers, the effect of ion channeling and radiation-stimulated diffusion on the spatial distributions of implanted ions as well as on the electrical properties of these layers.

Viktor Mikhailovich possessed exceptional generosity which was manifested in his sharing his experience with others. Workers of many leading institutes of our country as well as Hungary and the German Democratic Republic have trained in the laboratory he headed. The staff of the TsIFI Ion Implantation Laboratory, headed by I. Dyulai, regards V. M. Gusev as one of those scientists because of which work on ion implantation in semiconductors in Hungary was initiated and developed extensively.

V. M. Gusev used his experience on ion implantation to create radiation-resistant coatings on metals. Investigations, which V. M. Gusev first began, on chemical reactions during the interaction of hydrogen ion beams with various materials have taken on great importance.

In 1974 the scientific interests of Viktor Mikhailovich became linked with a new subject, i.e., working out materials science problems of thermonuclear fusion. He employed the ILU accelerator successfully to simulate the process of interaction of plasma with the first wall of a thermonuclear reactor.

Viktor Mikhailovich recently devoted particular attention to problems pertaining to the processes of synergism under the conditions of large-scale thermonuclear reactors. With his active participation work began on the creation of new devices with which it will be possible to simulate the concurrent action on the wall of various components of the corpuscular radiation of plasma and to imitate the effect of fast neutrons on the materials. Realizing that the conditions in large tokamaks are the closest to those in future reactors, he significantly facilitated the construction of a diagnostic complex for studying the processes of plasma interaction with the wall now being built in the T-10 tokamak.

The untimely death of V. M. Gusev is a great loss for Soviet physics. His bright image will remain in the minds of all who knew him.

DETERMINATION OF THE ABSOLUTE YIELDS OF 43.5-, 74.7-, AND 117.8-keV γ PHOTONS FROM ^{243}Am

Yu. S. Popov, D. I. Starozhukov,
V. B. Mishenev, P. A. Privalova,
and A. I. Mishchenko

UDC 539.163

The isotopic composition of our ^{243}Am sample, as determined by mass spectrometry, was 99.476 ± 0.019% ^{243}Am and 0.524 ± 0.019% ^{241}Am. The half-lives of ^{243}Am and ^{241}Am were taken as $T_{1/2}$ = 7370 ± 40 yr and 432.7 ± 0.7 years, respectively [2].

The americium was purified of plutonium, neptunium, and their decay products in a 1 × 8 Dowex anion-exchange column (25-50 min, column dimensions 3.5 × 10 cm). Pu (IV) and Np (IV) were sorbed successively from a nitric acid solution (8 moles/liter). The plutonium was stabilized in the IV-valence state by heating in nitric acid (8 moles/liter) with hydrogen peroxide. Np (V) was reduced to Np (IV) by hydrazine nitrate in HNO_3 (8 moles/liter) by heating in a water bath for 30 min.

Radiochemically pure americium in the form of a nitric acid solution with no more than a 2% content of inert admixtures by weight was deposited in a layer ∿0.6 μg/cm^2 thick on a ∿110 μm (∿8 μg/cm^2) polyethylene backing. No more than 2 h elapsed from the instant purification was stopped to the end of the measurements. During this time the ^{239}Np activity reached less than 2% of its equilibrium value.

The γ spectrometer included a coaxial 30-cm^3 Ge (Li) detector, an SÉS-03 spectrometer assembly, and a buffer register with output to a BÉSM-4M computer. The spectrometer ensured an energy resolution of 2.5 keV at half-height of the total absorption peak of ^{57}Co at 122 keV. The spectrometer was calibrated with two sets of standard spectrometric γ sources.

The values of the counting efficiencies were calculated from the nuclear physics constants used earlier in [3]. The specific α activity of the ^{243}Am solution was determined by absolute 4πα counting. The values of the absolute γ yield were calculated as the weighted mean of several series of measurements.

The errors of the absolute values of the γ yields were determined mainly by the errors of the areas under the total absorption peaks (2-20%), the errors in determining the absolute α activity of ^{243}Am in the sample (4-5%), and the error in the γ counting efficiency (4-9%). These errors amounted to ∿22, ∿7, and ∿14%, respectively, for 43.5-, 74.7-, and 117.8- keV γ

TABLE 1. γ Yields of ^{243}Am at Various Energies

Quantum yield, quanta/decay, %			Literature
43,5 keV	74,7 keV	117,8 keV	
4±1	69±3	~ 0,5	[4]
5,3*	61*	0,75	[5]
5±1	73±3	0,64±0,25	[6]
5,5±0,3	66±3		[7]
	100†	0,84†	[8]
	59,1±4,0		[3]
5,3±1,2	60±4	0,7±0,1	

*The authors of [5] did not cite the absolute errors of the values indicated.
†Relative measurements.

Translated from Atomnaya Énergiya, Vol. 46, No. 2, p. 111, February, 1979. Original article submitted February 2, 1978.

0038-531X/79/4602-0123$07.50

rays. The values cited for the relative errors correspond to a confidence coefficient of 0.95.

Our results are compared with other published data in Table 1. The values obtained for the quantum yields agree with data in [3, 5, 7].

LITERATURE CITED

1. L. Brown and R. Propst, J. Inorg. Nucl. Chem., 30, 2591 (1968).
2. F. Oetting and S. Gunn, J. Inorg. Nucl. Chem., 29, 2659 (1967).
3. D. I. Starozhukov, Yu. S. Popov, and P. A. Privalova, At. Energ., 42, No. 4, 319 (1977).
4. F. Asaro et al., Phys. Rev., 117, 492 (1960).
5. J. Van Hise and D. Engelkemeir, Phys. Rev., 171, 1325 (1968).
6. B. M. Aleksandrov, O. I. Grigor'ev, and N. S. Shimanskaya, Yad. Fiz., 10, 14 (1969).
7. J. Ahmad and M. Wahlgren, Nucl. Instrum. Methods, 99, 333 (1972).
8. J. Pate et al., Z. Phys., A272, 169 (1975).

ONE MICROWAVE METHOD OF DOSIMETRY FOR PULSES OF PENETRATING RADIATION

V. N. Kapinos and Yu. A. Medvedev

UDC 539.12.08

In an earlier paper [1] we considered the possibility of using microwave methods for the dosimetry of powerful short pulses of penetrating radiation in an air of quite low density when the electron lifetime θ is considerably longer than the pulse duration τ. In another paper [2] we considered possible microwave methods of dosimetry in air of high density when $\tau \gg \theta$. In this case one microwave method is used to measure the electronic conductivity G(t) of the air, which is in a linear relation with the exposure dose M(t) with $10^6 \leqslant M \leqslant 10^{11}$ R•sec^{-1}:

$$M(t) = 137 G(t), \text{ sec}^{-1*}.$$

The time dependence of the exposure dose rate can be determined by measuring any quantity which is proportional to the electronic component of the conductivity of the ionized air. Such a quantity which can be used conveniently is the damping of probing electromagnetic waves during their passage through a transmission line filled with ionized air:

$$\alpha(t) = P_1(t)/P(t),$$

where $P_1(t)$ and $P(t)$ are the intensities of the probing electromagnetic signal at the output of the transmission line with ionized and un-ionized air, respectively.

Using the data of [5], we can show that at sufficiently high electron collision rates $\nu_{eff} \gg \omega$, where ω is the cyclic velocity of the probing field, the wave intensity at the output of a transmission line uniformly filled with a conducting medium is related to the conductivity G(t) of that medium by

$$\Delta\eta(t) = |\ln 1 - \alpha(t)| = \frac{4\pi L}{c} G(t),$$

where L is the length of the transmission line. From this we find that for $10^6 < M < 10^{11}$ R•sec^{-1}, when the ionic component of the conductivity of the air can be neglected in comparison with the electronic component and the process of electron-ion recombination, for low damping $\alpha \ll 1$ we have:

$$M(t) = \frac{137c}{4\pi L} \alpha(t). \quad (1)$$

For experimental verification of the correspondence between the transient shape of the damping pulse (and, therefore, of the pulse of the exposure rate) and the transient shape of

*We used the values given in [3, 4] as constants.

Translated from Atomnaya Énergiya, Vol. 46, No. 2, pp. 112-113, February, 1979. Original article submitted February 22, 1978.

 0038-531X/79/4602-0124$07.50

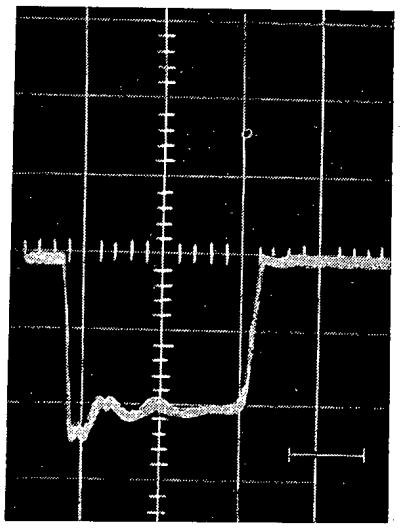

Fig. 1

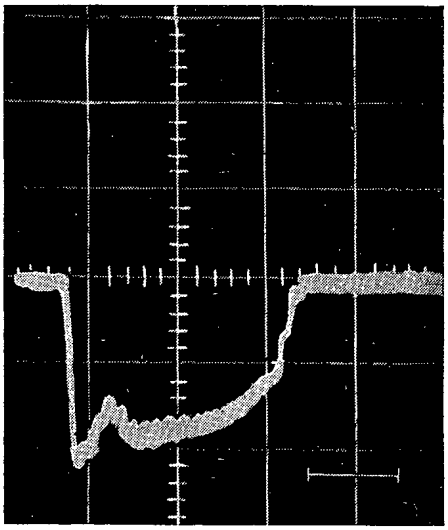

Fig. 2

Fig. 1. Oscillogram of pulse of exposure rate of electron radiation. Scanning rate 1 division/μsec.

Fig. 2. Oscillogram of electron current pulse with energy of 8 MeV. Scanning rate 1 division/μsec.

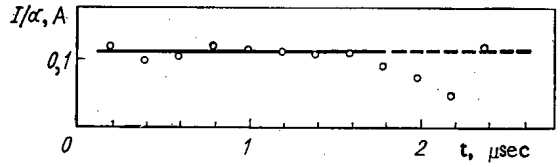

Fig. 3. Time dependence of ratio of electron current I(t) to damping α(t) of rf signal.

the pulse of ionizing radiation we simultaneously recorded the exposure rate pulse (Fig. 1) with a measuring instrument based on a strip line [6] with a length of 3.46 m, operating at a frequency of 900 MHz, and a pulse of electronic current of amplitude 31 mA (Fig. 2) with an energy of the order of 8 MeV by means of a Faraday cylinder. Comparison of the oscillograms shows that the shapes of the exposure rate and electron pulses are practically the same (Fig. 3). It follows from Fig. 3 that during the electron pulse the ratio $I(t)/\alpha(t)$ does not deviate from the value 0.31 by more than 5% (a somewhat larger deviation at the end of the pulse when $t \geqslant 1.8$ μsec was due to insufficiently high time characteristics of the Faraday-cylinder method). The results given in Fig. 3 experimentally confirm the validity of relations of the type of Eq. (1),

$$M(t) = K\alpha(t), \tag{2}$$

where K is a time-independent coefficient which can be calculated as follows. The exposure rate and the number Q(t) of electron pairs formed per cm^3 of air in 1 sec are related by

$$M(t) = Q(t)/2.08 \cdot 10^9, \tag{3}$$

and Q(t) can be written as

$$Q(t) = 7 \cdot 10^{18} \frac{\nu}{l} \frac{I(t)}{S}, \tag{4}$$

where I(t) is the time dependence of the electron-current pulse (in A), S is the area of the cross section of the Faraday cylinder (cm^2), and $\nu/l = 40\ cm^{-1}$ [7] is the number of secondary electrons formed in air per unit length by Compton electrons with a mean energy of the order of 1 MeV.

When Eqs. (2)-(4) are taken into account,

$$K = 3.3 \cdot 10^9 \frac{\nu}{Sl} \frac{I(t)}{\alpha(t)},$$

TABLE 1. Comparison of Results of rf and Thermoluminescence Dosimetry Methods

$M_{max} \cdot 10^{-7}$, $R \cdot sec^{-1}$	$M_{max,t} \cdot 10^{-7}$ $R \cdot sec^{-1}$	$M_{max,t}/M_{max}$
0,84	1,6	1,9
0,92	1,9	2,1
1,6	2,6	1,6
2,1	3	1,4
3,6	6,6	1,8
11	15	1,4
12	22	1,8
20	27	1,4
40	48	1,2

i.e., if it is noted that $I(t)/\alpha(t) = 0.31$ A and $S = 40$ cm^2, we get $K = 140$ c/4πL which is in complete agreement with Eq. (1).

In a number of experiments, along with measurements of the exposure rate by the rf method we measured the radiation dose D_t by the thermoluminescence method with VA-S-220 dosimeters (see Table 1). In the process, the relation

$$M_{max,t} = M_{max} \frac{D_t}{\int_0^\infty M(t)\,dt},$$

where M_{max}, the maximum value of the exposure rate M(t) recorded by the rf method in the same experiment as D_t was recorded, was used to convert the radiation dose D_t integrated over a pulse into the maximum dose rate $M_{max,t}$ obtained by the thermoluminescence method.

The fact that the ratio $M_{max,t}/M_{max}$ is constant within the limits of the error of measurement (the error of measurement is 15% in the case of the rf method and 25% in the case of the thermoluminescence method, the mean value of the ratio is 1.6) for a whole train of pulses attests to the applicability of the rf method for measuring the exposure rate of ionizing radiation, whereas the systematic deviation of these ratios from unity is due to the difference in the method of calibration of the rf and thermoluminescence dosimeters.

LITERATURE CITED

1. Yu. A. Medvedev et al., At. Énerg., 40, No. 1, 53 (1976).
2. Yu. A. Medvedev, N. N. Morozov, and B. M. Stepanov, At. Énerg., 45, No. 5, 374 (1978).
3. Yu. A. Medvedev, B. M. Stepanov, and G. V. Fedorovich, in: Problems of the Metrology of Ionizing Radiation [in Russian], Atomizdat, Moscow (1975), p. 183.
4. V. N. Kapinos et al., Zh. Tekh. Fiz., 44, No. 11, 2432 (1974).
5. V. Golant, Microwave Methods of Studying Plasma [in Russian], Nauka, Moscow (1968), p. 296.
6. A. L. Fel'dshtein, L. R. Yavich, and V. P. Smirnov, Handbook of the Fundamentals of Waveguide Engineering [in Russian], Sovet-skoe Radio, Moscow (1967), p. 214.
7. L. A. Artsimovich, Handbook of Nuclear Physics [in Russian], Fizmatgiz, Moscow (1963), p. 361.

ERRATA

In the article "Liberation of Hydrogen from Aqueous Solutions Irradiated in Nuclear Reactors" by M. V. Vladimirova and I. A. Kulikov (Vol. 45, No. 3, 1978) the formula on p. 927 should read:

$$I_\gamma + f.n = 2.5 \cdot 10^5 \varphi t.n,\ eV/ml \cdot sec.$$

USE OF THERMAL-NEUTRON PROBES TO MEASURE THERMAL-NEUTRON FLUX OF DISTRIBUTIONS

Yu. A. Safin, S. G. Karpechko,
P. G. Afanas'ev, V. I. Nalivaev,
V. B. Pampura, and V. I. Uvarov

UDC 621.039.51

At the present time considerable attention is being paid to the monitoring of energy release in the cores of nuclear reactors for various purposes [1]. Exact and reliable measurement of the neutron fields in reactor cores requires continuous improvement of old experimental methods and development of new ones. In-reactor measurements, however, always entail certain difficulties due to the difficult radiation and thermal conditions under which the detectors must operate, etc. In recent years there has been a great development of instrumental methods of measuring neutron fields, methods in which small fission chambers, electron-emission neutron, self-powered probes, thermal-neutron probes, etc. are used as the primary probes [2-5].

In the present paper we consider the possibility of employing specially developed thermal-neutron probes for operational measurement of the thermal-neutron flux distribution over the height and radius of the core of the IVV-2 research reactor [6]. A TND-A measuring probe was designed and built for this purpose. It consisted of two small thermal-neutron sensing elements: a high-sensitivity (HS) and a low-sensitivity (LS) sensing element [$3 \cdot 10^{-15}$ and $3 \cdot 10^{-16}$ V/(neutrons/cm^2•sec), respectively], placed in an aluminum can with a diameter of 54 mm (the diameter of the working part of the probe was 18 mm). The upper part of the can contains a device for moving the probe over the height of the reactor core in 50-mm steps. The design of the thermal-neutron sensing elements is much like that described in [4, 5]. The transmission line in the sensing element consists of a KTMS high-temperature cable with two aluminum thermoelectrodes. The signal is measured by a PP-63 potentiometer with recording on an EPP-09 M3 potentiometer.

The TND-A probe was installed in one cell of the reactor core and put in the lowest position, after which measurements were made. The probe was then raised 50 mm, fixed in that position, and the signal was measured once again. Measurements were made in succession over the entire height of the cell and the probe was then moved to the next cell. All the measurements were carried out at a reactor power of 200 kW and a water temperature of 35 ± 5°C. The reactor power and the position of the control devices (automatic regulator and shim rods) during the measurements were kept constant. The thermal-neutron flux distribution was measured in 24 reactor core cells: six water "traps," nine fuel assemblies, and nine beryllium slugs. A 0.9-mm copper wire was the indicator. The wire was fastened in special holders made of acrylic plastic. The irradiation was carried out for 10 min at a reactor power of 10 kW. The counting system consisted of a plastic scintillator of the BG type, an FÉU-19M photomultiplier, an amplifier, a power supply, and a PST-100 scaler. The position of the reactor control devices during the measurements of the distribution by the activation method was kept the same as in the measurements with the TND-A probe. The results of the measurements are given in Table 1 and Fig. 1.

It is seen from Table 1 that the signal from the HS sensing elements is almost an order of magnitude greater than that from the LS sensing element whereas the relative distributions of the thermal neutron flux, obtained by these elements, coincide with good accuracy in all the cells of the reactor core. This warrants the conclusion that the LS sensing element can be used to monitor the density of thermal-neutron fluxes $\sim 10^{14}$ neutrons/cm^2•sec. The relative distributions of the copper-wire activity and the readings of the TND-A probe with thermal-neutron sensing elements in the beryllium slug and in the fuel assembly are of the same character and coincide within the limits of error of measurement. In the water trap the results differ somewhat. This difference can be attributed to the different spectral

Translated from Atomnaya Énergiya, Vol. 46, No. 2, pp. 114-115, February, 1979. Original article submitted March 6, 1978.

0038-531X/79/4602-0127$07.50

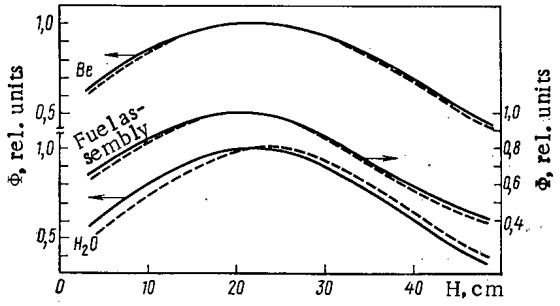

Fig. 1. Relative distribution of thermal-neutron flux, measured with TND-A probe (——) and by activating a copper wire (---) at various distances H from channel bottom.

TABLE 1. Signals from HS and LS Sensing Elements in Some Characteristic Cells of Reactor Core, mV

Distance from end of probe to bottom of reactor core, cm	Fuel assembly		Water trap		Beryllium slug	
	HS	LS	HS	LS	HS	LS
0	4,79	0,55	8,98	1,10	6,13	0,72
5	5,29	0,62	11,90	1,45	6,85	0,80
10	5,94	0,69	14,0	1,72	7,94	0,95
15	6,42	0,72	15,26	1,90	8,80	1,05
20	6,15	0,72	15,45	1,92	8,85	1,07
25	5,56	0,66	14,10	1,74	8,66	1,05
30	4,98	0,58	12,30	1,48	7,83	0,94
35	4,13	0,50	10,14	1,22	6,69	0,80
40	3,19	0,42	7,85	0,94	5,35	0,66
45	2,68	0,34	5,09	0,65	4,15	0,53
50	2,62	0,34	3,37	0,44	3,52	0,48

sensitivities of the copper indicator and the thermal-neutron probe as well as inadequate centering of the probe in the water trap (the coefficient of nonuniformity of the thermal-neutron flux distribution over the radius of the water trap is about 1.2). A similar effect was observed in [7].

The results permit the recommendation of probes with thermal-neutron sensing elements for operational in-reactor monitoring of the thermal-neutron flux distribution in the range from $5 \cdot 10^{10}$ to about 10^{14} neutrons/cm^2·sec.

LITERATURE CITED

1. I. Ya. Emel'yanov et al., Control and Safety of Nuclear Power Reactors [in Russian], Atomizdat, Moscow (1975).
2. A. B. Dmitriev and E. K. Malyshev, Neutron Ionization Chambers for Reactor Engineering [in Russian], Atomizdat, Moscow (1975).
3. V. B. Klimentov, G. A. Kolchinskii, and V. V. Frunze, Activation Measurements of Neutron Fluxes and Neutron Spectra in Nuclear Reactors [in Russian], Standarty, Moscow (1974).
4. I. Ya. Emel'yanov et al., At. Énerg., 30, No. 3, 275 (1971).
5. J. Boland, Monitoring Instruments for Nuclear Reactors [Russian translation], Atomizdat, Moscow (1973).
6. A. P. Zyryanov et al., in: Radiation Safety and Protection of Atomic Power Plants [in Russian], No. 2, Atomizdat, Moscow (1976), p. 110.
7. S. S. Lomakin et al., At. Énerg., 30, No. 3, 301 (1971).

TWO-DIMENSIONAL MODELING OF THE FUEL ASSEMBLIES OF HIGH-TEMPERATURE GAS-COOLED REACTORS

M. D. Segal' and V. I. Khripunov

UDC 621.039.517.5

High-temperature gas-cooled nuclear reactors (HTGR) [1] are becoming very important in power engineering and for producing high-potential heat. Such reactors are characterized by relatively high calorific intensity combined with long-term resources and strict requirements on the limiting fuel temperature. In this connection it is quite important to equalize the temperature fields of the fuel elements and the working substance, especially in the case of cluster-type reactors.

As a result of the slug effect and perturbations contributed by the regulating elements, etc., spatial nonuniformities can develop in the heat release field of the fuel assemblies (consisting of a large number of fuel-element rods) of such reactors. This nonuniformity gives rise to local overheating of the working substance and the fuel and therefore causes a reduction in the parameters of the fuel assemblies. A way to raise the output parameters of such assemblies that appears promising is the two-dimensional modeling of the energy-release field of fuel concentrations. Here we are of course speaking only of zone modelling, since it evidently would be technically impossible to individually choose concentrations of fuel for each fuel element (the Gulf General Atomic (U.S.A.) reactor uses assemblies containing 270 fuel elements). Physical modeling methods were discussed by Vinterberg [2] and further developed and experimentally justified by others [3-5]. It has been shown that changes in the concentration and the fuel-to-moderator volume ratio may possibly have a considerable effect on the distribution of energy-release sources in various systems. In many cases, the condition that the temperature at the surface or the center of a fuel element is kept constant reduces to an equalization of the density of energy release over the volume.

The optimization of these parameters with respect to the reactor as a whole is based on certain simplifying assumptions (a one-dimensional geometry, the few-group approach, etc.). In modeling a fuel assembly, it is also necessary to take into account the mixing of the working substance and the local characteristics of the energy distribution. The basis of the present approach consists in simultaneously using a multidimensional Monte Carlo neutron-physics calculation [6] and a heat-hydraulic calculation [7] to enable a rather effective equalization of the temperature fields of the fuel elements and the gas coolant. The temperature fields were calculated in three dimensions for a homogeneous heat-releasing medium, using a BÉSM-6 computer and a program which has been previously discussed [8].

In order to fix the spatial energy distribution in the inhomogeneous medium within the framework of the Monte Carlo method, a local estimate of the flux in extended (filament) mathematical detectors was proposed. For each collision of a neutron within the volume of the system, the contribution to the energy release is proportional to the integral

$$q \sim (1/A) \int_0^X \exp\left(-\sqrt{x^2+A^2}\right)/\sqrt{x^2+A^2}\, dx, \qquad (1)$$

where q is the contribution to the energy release due to the scattering of the neutron at a point, A is the optical distance between the detector and the point at which the neutron is scattered, and X is the optical length of the detector. In a correlated calculation for a large number of detectors, certain properties of the estimate (a single-parameter dependence on A which is due to rapid convergence with respect to the upper limit) make it possible to reduce the error in the local energy-release estimate in an r, φ geometry down to 3-5%. A relationship for the fuel concentration in the modeling zones was selected on the basis of the equality of the average values of the energy release in each zone. The constraint on the maximum allowable fuel temperature was represented by the equation

Translated from Atomnaya Énergiya, Vol. 46, No. 2, pp. 115-117, February, 1979. Original article submitted March 13, 1978.

0038-531X/79/4602-0129$07.50

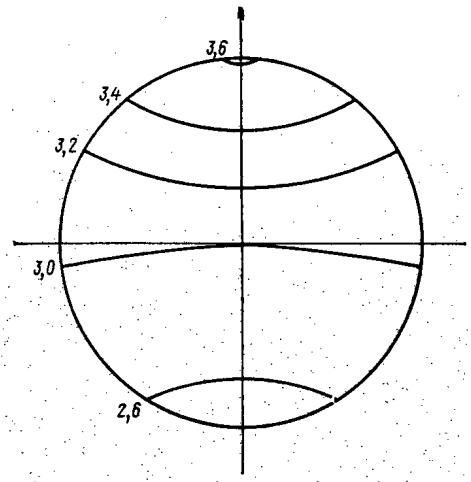

Fig. 1

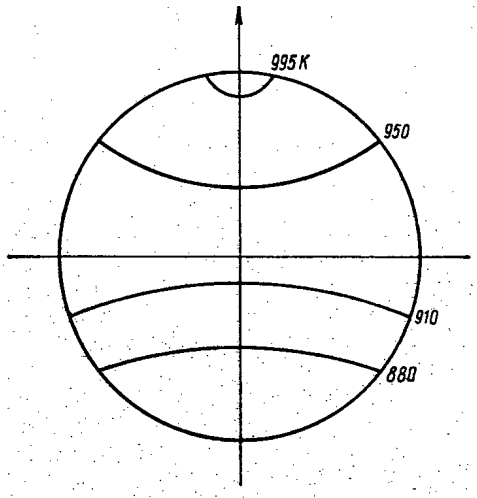

Fig. 2

Fig. 1. Lines of constant energy release (in arbitrary units) for an unmodeled fuel assembly.

Fig. 2. Isotherms of the gas at the exit of an unmodeled assembly.

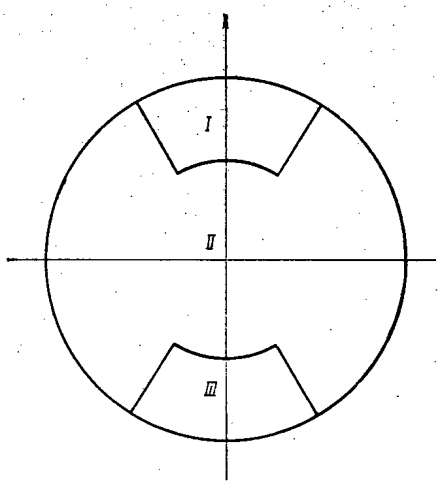

Fig. 3. Modeling zones.

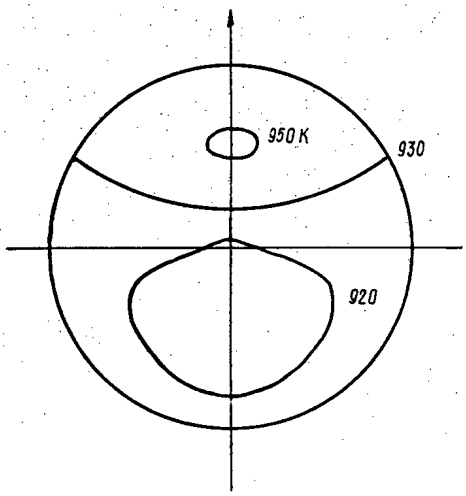

Fig. 4. Isotherms of the gas at the exit of a modeled assembly.

$$\int_{S_i}\int_{E} C_i(E)\,\Phi_i(r,\varphi,E)\,dE\,dS_i \Big/ \int_{S_i}\int_{E} \Phi_i(r,\varphi,E)\,dE\,dS_i = \text{const}, \qquad (2)$$

where S_i is the area of the modeling zone, E is the energy of the neutrons, C_i is the fuel concentration in the modeling zone, and Φ_i is the neutron flux in the modeling zone.

It should be noted that in the case of assemblies where the energy release fields have high gradients, it is desirable to model the fields on the basis of the equality of the maximum values of the energy release in the modeling zones. The choice of the number and configurations of the modeling zones is extremely important. Using a linear programming method described in [9], the zone configurations were chosen with respect to a certain energy-release field for a fixed number of fuel concentrations in a fuel element. The coefficient of nonuniformity of the energy release over the cross section of the modeling zones was minimized in the process. The zone configurations and the relation for the fuel concentration in them were finally corrected, taking into account the hydrodynamics and the local characteristics of the energy distribution.

The variational theory proposed in [10] can be applied to the problem of estimating the energy release to show that the correction to the exact value due to a change in the configuration of the modeling zone is of second order. Only two iterations were needed in a numerical

experiment to keep the error in the energy release distribution from exceeding 2-3%.

As an illustration of this method, we shall consider the modeling of a fuel channel with a hypothetical energy release field.

Characteristics of the channel	
Power, MW	1.5
Helium:	
consumption, kg/sec	0.85
intake temperature, °C	300
Number of fuel elements in a cassette	270
Diameter of the fuel element, mm	7.2

The hypothetical field of energy release is shown in Fig. 1, and the corresponding isotherms of the gas at the exit are shown in Fig. 2. Three fuel concentrations were used in modeling this channel. The configuration of the modeling zones is shown in Fig. 3. Figure 4 shows the isotherms of the gas at the exit which correspond to the new energy release field. The fuel concentrations in the zones are in the ratio $C_I/C_{II}/C_{III} = 0.848/1/1.19$. The nonuniformity of the exit gas temperature field thus decreased from 1.27 to 1.13 (with respect to the heating). This made it possible to increase the power of the fuel assembly by almost 10%.

It should be noted that the proposed method eliminates the radial and azimuthal nonuniformity of the energy release. In so doing, the number of fuel elements with different concentrations of fuel is no larger than in the case of radial modeling.

LITERATURE CITED

1. D. Bedenig, Gas-Cooled High-Temperature Reactors [Russian translation], Atomizdat, Moscow (1975).
2. F. Vinterberg, in: Transactions of Second Geneva Conference, FRG Proceedings [in Russian], No. 1055, Atomizdat, Moscow (1959), p. 453.
3. N. N. Ponomarev-Stepnoi and E. S. Glushkov, At. Énerg., 11, No. 1, 19 (1961); 12, No. 5, 415 (1962); 20, No. 6, 478 (1966).
4. N. N. Ponomarev-Stepnoi, E. S. Glushkov, V. I. Nosov, and S. N. Barkov, ibid., 28, No. 1, 58 (1970).
5. A. P. Rudik, Optimal Distribution of Nuclear Fuel [in Russian], Atomizdat, Moscow (1974).
6. D. V. Markovskii, V. I. Khripunov, and G. E. Shatalov, A Multigroup Calculation of Heterogeneous Reactors by the Monte Carlo Method [in Russian], Institute of Atomic Energy Preprint No. 2959, Moscow (1977).
7. M. D. Segal', Calculation of the Temperature Fields in an r,φ,z Geometry in Porous Media with a Spatial Nonuniformity of Heat Release [in Russian], Institute of Atomic Energy Preprint No. 2845, Moscow (1977).
8. M. D. Segal', A Brief Description and Instructions for the Use of a Program for Calculating Temperature and Velocity Fields [in Russian], Institute of Atomic Energy Preprint No. 2785, Moscow (1977).
9. C. Tzanos, Trans. Am. Nucl. Soc., 24, 195 (1976).
10. G. I. Bell and S. Glasstone, Nuclear Reactor Theory, Van Nos Reinhold (1970).

MAXIMUM RATE OF EMISSION OF LONG-LIVED γ-EMITTING AEROSOLS ALLOWABLE UNDER ATOMIC POWER STATION STANDARDS AND CONTROL

G. G. Doroshenko, E. S. Leonov,
Z. E. Lyapina, V. A. Fedorov,
and K. N. Shlyagin

UDC 543.52+614.73

In order to determine the radial distribution of ^{60}Co activity in the soil near an NVAÉS, natural measurements were taken at radial distances of 0.5, 1, 2, 3, and 5 km; the values obtained for the specific activity of ^{60}Co were 5, 4, 2, 1, and 0.5 mCi/km^2, respectively. Its total activity within a radius of 5 km was estimated by integration to be 97 mCi [1]. This value is in agreement with the result (113 mCi) obtained from measurements of the total emission during a 10-yr period of operation of the NVAÉS after taking into account the physical decay of the ^{60}Co.

Measurements of layered samples were used to estimate the distribution of ^{60}Co with respect to depth in the earth. It was approximately exponential, with a characteristic inverse length K = 0.5 cm^{-1}. These data could be used to calculate the exposure dose rate at a distance h = 1 m from the surface of the earth, using the equation [2]

$$P(E_0, h, K) = 1.44 \cdot 10^3 E_0 \gamma \nu f(E_0, h, K) F, \quad (1)$$

where E_0 is the photon energy in MeV; γ, electron conversion factor in cm^{-1}; ν, quantum yield in photons/decay; F, specific activity in mCi/km^2; and f, a tabulated function.

The values of dose rate P calculated for the above points are equal to 0.86, 0.69, 0.34, 0.17, and 0.086 mrd/yr, which are less than 1% of the natural radiation background for this region [3].

On the basis of the experimental data, and with the assumption that the distribution of specific activity F(R) remains the same for various values of the accumulated activity Q_0, a nomogram was constructed (see Fig. 1) in which the daily emission q is connected with the equilibrium quantity of total activity by the equation

$$Q_0 = qT_{1/2}/\ln 2. \quad (2)$$

It follows from the nomogram that in case the emission is due solely to ^{60}CO, an allowable rate of emission of long-lived aerosols of 0.5 Ci/day [4] leads to unjustifiably high dosages in the districts close to the atomic electric power station. Realistic emission levels from an NVAÉS correspond to 0.04 mCi/day and the maximum dose rate in the locality is at most 1 mrd/yr at a distance of 0.5 km from the atomic electric power plant. On the basis of this, it is proposed that the allowable operating level of ^{60}Co emission rate from an atomic power plant be set such that its equilibrium activity should not exceed 100 mCi; i.e., the quantity accumulated in the environment near the NVAÉS. Since it is difficult to measure a small allowable emission rate and is unnecessary for operative control, it is proposed instead of daily to set up a monthly allowable ^{60}Co emission rate of 1.2 mCi/month for a water-modulated—water-cooled power reactor with a total output of 1455 MW (electric) (which scales to 0.9 mCi/month for 1000 MW (electric)).

It is not possible to study other similar long-lived nuclides because of the smallness of the quantities being measured against the background of natural activity and global fallout. The maximum yearly emission of ^{134,137}Cs, ^{141,144}Ce, ^{103,106}Ru, ^{54}Mn, ^{95}Zr, ^{95}Nb, ^{51}Cr, and ^{110m}Ag for four NVAÉS units amounts to ∿460 mCi/yr or 1.26 mCi/day, which is 400 times as small as the maximum allowable emission. Assuming that the distribution of long-lived nuclides in the neighborhood of an atomic power plant is no different from the measured ^{60}Co distribution, and taking the maximum emission of each of the above radionuclides into account,

Translated from Atomnaya Énergiya, Vol. 46, No. 2, pp. 117-118, February, 1979. Original article submitted March 15, 1978.

 0038-531X/79/4602-0132$07.50

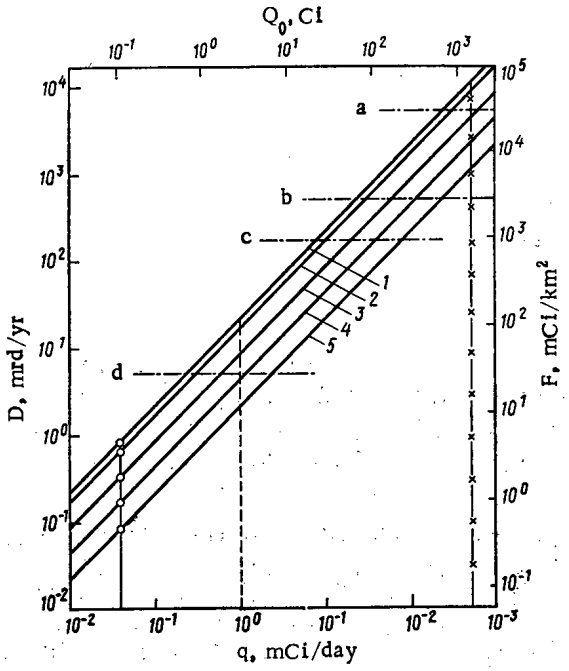

Fig. 1. A nomogram constructed according to data obtained from measurements on a NVAÉS. a, b, c, d) exposure dosages of 5, 0.5, 0.17, 0.005 rd/yr, respectively; 1, 2, 3, 4, 5) distance from the atomic energy power plant of 0.5, 1, 2, 4, 5 km; emission rate, mCi/day: ——) 0.04; — — —) 1; —×—×) 500; ○) experimental results.

we estimated the exposure dosage rate at a distance of 0.5 km from an NVAÉS. The calculation was carried out for an equilibrium activity of each radionuclide accumulated in the environment using Eqs. (1) and (2), with a result of 7.5 mrd/yr.

We see in this way that even when the activity level in the environment reaches equilibrium, including ^{137}Cs ($T_{1/2}$ = 30 yr), the exposure dosage rate near an atomic energy power plant is at most 5% of the natural background and is 0.5% at a distance of 5 km from the atomic energy power plant in a calculation assuming an output level of 1000 MW (electric). A rate of emission of long-lived γ-emitting aerosols of 460 mCi/yr or 300 mCi/yr for an output of 1000 MW (electric) may be taken as an approximate figure for purposes of setting a standard for the appropriate operating level of allowable emission rate.

LITERATURE CITED

1. G. G. Doroshenko, E. S. Leonov, K. N. Shlyagin, and V. A. Fedorov, in: Proceedings of the COMECON Scientific—Technical Conference, Prague (1976), pp. 24-31.
2. G. A. Fedorov, I. E. Konstantinov, and V. V. Pavlov, in: Dosimetry and Radiation Shielding [in Russian], No. 7, Moscow (1967), pp. 87-98.
3. E. I. Vorob'ev et al., At. Énerg., 43, No. 3, 374 (1977).
4. Safety Rules for Atomic Electric Power Plant Design [in Russian], Ministry of Public Health of the USSR, Moscow (1969).

A CONTACTLESS METHOD OF STUDYING THE THERMAL STATE OF FUEL ELEMENTS DURING IRRADIATION

V. N. Murashov, L. S. Kokorev, and V. V. Yakovlev

UDC 621.039.517.5

Previous studies [1-4] have shown that the thermophysical properties of fuel elements can undergo considerable change during irradiation. The results of Asamato [5] and MacDonald and Weisman [6] indicate that during the initial period of irradiation (100-300 h) the temperature at the center of the fuel elements rises, and then drops during the subsequent period of operation at a constant output level.

The authors of the present study propose a method of contactless control of the thermal state of fuel elements during a process of prolonged operation. The method is based on the use of nonstationary regimes with intermittent changes of output, interruptions, actuations of the emergency protection of the reactor, and fluctuations of output. A neutron flux detector at the TVS and a thermocouple in the coolant flux at the exit of the active zone serve as detecting elements. A relation between the perturbations of the coolant temperature (u) and the perturbations of the linear thermal load of the TVS (S) is obtained by solving the system of energy equations for the coolant and fuel element. The solution is obtained in the form

$$u(t)=\exp(-az)\int_0^t u(0,\ \vartheta)\exp[-m(t-\vartheta)]\sqrt{lz/(t-\vartheta)}\ I_1[2\sqrt{l(t-\vartheta)z}]\,d\vartheta$$

$$+M\int_0^z \exp[-a(z-\xi)]\int_0^t S(\xi,\vartheta)\exp[-m(t-\vartheta)]\,I_0[2\sqrt{l(t-\vartheta)\xi}]\,d\vartheta\,d\xi, \qquad (1)$$

where $m = \Pi/(CR)$, R is the integral coefficient of the thermal resistance between the fuel and the coolant (including the thermal resistance of the fuel, the contact clearance between fuel element and jacket, and the convection heat exchange), C is the heat capacity per unit length of the fuel element in the TVS, Π is the perimeter of heat exchange of the fuel elements in the TVS, $a = \Pi/RG_{z}lC_{z}l$, $G_{z}l$ and $C_{z}l$ are the mass consumption and heat capacity of the coolant, $l = am$, $M = m/G_{z}lC_{z}l$, and I_0 and I_1 are Bessel functions of imaginary argument.

It follows by definition that m is proportional to the integral thermal conductivity from the fuel to the coolant.

The required parameter here is $m = 1/\tau$, i.e., the reciprocal of the temperature field period of relaxation τ. The relationship between the relaxation period and the thermophysical properties of the fuel element was found in [4]. They found the unknown parameter by minimizing the mean squared deviations during time T between the calculated (u) and experimental (u_e) relations for the perturbations of coolant temperature at the TVS exit, using Eq. (1) to calculate u. The method of least squares can be used to obtain and equation for determining m:

$$\int_0^T (u_e-u)\frac{du}{dm}\,dt=0, \qquad (2)$$

which was solved on a computer.

The experimental measurements were made on an assembly with fuel elements of the water-moderated—water-cooled power reactor type, in an MR reactor. A TVS with 18 fuel elements was equipped with thermocouples at the entrance and exit and a thermal neutron detector so that the variations in the energy release could be observed. Figure 1 shows the results of

Translated from Atomnaya Énergiya, Vol. 46, No. 2, pp. 118-120, February, 1979. Original article submitted March 27, 1978.

 0038-531X/79/4602-0134$07.50

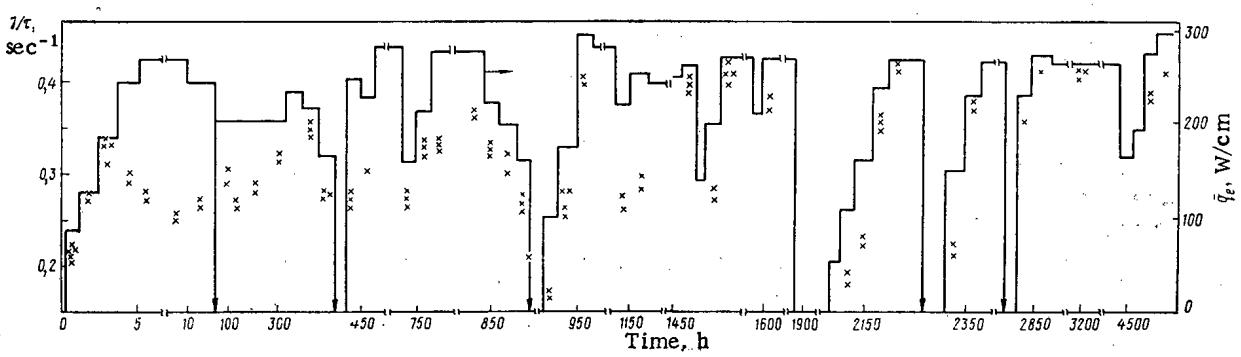

Fig. 1. Variation of the relaxation period (×) and of the linear thermal load averaged over the TVS $\bar{q}_\ell$ (solid curve) during irradiation.

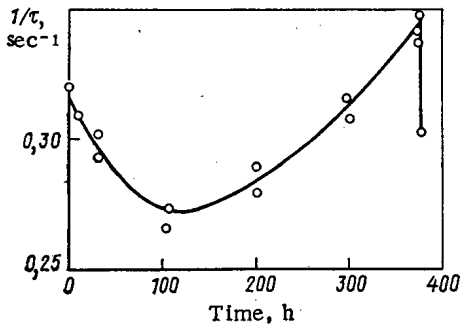

Fig. 2

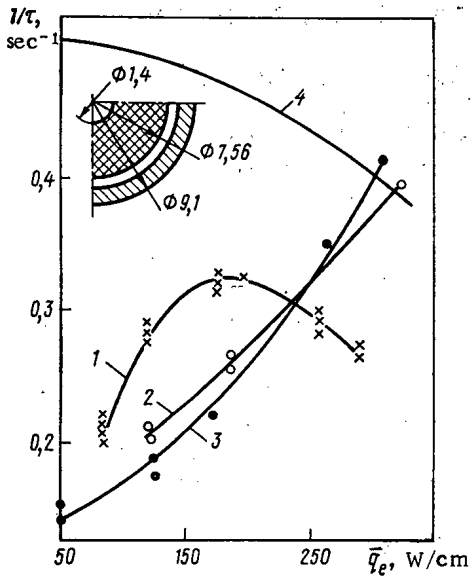

Fig. 3

Fig. 2. Variation of the period of relaxation of the temperature field during the initial stages of the irradiation.

Fig. 3. Dependence of the period of relaxation on the linear thermal load of the fuel element. 1) starting dependence; 2) 850 h of irradiation; 3) 2150 h of irradiation; 4) calculated curve.

the measurements of m during a period of over 4500 h from the start of the irradiation. During the operation the output was repeatedly changed and the emergency protection actuated (indicated by the arrows). As indicated by the experimental data, the thermal conductivity of a fuel element drops during the first 100 h but subsequently increases (Fig. 2). The data shown are for a linear thermal fuel element load averaged over the TVS $\bar{q}_\ell \sim 200$W/cm. Actuation of the emergency protection after ∿380 h results in a sharp reduction in the conductivity, and with subsequent operation at constant output the conductivity increases to a certain stable level. It follows from Fig. 3 that during operation the period of relaxation drops by a factor ∿1.4, corresponding to a temperature drop at the center of a WMWR-1000 type fuel element from 2100 to 1600°C for a thermal load of 500 W/cm. Under prolonged operation in the high thermal load region, the fuel element reaches a state in which the thermal resistance of the fuel-jacket contact becomes negligibly small in comparison with the total thermal resistance (curve 4 in Fig. 3). These results are in qualitative agreement with the data on the behavior of oxide fuel [1-6].

LITERATURE CITED

1. B. Lastman, Radiation Phenomena in Uranium Dioxide [Russian translation], Atomizdat, Moscow (1964).

2. I. G. Lebedev et al., in: Problems of Atomic Science and Engineering. Series "Radiation Materials Science, Methods and Techniques of Irradiation" [in Russian], No. 6, Dimitrovgrad (1975), p. 19.
3. Kh. Khoffman, At. Tekh. Rubezhom, No. 4, 19 (1976).
4. V. N. Murashov et al., A Design Calculation and Experimental Study of the Center Temperatures in Uranium Dioxide Fuel Elements, Institute of Atomic Energy Preprint No. 2936, Moscow (1978).
5. R. Asamoto et al., Center Temperature Measurements of Mixed Oxide Fuel from Zero to $3 \cdot 10^3$ MWd/Te, GEAP-13603 (1970).
6. P. MacDonald and J. Weisman, Nucl. Technol., 31, No. 3, 357 (1976).

DISTRIBUTION OF TRITIUM IN TECHNOLOGICAL SYSTEMS OF THE NOVOVORONEZH NUCLEAR POWER PLANT

D. P. Broder, L. I. Golubev,
V. M. Ilyasov, A. I. Lur'e,
B. N. Mekhedov, I. R. Nurislamov,
L. N. Sukhotin, L. P. Kham'yanov,
and V. M. Arkhipkin

UDC 621.039.524.44

The radioactive hydrogen isotope tritium presents a definite radioactive danger to nuclear power plant personnel and to the population. It is formed as a result of the activation of the coolant and impurities in it, and also by ternary fission of the nuclear fuel.

The principal state of tritium in water coolant is HTO, which does not differ chemically from ordinary water and cannot be separated by special water purification devices. Therefore as a result of leaks in the primary loop tritium is freely propagated through the technological systems of the power plant and escapes into the service rooms and into the environment. In rooms with tanks of pure distillate for the primary loop where the total radioactivity (without tritium) is below $3 \cdot 10^{-10}$ Ci/liter, the concentration of tritium can reach 10^{-5} Ci/liter. Therefore practically the total dose to personnel coming into close contact with this water is determined by tritium.

To estimate tritium doses and emission during a run it is necessary to know the tritium concentration in the technological loops of the power plant. To find this concentration we used a mathematical model which takes account of the connection of the loops of the third and fourth units of the Novovoronezh Nuclear Power Plant with the feedwater and discharge system.

For steady-state water exchange (Fig. 1) the dilution ratio of the coolant in the feedwater system by uncompensated water can be assumed constant. The concentration of tritium in the coolant of the primary loop can be calculated by solving the tritium balance equation in the technological system of the primary loop:

$$\frac{dC}{dt} = \overline{\Sigma_0 \Phi} \left(1 - \frac{t}{T}\right) \frac{V_c}{V_p} - [\lambda + \omega (1 - \varepsilon)] C, \quad (1)$$

where C is the concentration of tritium in the coolant, Σ_0 is the macroscopic cross section for the formation of tritium in the reaction $^{10}B(n, 2\alpha)^3H$ at the beginning of the run, $\overline{\Sigma_0 \Phi}$ is the reaction cross section averaged over energy, T is the time of a run, $\Sigma_0[1 - (t/T)]$ corresponds to the decrease in the concentration of boron in the coolant to zero at the end of the run, V_p is the volume of coolant in the primary loop of the third and fourth units, V_c is the volume of coolant in the core, $\lambda = 1.53 \cdot 10^{-4}$/day is the tritium decay constant, $\omega = (3.9 \pm 0.7) \cdot 10^{-2}$/day is the fraction of the coolant removed per day from the primary loop system, $\varepsilon = 0.05 \pm 0.01$ is the dilution ratio of the coolant in the feedwater system by uncompensated water. Since $\lambda \ll \omega$ we neglect the decay of tritium. The solution of Eq. (1) for a second and subsequent runs can be written in the form

Translated from Atomnaya Énergiya, Vol. 46, No. 2, pp. 120-122, February, 1979. Original article submitted March 27, 1978.

 0038-531X/79/4602-0136$07.50

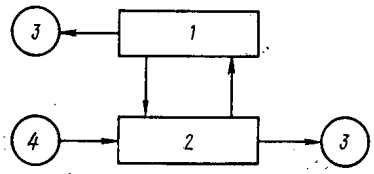

Fig. 1. Equivalent flow diagram of water exchange: 1) Primary loops of third and fourth units; 2) feedwater and discharge system; 3) leakage channels; 4) channel for entrance of uncompensated water.

TABLE 1. Concentration of Tritium in Water Supply Systems, Ci/liter

Unit	Av. thermal power of reactor, MW	Primary loop	Tanks of contaminated condensate	Drainage and discharge system	Secondary loop
I	755	$4{,}1\cdot10^{-6}$*	—	$0{,}8\cdot10^{-6}$	$<4\cdot10^{-7}$
II	1275	$5{,}3\cdot10^{-5}$	$1{,}2\cdot10^{-5}$	$1{,}8\cdot10^{-6}$	$<<4\cdot10^{-7}$
III	1376	$4{,}4\cdot10^{-5}$	$3{,}1\cdot10^{-5}$	$2{,}8\cdot10^{-6}$	$<<4\cdot10^{-7}$
IV	1467	$6{,}7\cdot10^{-5}$	$3{,}1\cdot10^{-5}$	$2{,}8\cdot10^{-6}$	$<4\cdot10^{-7}$

*The reactor of the first unit has only rod control of power.

$$C(t)=\frac{\overline{\Sigma_0\Phi}}{\omega(1-\varepsilon)}\frac{V_C}{V_p}\left\{1-e^{-\omega(1-\varepsilon)t}-\frac{1}{T}\left[t-\frac{1}{\omega(1-\varepsilon)}\right]\right\}. \tag{2}$$

The specific activity of the tritium in the water of the primary loop is

$$A(t)=\frac{\overline{\Sigma_0\Phi}V_C\lambda}{3{,}7\cdot10^{10}V_p\omega(1-\varepsilon)}\left\{1-e^{-\omega(1-\varepsilon)t}-\frac{1}{T}\left[t-\frac{1}{\omega(1-\varepsilon)}\right]\right\}. \tag{3}$$

The errors in the calculation of the specific activity resulting from the inaccuracies in the determination of ω and ε are found from the equations

$$\left(\frac{dA}{A}\right)_\omega=\left\{1+\frac{\left[\omega(1-\varepsilon)te^{-\omega(1-\varepsilon)t}-\frac{1}{T\omega(1-\varepsilon)}\right]}{1-e^{-\omega(1-\varepsilon)t}-\frac{1}{T}\left(t-\frac{1}{\omega(1-\varepsilon)}\right)}\right\}\frac{d\omega}{\omega}; \tag{4}$$

$$\left(\frac{dA}{A}\right)_\varepsilon=\left\{\frac{\varepsilon}{1-\varepsilon}-\frac{\left[\omega\varepsilon te^{-\omega(1-\varepsilon)t}+\frac{\varepsilon}{T\omega(1-\varepsilon)^2}\right]}{\left[1-e^{-\omega(1-\varepsilon)t}-\frac{1}{T}\left(t-\frac{1}{\omega(1-\varepsilon)}\right)\right]}\right\}\frac{d\varepsilon}{\varepsilon}. \tag{5}$$

The total error is

$$dA/A=(dA/A)_\omega+(dA/A)_\varepsilon. \tag{6}$$

Equation (3) corresponds to both units starting runs at the same time. Actually, in the Novovoronezh power plant when one of the units is shut down the other continues to operate at power; under these conditions the average concentration of tritium in coolants can be calculated from the expression

$$A(t)=\frac{1}{2}[A_1(t)+A_2(t-\Delta T)], \tag{7}$$

where A_1 and A_2 are concentrations of tritium in the coolant in the two units calculated by Eq. (3), and ΔT is the time between the starts of the runs of the units.

Figure 2 shows the dependence of the average concentration of tritium in the primary loops of the third and fourth units for various values of ΔT calculated by Eq. (7), the confidence interval of the values of the concentration for ΔT = 50 days, and the results of measuring the concentration of tritium in the primary loop.

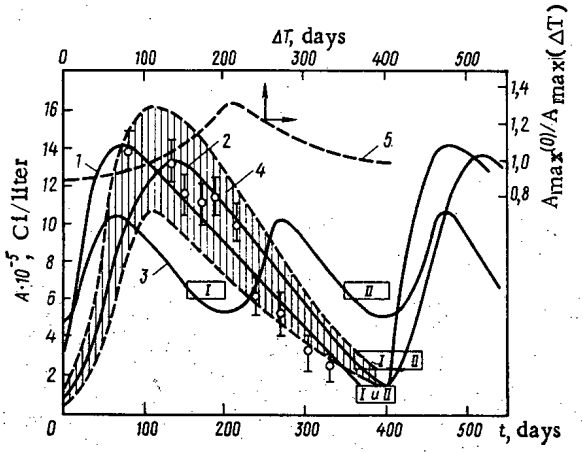

Fig. 2

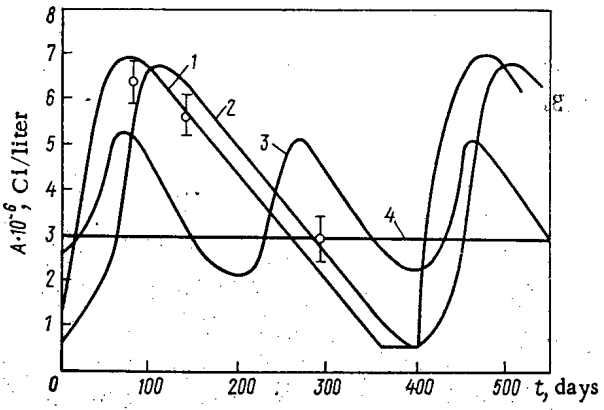

Fig. 3

Fig. 2. Concentrations of tritium in the coolant of the primary loops: 1) ΔT = 0; 2) ΔT = 50; 3) ΔT = 200 days; 4) confidence interval for ΔT = 50 days; 5) ratio of maximum concentration for ΔT = 0 to maximum concentration for various ΔT; ○ experiment for T = 50 days; I and II, scheduled preventive maintenance of first and second units.

Fig. 3. Concentration of tritium in feedwater and discharge system: ——) calculated; ○) experiment.

Samples of water were withdrawn from the primary loop, the special water purification system, and the auxiliary equipment and tanks connected with it. These samples were distilled twice to remove chemical impurities and associated radioactivity, and then analyzed on a beta spectrometer using standard ZhS-8 and ZhS-50 liquid scintillators. Figure 2 shows satisfactory agreement between calculation and experiment. The average concentration of tritium in the feedwater and discharge system, calculated from the relation

$$A_a(t) = \varepsilon A(t) \tag{8}$$

for 1) ΔT = 0; 2) ∿50; 3) 200 days, and the experimental data on the concentration of tritium in tanks of pure distillate for ΔT = 50 days (4) plotted in Fig. (3) are in satisfactory agreement. The maximum concentration of tritium in the feedwater and discharge system when the two units are started up at the same time is 1.4 times higher than when there is a 200-day interval between starts. Comparing with the value of the average permissible concentration of tritium in water ($3.2 \cdot 10^{-6}$ Ci/liter) we note that for ΔT = 200 days the concentration of tritium in the discharge water is closest to the permissible value, and a rather insignificant dilution of the discharge water is required to achieve the permissible level of tritium radioactivity. The measured distribution of tritium activity in the water supply systems of units I-IV, averaged over December, 1976, is shown in Table 1.

Comparison with known [1] data on the concentration of tritium in the primary coolant of pressurized water reactors shows that the concentration of tritium in the primary coolant of VVÉR-440 reactors is lower than in RM 3A reactors ($9 \cdot 10^{-4}$ Ci/liter), Saxton ($5 \cdot 10^{-4}$ Ci/liter), SELN ($7.5 \cdot 10^{-4}$ Ci/liter), Yankee ($4 \cdot 10^{-3}$ Ci/liter), Indian Point ($1.5 \cdot 10^{-4}$ Ci/liter), and higher than in the Rheinsberg Nuclear Power Plant ($5 \cdot 10^{-6}$ Ci/liter). These differences in the tritium concentration can be accounted for both by the differences in reactor powers and by the system of water exchange between the primary loop and other technological systems with auxiliary equipment and the associated system of tanks.

Thus, with a common (or two-unit) water purification system, feedwater and discharge system, the concentration of tritium in technological systems of nuclear power plants depends not only on the water exchange system and the power level, but also on the time between the startups of the units; for the production of the same amount of tritium the selection of the optimum interval can lower the concentration of tritium in the discharge water and eliminate the need for preliminary dilution.

LITERATURE CITED

1. A. S. Chopornyak, Nuclear Power Plants and the Environment [in Russian], Atomizdat, Moscow (1973).

EFFECT OF HELIUM-ION ENERGY AND IRRADIATION TEMPERATURE ON THE BLISTERING OF NICKEL

V. I. Krotov and S. Ya. Lebedev

UDC 621.039.51

The present work reports the preliminary results of an investigation of the blistering of nickel irradiated by helium ions of energy 20, 40, and 80 keV at a dose of $5 \cdot 10^{17}$, 10^{18}, $2 \cdot 10^{18}$, and $5 \cdot 10^{18}$ ion/cm^2 and a temperature of 300, 500, and 700°C; the ion-current densities corresponding to these ion energies are 80, 40, and 20 μA/cm^2, respectively. Thus, for all conditions of irradiation, the same heat liberation in the samples from the ion beam is ensured. The given temperature was maintained by radiant heating from a plane tungsten heater positioned behind the cassette with samples in the form of electrically polished disks (diameter 3 mm) of 0.2-mm-thick annealed nickel foil. An ILU-100 accelerator was the source of the irradiation [1]. After irradiation, the sample was inspected and photographed on a MIM-7 metallographic microscope (see Fig. 1 and Table 1).

On samples irradiated at 300°C, we observed group relief of the surface, which originated after the section of the blister roof (see Fig. 1a, b). The second-generation blisters have a size from 3 to 4 μm and are enlarged from 20 μm with higher energy ions. On samples irradiated at 300°C with a dose of $\geqslant 2 \cdot 10^{18}$ ions/cm^2 with ion energies of 40 and 80 keV, we also observed third-generation blisters, while for ion energies of 20 keV we did not observe even second-generation blisters. At 500°C the size of the blisters decreased (see Fig. 1c).

TABLE 1. Results of Inspection of Irradiated Samples

Sample temp., °C	Ion-current density, μA/cm^2	Helium-ion energy, keV	Concn. of first generation blisters, 10^6 cm^{-2}	Blister size, μm	
				max.	mean
300	20	80	0,3—0,5	40	10—14
	40	40	1—7	20	4—6
	80	20	4—40	2—3	0,5—1,5
500	20	80	2—3	10	3—4
	40	40	2—7	7	1—1,5
	80	20	4—40	2	0,5

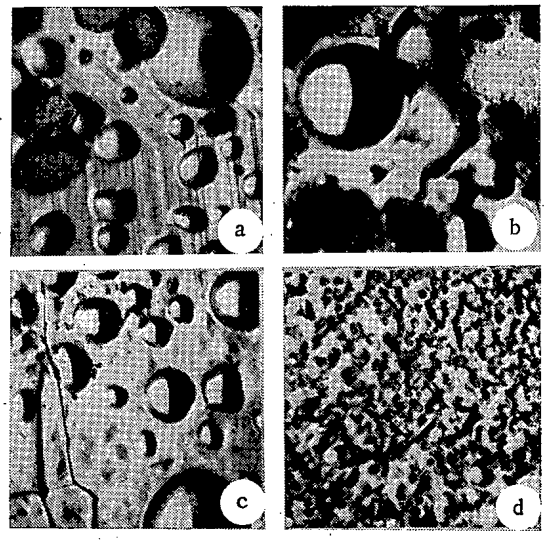

Fig. 1. Microphotograph in transverse illumination (from left to right) of a nickel sample (×1350) after irradiation by helium ions of energy 40 keV at 300°C in a dose of $5 \cdot 10^{17}$ (a) and $2 \cdot 10^{18}$ ion/cm^2 (b); and of energy 80 keV in a dose of 10^{18} ion/cm^2 at 500 (c) and 700°C (d).

Translated from Atomnaya Énergiya, Vol. 46, No. 2, pp. 122-123, February, 1979. Original article submitted April 17, 1978.

0038-531X/79/4602-0139$07.50

In all the samples, irradiation at 700°C creates coarse rough relief, possibly as a result of the rupture of blisters formed previously (Fig. 1d). The step height between the irradiated and unirradiated sections of the sample surface varies approximately from 0.1 to 0.5 μm; it is larger for lower temperatures and higher radiation doses, which indicates extremely strong swelling of the irradiated surface.

The great spread in the values of the blister concentration (Table 1) at energies of 20 and 40 keV is due to the formation of two groups of blisters, as observed for niobium in [2]. The blistering of nickel at room temperature has been observed by a number of investigators (see [3], for example), but comparison of the results is difficult because of discrepancies in the conditions of irradiation.

It remains to thank G. G. Gunin, G. P. Fokin, L. A. Zhdamirova, and V. D. Nedikova for assistance in carrying out the experiments and analyzing the results.

LITERATURE CITED

1. S. Ya. Lebedev et al., Prib. Tekn. Eksp., No. 4, 225 (1968).
2. S. Das and M. Kaminsky, J. Nucl. Mat., 53, 115 (1974).
3. V. M. Gusev et al., Fiz. Khim. Obrab. Mater., No. 1, 15 (1976).

KINETICS OF INSTANTANEOUS NEUTRONS IN A SYSTEM WITH A CAVITY

A. S. Chistozvonov, I. P. Matveenko, V. P. Polivanskii, and G. M. Vladykov

UDC 621.039.514

In reactor experiments, cases in which there are cavities in the breeder system are often encountered. This situation is observed both in the investigation of piles with an unloaded section of the active region and also for the associated reactors. In this case, a number of specific properties must be taken into account in using the pulsed neutron method. In such a system, the following condition is satisfied

$$\alpha^* \equiv \min \{v\Sigma_{\text{tot}}(\bar{r}E)\} \approx 0.$$

This means that for a subcritical system the fall in instantaneous neutron flux φ in pulsed experiments is described by the expression [1, 2]

$$\varphi(\bar{r}Et) = \int_{\alpha} f(\bar{r}E\alpha)\, e^{\alpha t}\, d\alpha,$$

where α is a complex number (Re $\alpha \leqslant -\alpha^*$).

However, for a relatively small cavity, the effect of the neutrons passing through it does not radically change the picture of the fall in neutron flux, although this process is somewhat slowed. It is then possible to use effective mean values, approximating this fall (which, strictly speaking, is nonexponential) by an exponential over a short time interval

$$\varphi(\bar{r}Et) \approx \varphi(\bar{r}E) \exp(-\alpha_{\text{eff}} t)\ (t_1 \leqslant t \leqslant t_2).$$

Over the time of flight through the slit, the neutrons are "conserved" in the cavity and are not involved in processes which lead to their destruction. Of course, the parameters characterizing the neutron residence time in the system (the lifetime and time of generation) are higher in this case than the analogous parameters for a continuous medium. For a fixed cavity size, this effect is found to increase with decrease in neutron energy.

The kinetics of instantaneous neutrons was investigated experimentally in a system consisting of two identical plane breeder piles. The piles took the form of a thin-walled steel tank of 150 × 600 × 785 mm filled by an aqueous solution of uranium salt. The uranium concentration in the solution was 36.1 g/liter and the uranium enrichment 90%. The pile construction allowed the distance between the tanks to be varied from 0 to 1200 mm. The emitter

Translated from Atomnaya Énergiya, Vol. 46, No. 2, pp. 123-125, February, 1979. Original article submitted April 21, 1978.

 0038-531X/79/4602-0140$07.50

TABLE 1. Values of System Parameters for Different Cavity Sizes

Slit size, cm	α, sec^{-1} (expt.)	η (calc.)	ρ_α, β_{eff}	ρ, β_{eff} (calc.)
0,0	110±10	1,0	0	0
2,3	585±25	1,06	−4,65±0,61	−4,7
4,7	1100±40	1,12	−10,2±1,1	−9,2
9,3	1640±70	1,24	−17,4±1,7	−17,5
18,6	2290±70	1,28	−25,5±2,4	−27,2

of TGI-91 pulsed neutron generator (E_n = 14 MeV) was placed at the outside of one of the tanks (at the midpoint of its height). SNM-12 counters were used as neutron detectors. To establish the dependence of the detector reading on its position, detectors were placed in each of the tanks and also in the gap between them. A Nairi computer was used for the analysis of the apparatus spectra.

The results of a series of experiments with cavity sizes of 0-200 mm show that, over a time in the range $(1/\alpha)$-$(5/\alpha)$, the fall in neutron density is approximated by an exponential; within the limits of experimental error (up to 5%) the decay constant α is independent of the detector position. The values of the reactivity $\rho/\beta \equiv (\alpha/\alpha_{cr})(\Lambda/\Lambda_{cr}) - 1$ calculated on the basis of the α method are found to be in agreement with the calculated data (Table 1). The correction for the variation in generation time $\eta \equiv \Lambda/\Lambda_{cr}$ was calculated in a multigroup approximation.

The determination of the nonsteady distribution of neutrons reduces to the solution of a system of multigroup transfer equations, which take the following form in the $2P_0$ approximation (in conditions of plane geometry)

$$\frac{1}{v_j}\frac{\partial}{\partial t}(u^j+w^j)+\frac{1}{2}\frac{\partial}{\partial x}(u^j-w^j)+\sigma_0(u^j+w^j)=\sum_{i=1}^{j-1}\sigma_0^{i\to j}(u^i+w^i)+\chi^j\sum_{k=1}^{m}(\nu_f\sigma_f)^k(u^k+w^k);$$

$$\frac{1}{v_j}\frac{\partial}{\partial t}(u^j-w^j)+\frac{2}{3}\frac{\partial}{\partial x}(u^j+w^j)+\sigma_1(u^j-w^j)=\sum_{i=1}^{j=1}\sigma^{i\to j}(u^i-w^i),$$

with the additional conditions

$$u^j(0,\ t)=0;\quad u^j(x,\ 0)=u_0(x);$$
$$w^j(0,\ t)=0;\quad w^j(x,\ 0)=w_0(x),$$

where $u^j(x,\ t)=\int_0^1\varphi^j(x,\ \mu,\ t)\,d\mu$; $w^j(x,\ t)=\int_{-1}^0\omega^j(x,\ \mu,\ t)\times d\mu$, and $u_0(x)$ and $w_0(x)$ are given functions determining the shape of the initial neutron pulse.

Since the real system is finite, although here it has been considered to be of infinite extent, it will be assumed that the main contribution to the neutron flux within the limits of the slit is that of neutrons flying at angles of $|\mu| \geq \mu_0$, for which the following expression may be written

$$\varphi^j(x,\ \mu,\ t)-\frac{l}{|\mu|v^j}=\varphi^j(x,\ \mu,\ t)\ \frac{l}{|\mu|v^j}\frac{\partial\varphi(x,\ \mu.\ t)}{\partial t}+O\left(x,\ \frac{l^2}{\mu^2v^{j2}},\ t\right).$$

Within the framework of the approximation adopted, this condition reduces to the form

$$\gamma u^j(x,\ t)|_{x=a}-u^j(x,\ t)|_{x=a+l}=\gamma\frac{2l}{v^j}\frac{\partial u^j}{\partial t}\Big|_{x=a};$$

$$\gamma w^j(x,\ t)|_{x=a+l}-w^j(x,\ t)|_{x=a}=$$

$$=\gamma\frac{2l}{v^j}\frac{\partial w^j}{\partial t}\Big|_{x=a+l},$$

where a and $a + l$ are the coordinates of the edges of the slit; l is the slit width.

TABLE 2. Relative Values of Λ for Systems with and without Cavities at Different Values of K_{eff}

K_{eff}	System with a cavity $\eta = \Lambda/\Lambda_{cr}$	System without a cavity $\eta_0 = \Lambda^0/\Lambda^0_{cr}$	η/η_0
1,00	1,00	1,00	1,00
0,97	1,06	1,03	1,03
0,94	1,12	1,06	1,06
0,889	1,24	1,12	1,11
0,837	1,28	1,19	1,08

The coefficient γ reflects the attenuation of the neutron flux on passing through the slit as a result of the finite dimensions of the real system in the direction of the y and z axes; it may be chosen in accordance with the recommendations of [3]. An approximate version of the initial problem was solved by replacing the time derivatives by difference relations at the chosen system of points $t = 0, t_1, \ldots, t_n = T$. At each time layer, the solution of the steady problem was found by the method described in [4]. The decay constant at each moment of time was found from the formula

$$\alpha(x, t_k) = \frac{1}{\Delta t_k} \ln \frac{\sum_{j=1}^{n} \varepsilon^j [u^j(x, t_k) + w^j(x, t_k)]}{\sum_{j=1}^{n} \varepsilon^j [u^j(x, t_{k-1}) + w^j(x, t_{k-1})]},$$

where ε_j is the spectral sensitivity of the detector.

The value of K_{eff} (and correspondingly the reactivity ρ) was determined by the standard procedure. The instantaneous-neutron generation time was calculated from the relation

$$\Lambda = [\psi^+, v^{-1}(u+w)]/[\psi^+, \chi\hat{q}(u+w)];$$

the importance function ψ^+ was found from the conditionally critical equation. The calculations were made using three-group constants obtained by means of the convolution operation from the 21-group calculations of the 9M program.

On the basis of this investigation of instantaneous-neutron kinetics in plane interacting thermal-neutron piles, the following conclusions may be drawn.

1. Despite the presence of a cavity, which has a pronounced effect on the kinetic parameters of the instantaneous neutrons, the fall in neutron intensity may be approximated as exp (−αt) (on the section where the main harmonic falls by a factor of 10^2 with an error of $\Delta\alpha/\alpha \sim 5\%$). The time required to establish this quasiasymptotic decline at different points of the system is $(1/\alpha)$-$(5/\alpha)$ and depends on the relative positions of the detector and neutron source.

2. The theoretical parameters derived on the basis of the multigroup $2P_0$ approximation are found to be in agreement with the experimental results.

3. In systems with cavities, the increase in neutron generation time with decrease in K_{eff} is found to be faster than in systems of the same composition but without a cavity [2]. This difference reaches a maximum at $l \approx 10$ cm, and then begins to decrease, evidently as a result of a decrease in the proportion of neutrons reaching the other half of the system because of the escape of neutrons through the cavity to the outside (Table 2).

4. The pulsed α method of determining reactivity may be successfully used to study systems with very considerable cavities.

LITERATURE CITED

1. M. Nelkin, in: Proceedings of a Symposium on Pulsed Neutron Research, Vol. 2, Karlsruhe (1965), p. 85.
2. É. A. Stumbur, in: Theoretical and Experimental Problems of Nonsteady Neutron Transfer [in Russian], Atomizdat, Moscow (1972), p. 80.

3. H. Clark, Nucl. Sci. Eng., 15, No. 1, 20 (1963).
4. Sh. S. Nikolaishvili and V. I. Polivanskii, in: Problems of Reactor-Protection Physics [in Russian], No. 5, Atomizdat, Moscow (1972), p. 64.

TRACK-DETECTOR DETERMINATION OF NUCLEAR-FUEL CONTAMINATION OF PRIMARY-CIRCUIT SODIUM COOLANT

V. P. Koroleva, P. S. Otstavnov, and V. S. Shereshkov

UDC 621.039.5

Chemical and radiochemical methods are used extensively today to determine the nuclear-fuel contamination of the sodium coolant and the contamination of the primary-circuit equipment of fast reactors [1, 2]. These methods are based on taking a sample of coolant from the circuit, treating it chemically to isolate and concentrate the relevant elements, and then making a radiometric or colorimetric analysis of the content of fissile elements. The principal drawback of these methods is that a complex procedure is required for isolating from the sample fissile elements which may be present in different chemical compounds with the coolant, fission products, and impurities present in the coolant.

The method of weighing the fuel elements before and after irradiation [3] was used to determine the penetration of fuel into the coolant. Rather than characterizing the content of fuel in the coolant, this method characterizes the total change in the mass of the fuel elements because of losses of nuclear fuel, leaks of gaseous fission products, and penetration of coolant into the fuel elements.

In the present paper we study the possibility of employing nitrocellulose track detectors to assess the degree of α-contamination of the surface of the film of coolant on the primary-circuit equipment of the BR-10 reactor [4] with nuclear fuel.

Solid-state track detectors (glasses, micas, polymer films, nitrocellulose, etc.) possess a number of significant advantages for extensive use in reactor experiments [5]: a quite high efficiency of charged-particle detection, insensitivity to γ and β rays, a simple and reliable method of processing, absence of electronic equipment, small detector size, unlimited memory, etc. From the various types of track detector, nitrocellulose was chosen for decting α particles from fuel, the use of nitrocellulose being preferable to other forms of track detectors, e.g., detectors with glasses. In this case use is made of the natural α activity of fissile elements whereas for glasses detecting fission fragments require irradiation in a neutron flux. Moreover, since it is quite flexible, nitrocellulose can assume the shape of any bent surfaces and, therefore, can be used in places which are almost inacessible to other detectors.

We determined the α activity of the inner surface of the bypass pipe with a residual film layer of sodium, drained at a temperature $\sim$200°C, as well as that of the end section of the pipe and of the surface of a technological instrument in the radioactive circuit, after rinsing of the instrument. Nitrocellulose (the base of the RF-5 x-ray film) with a thickness of 0.12 mm was used as a detector for the α rays of uranium and plutonium. For greater reliability of results three specimens of nitrocellulose were placed at various points in close contact on each of the surfaces examined. After exposure, the nitrocellulose specimens were etched in an aqueous solution of NaOH with a 30% concentration (by weight) at 60°C for 30 min. The nitrocellulose detectors were then examined visually in a PMT-3 microscope (×360). Tracks from the α rays of the fuel were observed in nitrocellulose specimens which had been in contact with the inner and end surfaces of the pipe coated with a sodium film. No α-ray tracks from the fuel are observed on the surface of the instrument with the residusl layer of sodium washed off. For quantitative determination of the track density on the inner surface of the pipe we counted 120 microfields (microfield diameter 0.46 mm) with roughly 140 tracks in each. With the background microfields taken into account, all told $\sim$17,000 tracks were counted. It was found that the mean track density minus the background is 630 tracks/mm^2.

Translated from Atomnaya Énergiya, Vol. 46, No. 2, pp. 125-126, February, 1979. Original article submitted July 24, 1978.

0038-531X/79/4602-0143$07.50

The number of background tracks was determined by means of nitrocellulose control specimens, also set up on the surfaces under examination but protected from the effect of α particles. The chemical treatment of the control specimens was carried out along with the working specimens. In the experiment the background constituted about 23%. The spread of the track densities for the three nitrocellulose specimens, which also characterizes the nonuniformity of the fuel distribution, is equal to ∿15-20%.

On the nitrocellulose specimens exposed on the end section of the pipe, the microfields with α-ray tracks lay on the line of a clearly defined circle with a diameter corresponding to the inner surface of the pipe. These microfields were examined only qualitatively. The absolute efficiency of α-ray detection determined earlier for uranium and plutonium with allowance for differences in the energy in them for the given etching conditions is equal to 25 ± 5%. For this efficiency the α activity of the inner surface of the pipe is $(2.0 \pm 0.2) \cdot 10^{-5}$ μCi/cm². It should be added that the measured surface contamination with a residual film of the coolant on the equipment does not yet characterize the contamination of the entire circuit and the coolant as a whole. For a complete picture further studies must be made of the contamination over the entire circuit and volume of the coolant.

On the basis of the studies done it may be concluded that the track-detector method is applicable to the determination of contamination, with nuclear fuel, of the equipment and sodium coolant of the primary circuit of the reactor. The possibility of using nitrocellulose for such purposes is limited in practice only by the ratio of the exposed tracks to the intrinsic background tracks of the nitrocellulose.

LITERATURE CITED

1. V. K. Markov et al., Uranium, Methods of Determination [in Russian], Atomizdat, Moscow (1960).
2. R. Hart, Distribution of Fission Product Contamination in the SRE, NAA-SR-6890, North American Aviation (1961).
3. A. Thorley, F. Findlay, and A. Hooper, Fission and Corrosion Product Behavior in Primary Circuit of LMFBR's. Specialists' Meeting, Dmitrovgrad, USSR (1975).
4. N. N. Aristarkhov et al., in: Proceedings of the Second COMECON Symposium "State of the Art and Prospects of Work on the Construction of Design of Atomic Power Plants with Fast Neutron Reactors" [in Russian], Vol. 1, Izd. Fiz. Énerg. Inst. (FÉI), Obninsk (1975), p. 374.
5. V. A. Kuznetsov et al., At. Énerg., 32, No. 6, 481 (1972).

BOOK REVIEWS

I. N. Aborina

PHYSICAL RESEARCH ON WATER-MODERATED—WATER-COOLED POWER REACTORS*

Reviewed by V. I. Pushkarev

The book has been published in the "Nuclear Reactor Physics" series. Experiments performed on physical stands for water-moderated—water-cooled power reactors (VVÉR) have an almost 25-year-old history. The results of these experiments have made it possible to correlate design methods for the cores of water-moderated—water-cooled reactors, to draw up recommendations for increased operating reliability and safety of functioning reactors, and proposals for the construction of more powerful and economical reactors. The main attention has been devoted to experiments which precede the entry of a reactor into service. The scheme and sequence of the experiments built up in the course of the investigations are presented.

The book consists of an introduction, two chapters, and a conclusion.

The introduction briefly enumerates the principal advantages of water-moderated—water-cooled power reactors and considers the reactor core and its design and control systems within the limits necessary for subsequently describing the technique of the experiments.

The first chapter is devoted to research done on subcritical and critical assemblies, i.e., mainly to experiments providing confirmation for concepts for water-moderated—water-cooled reactors, verifying the main metholodological assumptions, and developing computational methods of research. The experiments determined the material parameters of various lattices, neutron spectra, and multiplication factors and their components (in the approximation of the "four-factor formula"). The author presents and analyzes different methods of determining each parameter, the technique of conducting experiments, and the methodological basis of the experiments. A description is given of neutron spectra and methods of measuring the reactivity, including research on controls.

The second chapter describes experiments performed during the reactor startup. Startup experiments differ considerably from experiments on physical stands in respect to both the conditions under which they are carried out and the methods and apparatus employed. The important thing is that usually an extremely short time is set aside for these experiments, thus necessitating particular care in planning the experiments and organizing the work. In the course of startup experiments the asymmetry of the reactor-core properties is revealed, the reactivity excess and the efficiency of means of compensating it are determined, and the temperature coefficient of reactivity and other reactivity coefficients are measured.

In the conclusion the author points out certain areas of experimental investigations which it is desirable to expand. These include experiments on the determination of little-investigated effects in the upper neutron-energy regions, the anisotropy of neutron diffusion in inhomogeneous media, and the determination of the effective delayed-neutron fraction. Many experiments should be performed in connection with the transition to boron control in water-moderated—water-cooled power reactors. It is necessary to experimentally verify such an important reactor parameter as plutonium buildup and there is a need to verify the methods of in-reactor monitoring as well as methods for early detection of deviation from normal operating conditions, including statistical methods of investigation. All of this indicates that very much still remains to be done in studying the physics of water-moderated—water-cooled reactors. And one of the shortcomings of the book is that these tasks are only enumerated but are not discussed to the necessary degree. This would have made the book much fuller and more useful.

*Atomizdat, Moscow (1978).

Translated from Atomnaya Énergiya, Vol. 46, No. 2, p. 126, February, 1979.

0038-531X/79/4602-0145$07.50

It is difficult to agree with the author when she gives reasons why the book does not give certain experimental results for commercial water-moderated—water-cooled power reactors: these results would be extremely useful to those to whom the book is addressed, i.e., specialists and students.

On the whole, the book is unquestionably interesting. Much of the material presented in it is applicable not only to water-moderated—water-cooled reactors but also to reactors of other types.

YULII BORISOVICH KHARITON (75th BIRTHDAY)

A. P. Aleksandrov, E. P. Velikhov,
E. I. Zababakhin, Ya. B. Zel'dovich,
I. K. Kikoin, and M. A. Markov

Yulii Borisovich Khariton is an eminent scientist. For more than 50 years he has devoted his talent and his effort to Soviet physics, and, of them, 40 years to nuclear technology. He has continuously headed one of the most important trends of this problem.

The work carried out by Yu. B. Khariton has received nation-wide recognition: Yulii Borisovich — three times Hero of Socialist Labor, Laureat of the Lenin and three State Prizes, Deputy of the Supreme Soviet of the SSSR, and Academician.

Yulii Borisovich was born on Feb. 28, 1904, in Petersburg in a highly cultured family. He soon became interested in mathematics and physics. Then as a schoolboy he made experiments and read popular books. In 1920 he entered the Electrotechnical Faculty of the Polytechnic Institute, in the next year he transferred to the Physicomechanical Faculty of the same Institute, and from the second course he started work in the Laboratory of N. N. Semenov in the Leningrad Physicotechnical Institute. We recall that the Physicotechnical Institute was founded shortly before this by A. F. Ioffe, as was the Physicomechanical Faculty of the Polytechnical Institute.

Soon after, Khariton, together with Z. I. Valt', made an eminent discovery — he demonstrated the existence of critical conditions for the oxidation of phosphorus. This work played an important role in the development of the theory of branched-chain reactions, attributed to N. N. Semenov. In the Journal "Atomnaya Énergiya," there is no need to remind the reader that the explosion of nuclear fuel is the result of a supercritical chain reaction with neutron multiplication, but in a reactor this same process is accomplished in strictly critical conditions.

Translated from Atomnaya Énergiya, Vol. 46, No. 2, pp. 129-130, February, 1979.

0038-531X/79/4602-0147$07.50

In 1927, V. N. Kondrat'ev, N. N. Semenov, and Yu. B. Khariton published the monograph "Electron Chemistry," which played a large role in the future development of chemical physics in the Soviet Union. In a subsequent work Khariton discovered the critical phenomena during the condensation of mercury vapor on a supercooled glass surface. He introduced the concept of the two-dimensional gas of mercury atoms, adsorbed on the surface, and he demonstrated the mobility of these atoms. This work, together with theoretical work, was of practical importance in connection with the preparation of colloid mixtures and in the technology of semiconductors. Yu. B. Khariton and A. I. Shal'nikov in 1934 published the book "Condensation and Formation of Colloids."

In 1927-1928 Yulii Borisovich worked in England at the Rutherford Laboratory — a universal center for nuclear research at that period. In connection with the scintillation method of observing α particles, Khariton investigated the luminescence of zinc sulfide, demonstrated the migration of energy in the crystal, and determined the sensitivity of the human eye: even four quanta of light make a visual sensation. The creative circumstances in the laboratory, contact with Rutherford and many other outstanding physicists, were of great importance in shaping Khariton as a scientist and scientific organizer.

On returning to his native town, Khariton organized the Explosives Laboratory in the Institute of Chemical Physics. For the first time, the processes of origination and propagation of an explosion were analyzed from the aspect of chemical physics, for the purpose of relating the elementary processes at atomic level with the practical characteristics of explosives, their power and sensitivity. Khariton discovered and explained the existence of the critical diameter of detonation of a charge. This discovery enabled him subsequently in wartime to develop the technology of the application of substitute explosives in aircraft bombs. The work received high appraisal.

In 1930-1943 Khariton was the deputy of the editor-in-chief of the Journal of Experimental and Theoretical Physics (JETP). Many authors of articles still recall with gratitude the benevolent and responsible consideration of Yulii Borisovich, and his help. Many Soviet physicists remember that in their youth the most popular book on problems of physics for universities was the book by Valter', Kondrat'ev, and Khariton.

Let us return to the work of Yulii Borisovich, which is concerned directly with nuclear energy.

In 1937 Khariton published an investigation into the separation of air into oxygen and nitrogen by means of the centrifuge. The results are transferred easily to the separation of the isotopes ^{235}U and ^{238}U. He noted in the paper that centrifugal separation is possible in principle with the minimum expenditure of energy. This is specially important to find the maximum possible output of the equipment for a given peripheral velocity of the centrifuge. This output cannot be exceeded for any cascade systems whatsoever.

In 1939-1941 Khariton published (jointly with Ya. B. Zel'dovich) several papers, in which the possibility was investigated of a nuclear chain reaction in natural uranium by fast and slow neutrons, and the kinetics of a nuclear reaction in a system close to critical. He noted the necessity for enrichment of the uranium in the isotope ^{235}U in order to conduct the reaction with a water moderator, and also the necessity for searching for better moderators. It is shown that control of the reaction is facilitated owing to the emission of delayed neutrons.

The combination of experimental talent and a deep theoretical understanding of the problems of nuclear energy, together with the exceptional personal qualities of Khariton, has predetermined his future destiny. With the start of an extensive expansion of work on the new technology, Khariton was commissioned as the director of one of the most important parts of the problem. In collaboration with I. V. Kurchatov and A. P. Aleksandrov, Yulii Borisovich brilliantly achieved the work entrusted to him. He founded an outstanding scientific school, which he continues to head at the present time. He was, and will remain, an outstanding teacher and educator of scientific personnel. Among his students are academicians, corresponding members, and Doctors of Science.

Khariton distinguishes the combination of scientific phantasy, boldness, and feeling — and simultaneously scrupulous attention to every "trifle," to every nebulous or difficult problem, on the solution of which depends success.

The motto of Khariton is total lucidity and absolute honesty. Responsibility for the work and fundamental exacting demands are combined for Khariton with benevolence, humanity,

and the charm of a highly intelligent and sincere person. Without these humanitarian qualities and total self-efficiency, it is doubtful whether Khariton would have been able to do what he has done.

In the important day of the 75-year old, colleagues and scientists wish their dear friend Yulii Borisovich many years of life, health, and creative work.

INFORMATION

WORK ON FAST REACTORS IN ITALY

V. M. Arkhipov

In July 1978 Soviet specialists visited the research centers of Italy, where they familiarized themselves with the work in the field of research and development of fast reactors and their principal components.

The development of fast reactors in the country characterizes the close contact with France. Italy has a considerable share of participation (33%) in financing the development of Superphoenix. The efforts of the Italian specialists are directed at the establishment and development of systems of the RES reactor and certain facilities of Superphoenix (pumps, steam-generators, heat exchangers, etc.). RES, with a capacity of 118 MW, is a facility for testing fuel elements in thermal loading conditions (540 kW/liter) and neutron flux densities ($4.35 \cdot 10^{15}$ neutrons/cm^2·sec) which approach the operation of fast power reactors. The special feature of the reactor is the presence of a central experimental channel with an autonomous heat-transfer system, calculated on a thermal capacity of 3 MW. The inside diameter of the channel at the core level amounts to about 110 mm, and the overall length of the vertical part is 16 m.

The experimental loop is calculated on an operating temperature of up to 650°C; it has two pumps and a heat exchanger located in a single tank. Experiments on boiling sodium and the investigation of the interaction of the fuel with sodium can be conducted in the experimental channel. The program of investigations includes also a large volume of work on the study of the behavior of structural materials. All these investigations, which it is proposed to carry out in RES, are directed at the development of prospective types of fuel, structural materials, and the design of fuel elements for fast power reactors.

At present, work is being carried out inside the secondary containment shell on the assembly of the reactor shaft, its outer shell is installed, preparations are being made to install the cooling shell of the reactor biological shield, which also serves the function of an antiexplosion barrier and is calculated on an energy release in the reactor of 200 MJ. The foundation of the rooms adjacent to the reactor building is being concreted. It was reported also that 80 % of the RES plant has been manufactured. Startup of the reactor is planned in 1981.

The work carried out at present in the nuclear centers of Kassachi and Brazimone, is associated, on the one hand, with the establishment and development of the RES plant components and, on the other hand, is directed at the establishment of selected components of Superphoenix. Work is being carried out at Kassachi on:

the development of a fuel recharging mechanism and the reactor control and safety rod mechanisms, and the development in sodium of a mechanism for the operation of the lugs of a device, preventing flotation of the fuel assemblies;

investigation of the thermohydraulic characteristics of the fuel assemblies on models of 7 and 19 fuel element simulators with electrical heating;

safety — investigation of sodium boiling in a bundle of rods and the interaction of uranium oxide with sodium, using electrical heating for melting the uranium oxide. In association with these problems, an experimental base has been constructed — full-scale test-rigs for fuel recharging mechanisms and test-rigs for testing the control rod mechanism and plant components to thermal shocks (rate of change of temperature 50 deg C/sec).

For the investigation of the RES fuel, a room with 10 hot boxes has been constructed. Several series of experiments have been carried out on the boiling of sodium in a fuel assembly and the interaction of sodium with the fuel (with electrical heating). From the preliminary results, the energy of interaction between the sodium and the fuel can be recorded as 1-3 J/g UO_2, which is more than an order of magnitude less than calculated.

Translated from Atomnaya Énergiya, Vol. 46, No. 2, pp. 131-132, February, 1979.

 0038-531X/79/4602-0150$07.50

In Kassachi, work is also proceeding on the investigation of materials for the steam generators of Superphoenix to thermal fatigue, mechanical properties, corrosion in sodium and steam—water mixtures. The effect of a 1-10% solution of caustic on the intercrystallite corrosion of steel is being studied. In Brazimone, the main problem is the construction of the RES. One of the largest scale and most equipped in this center is the complex full-scale test rig for developing the technology of discharging the fuel assemblies from the experimental loop of the RES and for conducting operating-life tests on the plant, in conditions of heat exchange and thermal shocks. The full-scale plant of the loop is used on these test-rigs. Of the experimental work associated with the Superphoenix project, the investigations of large and small water leaks in the steam-generators should be mentioned. An experiment has been conducted on the large-leak test-rig, in which 160 kg of water entered the sodium, and a further 60 kg due to secondary failures in consequence of accidental damage to the tubes. A test rig has been constructed for operating-life tests of the rotary parts of the Superphoenix pump, including under seismic loading conditions. This program should be completed at the end of 1979.

On the whole, the program of work on fast reactors in Italy is directed at the most rapid introduction of fast power reactors into the country's energy generation.

CONFERENCES, SYMPOSIA

SYMPOSIUM ON HIERARCHY IN LARGE POWER GENERATING SYSTEMS

N. A. Trekhova

An All-Union symposium, organized by the Scientific Council on Complex Problems of Energy Generation, Academy of Sciences of the USSR, and the Siberian Power Generation Institute, Siberian Branch of the Academy of Sciences of the USSR, was held in September 1978 in Irkutsk.

The structure of the rational hierarchy of control in large power generation systems is one of the central and methodologically most complex problems in the theory of control. At the same time, it has great practical importance as the constant improvement of the mechanism of centralized control by the national economy and all its elements (in particular, power generation) is an integral feature of the socialistic method of production.

In the investigations undertaken, the nature of the hierarchical organization of large power generation systems is being studied, the principles of constructing a rational hierarchy of systems and the problems of control by them at different time stages and hierarchical levels are being worked out, and methods are being established for the coordination of solutions in the complex hierarchy of mathematical models, including in the case of ambiguity of the starting information. Academician L. A. Melent'ev, in a report at the plenary session, noted that it is not possible to study and improve the structure of control in large power generation systems separately from the hierarchy of control by the national economy as a whole. The production and territorial criteria are set up on the basis of the hierarchical structure. In this case, the principal large systems in power generation (interbranch – general power generation and the functional branches involved in it) are subdivided territorially according to basic levels (country – region – power generating unit – undertaking), creating a hierarchical assembly of vertically and horizontally disposed and relatively autonomously functional large systems. If this scheme is represented according to the control hierarchy, then it would have a pyramidal form. At its upper level are to be found problems of control in the development of a general power generation system, i.e., common problems of the shaping of the proportions of development of the power generation economy; next, there are disposed the more specific problems of development and operation of the individual functional systems as a single economic entity. One of these problems is the development of the nuclear power generation of the country, and then the even more specific problems of development and operation of local systems of their subdivisions (e.g., nuclear power stations). A similarly structured information system must match this pyramidal hierarchy of problems of control.

L. A. Melent'ev paid particular attention to the fact that the subject of the investigation are the hierarchical structures of actual systems, and not an abstractly represented and arbitrarily shaped structure, originating from convenience of observation of the hierarchy of information links.

The work of the Symposium was conducted in three sections.

To the first section – "Hierarchy of Control in the Development of Large Power Generation Systems" – 19 reports were devoted, of which the actual hierarchies of systems were considered in 12, and in 4 of them methods of coordinating solutions by the analysis of an actual hierarchy were considered. The solution of problems of actual hierarchy was concerned with finding not the optimum, but even acceptable solutions. The following problems were proposed for discussion in the first section: what time level of control (planning, economic, or operative-dispatcher control) should the shaping of the hierarchy of large power generation systems accept in principle, which problems of control – optimization or achievement of solutions – are in this case the principal ones, what major aspects of control determine the structure of the hierarchy, what are the principles of coordination of the solution in an actual hierarchy of power generation development control and the requirements imposed on mathematical methods and models of coordination of the hierarchial solutions.

In the second section – "Hierarchy of Economic and Dispatcher Control with Large Power Generation Systems" – 12 reports were discussed devoted to the hierarchy of control, interbranch

Translated from Atomnaya Énergiya, Vol. 46, No. 2, pp. 132-133, February, 1979.

 0038-531X/79/4602-0152$07.50

interaction, hierarchy and interaction of mathematical models, and systems of operative control.

In the third section — "Mathematical Models and Methods of Coordination of Solutions in Hierarchical Systems" — 9 reports were presented on the application of existing treatments — theory of nonantagonistical games, models of economic equilibrium, programmed-specific approach, system-information method; on the use of mathematical programming, designed for the optimization and achievement of solutions under actual conditions of functioning of large power generation systems.

Control of a large power generation system inevitably requires the participation of people. In this case, a high degree of automation of this process is necessary, as even if a person has available all the necessary information concerning the state of the individual elements and of all the system as a whole, he might not always select from it the most important, and take and effect the correct solution. Moreover, control is possible only in the presence of criteria of efficiency, and therefore the whole problem must precede the choice of the criteria hierarchy.

The problem of future research in the field of hierarchical structures of large power generation systems can be formulated in the following way: 1) to continue to study closely the experience of control of the hierarchical structure of the large power generation systems of the Soviet Union and other Socialist countries, and also to interpret critically the experience of controlling nationalized power generation systems in capitalist countries. Serious attention should be paid to a master unit of control — economic control; 2) to generalize this experience and to develop the most reasonable alternatives of a possible structure, to assess them from the point of view of efficiency of the controlled systems, and to create on this basis the appropriate practical recommendations.

The proceedings of the Symposium have been published by the Siberian Branch of the Siberian Power Institute of the Academy of Sciences of the SSSR.

CONFERENCE ON LARGE TOKAMAKS

G. N. Popkov

In September 1978 a conference was held in Paris of the Technical Committee of the IAEA on engineering problems of experimenters on large tokamaks, at which was discussed the course of designing and construction of large-scale thermonuclear facilities of the tokamak type, and also the construction of other planned large-scale devices was discussed. Individual engineering problems were considered in eight sectional sessions. Seventy-seven specialists from 16 countries and the representatives of firms developing and supplying plants for tokamaks participated in the Conference.

TFTR (U.S.A.). The installation project has been completed, and its startup is designated at the end of 1981. The cost of the project is 239 million dollars, with 166 million dollars appropriated at the end of 1978. The successes achieved recently on PLT have influenced the ideology of TFTR. At present, a program is being developed for modernizing the facility. Its purpose is to increase the peak power of the fusion reaction and to lengthen the discharge pulse. It is proposed to increase the power of the injected beam of fast atoms from 20 to 45 MW. Because of this, the power of the fusion reaction will reach 75 MW instead of 18 MW. Now, construction work is going into operation, and a considerable part of the technological plant has been completed.

JET (Euratom). After official approval by ministers of the European Economic Community, the project has become an independent undertaking. In October, 1977, the site of the facility was approved — next to Culham (Great Britain). The cost of the project in the 5 years of its installation (to the beginning of 1983) will amount to 123 million pounds. The construction project, because of the delay in selecting the site of installation, will be launched with a delay. In the near future, it is proposed to place orders on 80% of the plant.

Translated from Atomnaya Énergiya, Vol. 46, No. 2, pp. 133-134, February, 1979.

0038/531X/79/4602-0153$07.50

JT-60 (Japan). Planning is at the stage of completion. The chosen construction site has not yet been finally formulated. In April, 1978, the Hitachi firm issued a contract on the manufacture of the plant. The cost of the whole complex is estimated at 700 million dollars. Construction of the facility should be completed in 1982. The first phase of experiments postulates the injection of neutral beams of atoms with a power of 12 MW, and the second phase (1984) — 80 MW.

T-10M (USSR). Planning of the complex is at the stage of completion. The alloy Nb_3Sn has been chosen as the superconducting material for the winding of the toroidal field. This, it is hoped, will permit a toroidal magnetic field greater than proposed earlier to be obtained — 4.5-5 T instead of 3.5 T. Construction of the facility is designated for completion in 1983.

Other projects were also considered at the Conference: SLPX (Superconducting Long-Pulse Experiment), Princeton, U.S.A.; LPTT (Long-Pulse Technological Tokamak), Oak Ridge, U.S.A.; JT-4, Japan; Torus-II Supra, France, etc. Of these, SLPX should be distinguished, as according to the plant this facility will be the next generation by comparison with TFTR. A site has been reserved for it during construction of the latter. The facility will have niobium—tin superconducting toroidal windings, creating a magnetic field on the axis of the torus of 7.2 T. The parameters of the facility are: $R = 3.5$ m; $a = 0.7$-0.95 m; $e/a = 1.6$; $I = 3$-5 MA. The pulse duration is $\sim$100 sec. The purpose of constructing the facility is to demonstrate the efficiency of the superconducting magnetic system in facilities which approximate to reactors, and to obtain a prolonged plasma cycle with thermonuclear parameters. Construction is designated for completion in 1986.

The following sections worked at the Conference: diagnostics; magnetic systems; power supply systems; shielding, remote control and servicing; operating modes and supplementary heating; vacuum systems; control and processing of data; and the organization of construction and quality assurance.

New procedures of plasma diagnostics were not discussed, as by common agreement the planned diagnostic complexes as it is are adequately large and will provide the requirements of experiment. In all projects, total automation of the extraction and processing of experimental information was provided. The results obtained on PLT have forced the planners to further improve the project in the direction of increasing the duration of the working pulse and the power of the supplementary heating. In all projects, the possibility is being considered of using different types of high-frequency heating together with the injection of neutral beams of atoms. The refinement of the magnetic system designs during 1977-1978 have taken place along the lines of providing high β values. In the JET project, e.g., this has led not only to an increase of the copper in the windings, but also to an increase of the cross section of the magnetic conductor supports. In all projects, the forces acting on the winding have been refined, and the mechanical structures have been strengthened.

The TFTR and JET facilities are intended for operating on a mixture of deuterium and tritium. This has necessitated careful development of the shielding and of the remote control facilities. JET is located in a room which has a concrete shield 2.5 m thick. TFTR, in addition to the shielding of the room where it is located, is surrounded by a protective hut (igloo) of concrete, 1.2 m thick. This shielding simplifies servicing of the diagnostic plant. The requirements for remote-controlled reassembly of the facilities have significantly influenced the construction of the individual components and units, i.e., they have been designed jointly with the equipment for remote-control reassembly. All remote-control operations have been carefully worked out on simulators. As applicable to TFTR, about 20 of these simulators have been developed and tested, and the cost of one of them frequently exceeds one million dollars.

Work on the construction of the control system in the TFTR complex is proceeding with considerable determination, in comparison with other systems. At present, 13 computers have been purchased. The development of peripheral electronic equipment is proceeding at full speed. It should be mentioned that only one-third of the simulators is of series production and has been purchased. Another third has been developed specially and has been placed with firms, and the other third has been developed in the Princeton Laboratory. The volume of the operative memory of the control system is 5.75 Mbit, and the memory in the disks is 1280 Mbit. It is proposed to process about 13,000 signals from the various systems of the facility. Work on the construction of the TFTR control system provides for testing of the components of this system on PLT. The control system will be ready in 1980.

Monitoring for the progress of the work and methods of control in the project were analyzed in detail at the Conference. This problem has been studied most thoroughly on TFTR. The state of affairs and control will be analyzed through a system of network planning, which will monitor the sequence of operations, their duration and terms, labor resources in man-days, and costs. The data will be processed and analyzed with the use of a computer.

The Conference showed that the engineering difficulties facing the originators of large-scale thermonuclear facilities are being overcome successfully, and there is the basis for hoping for startup of a facility in the period contemplated.

The next conference on engineering problems of experiments on large tokamaks is planned to take place in 1980 in Tokyo.

INTERNATIONAL CONFERENCE ON THE APPLICATION OF THE MÖSSBAUER EFFECT

A. N. Artem'ev

At the Conference, held in August-September 1978 in Kyoto (Japan), the following sections functioned: Progress in Methodology, Surface Phenomena and Catalysis, Amorphous Materials, Magnetic Hyperfine Interactions, Magnetic Materials, Chemical Structures, Aftereffects of Nuclear Transformations, Earth Sciences and Archeology, Biological Systems, Radiation Damage and Defects, Engineering Materials, Metals and Alloys, and Lattice Dynamics.

The paper by R. Pound et al. (U.S.A.) aroused great interest; it described "light guides" for γ radiation based on the principle of total external reflection. The light guide was a bundle of fine glass tubes. The observation of the unbroadened γ-resonance line of ^{57}Fe by means of a source and absorber, separated by this light guide, demonstrates the elasticity of the reflection process. V. Wildner and U. Gonzer (Federal Republic of Germany) worked with the extremely sharp Mössbauer line of the 88-keV transition in ^{109}Ag (τ = 58 sec). Carrier-free ^{109}Cd was introduced into the silver crystal by thermal diffusion. The search for the resonance effect was conducted according to the temperature dependence of the 88-keV γ-emission absorption. When measuring the temperature from 78 to 4.2°K, the count rate decreased by 0.1%, which coincides with the estimates and confirms the resonance absorption.

Work on the research application of Mössbauer diffraction, started at the end of the 1960s, has been introduced intensively into laboratory practice.

Among the papers on this trend, the one is interesting in which the cirtical scattering during phase transition in a monocrystal of $RbCdF_3$ was studied by Mössbauer diffraction (J. Maetz et al., Federal Republic of Germany). A Mössbauer diffractometer with a 200 mCi source of ^{57}Co was used. The radiation, diffracted by the monocrystal, was analyzed with a "black" absorber with ΔE = 60 eV. The Si (Li) detector, with an area of 80 mm^2, was stationary, but the source was rotated around the axis 2θ of the monocrystal, which eliminated acoustic pick-up at the detector. In this way, the intensity of elastic and inelastic scattering from 1/2 (311) plane was measured, over the temperature range up to 150°K. The temperature dependences of both components are identical and do not contradict the data obtained by x-ray and neutron diffraction.

B. Furubayasi et al. (Japan) used the selective excitation of Mössbauer sublevels (SEDM) for observing spin relaxation. The temperature dependence of the SEDM spectra was obtained in symmetrical (555) Bragg reflection in the vicinity of the Morin transition (254°K). The results of the experiment were compared with the theory of A. M. Afanas'ev and V. D. Gorbachenko (I. V. Kurchatov Institute of Nuclear Energy). Relaxation phenomena in Ferrichrome A were investigated by selective excitation of Mössbauer levels (B. Balko et al., U.S.A.). Ferrichrome A was chosen for the first experiments as a simple model, already studied by other methods. The SEDM spectra were measured. The speed of the source corresponded to the excitation of one of the resonances in the scatterer. The scattered radiation was analyzed with a single-line absorber. The evidence of relaxation was the broadening and shift of the line.

Translated from Atomnaya Énergiya, Vol. 46, No. 2, pp. 134-135, February, 1979.

0038-531X/79/4602-0155$07.50

The attention of researchers continues to be drawn by time experiments with resonance γ radiation. The reports "Phase Coherence of Frequency-Modulated γ Radiation" (J. Kashon, Australia) and "The Time Dependence of Line Width and the Resonance Fraction in the Mossbauer Spectrum of $^{57}Co^{2+}[Fe^{III}(CN)_6]^{3-}$" (T. Kobayasi, Japan), "The Time Dependence of Filtered Resonance Emission of ^{119}Sn" (N. Hayasi, Japan), "Frequency Modulation of the 6.2-keV Mössbauer Level of ^{181}Ta" (P. West et al.), and other papers were devoted to this.

The reports on the possibility of using synchrotron radiation (SR) in Mössbauer spectroscopy (report by A. N. Artem'ev et al., USSR) caused great interest and a lively discussion. Attempts to formulate this experiment have already been undertaken during several years in the U.S.A. and the Federal Republic of Germany. Synchrotron radiation can be a powerful instrument for giving information which is new in principle. Thus, in the paper by Yu. Kagan et al. (USSR), the advantages and prospects of this method are shown. Interest in the use of SR was so great that a separate previously unplanned conference was set up, at which the creation of a working group under the chairmanship of Maier-Leibnitz was discussed. The group will publicize the unique possibilities of SR in different fields of research — in solid-state physics, atomic and molecular physics, chemistry, biology, medicine, et al. It is significant that the flux of SR exceeds the flux of a normal x-ray tube by a factor of more than 10^6–10^8, has a continuous spectrum, low divergence (10-20"), a time structure (pulses of 0.1-1 nsec with an interval of 100-200 nsec) and polarization. Work on SR is being developed at the present time in three of the largest centers. However, the radiation of storage rings is not being successfully used sufficiently effectively, as these facilities are loaded by high-energy physics programs. Therefore, in particular, the ultimate aim of the working group is the construction of a Joint European Storage Ring — a specialized source of SR in the x-ray energy range. The possibilities of SR for Mössbauer spectroscopy were considered in detail at the conference, and the essential parameters of the SR beams and scientific problems which must be solved were discussed.

The Conference was conducted in a businesslike manner, was well organized, and brought great benefit.

ALL-UNION PROBLEM SYMPOSIA ON REAL-TIME DATA-COMPUTING SYSTEMS

V. I. Vinogradov

The solution of extensive national-economic problems in science, power generation, industry and other fields, necessitates the automation of the actual processes, the application of modern electronics facilities and computer technology at the level of international standards. The creation and development of modern automation systems in the various fields of science and technology have been the subject of symposia on modular data-computing systems. The first of them was held in February 1977 in Moscow. Its theme was the language, translators and programming of CAMAC systems. 110 people from 53 organizations participated in the work of the Symposium, and 15 reports and communications were presented, devoted to means of automation of programming and the attempt to use modular systems in standard CAMAC. Seventeen people took part in the discussions.

The participants of the Symposium noted that modular systems in standard CAMAC are finding even more extensive application in the automation of experimental investigations and production processes both in the Academy of Sciences of the USSR and in other departments, so that programming automation of these systems is becoming urgent. The development and efficient utilization of modular data-computing systems is a new scientific-technical trend, requiring an integrated approach to the creation of program-equipment means, for which specialists of a new pattern are necessary.

At the present time, in the majority of organizations there are no programming automation facilities for CAMAC (compilers, interpreters, etc.). At the same time, the following successful work may be noted: SICL and CAMIN interpreting systems (Institute of Atomic Energy,

Translated from Atomnaya Énergiya, Vol. 46, No. 2, pp. 135-136, February, 1979.

 0038-531X/79/4602-0156$07.50

Siberian Branch of the Academy of Sciences of the USSR) and BASCAL (Institute of Nuclear Research, Academy of Sciences of the USSR); CAMILA assembler preprocessor (Institute of Nuclear Research, Academy of Sciences of the USSR); preprocessor, executing high-level CAMAC-language (Joint Institute of Nuclear Research); a unified set of subprograms (P. N. Lebedev Institute of Physics of the Academy of Sciences of the USSR), etc.

A comparative analysis of methods and means of programing automation of real-time modular systems showed the advisability of developing certain trends of programmed security of automation systems in science and technology. Thus, in order to operate with CAMAC equipment, it is necessary to create a unified set of programs, originated from languages of different levels, and it is necessary to develop interpreting systems within the scope of real-time BEISIK. It is necessary to execute a unified language of intermediate level for the programming of systems which impose rigid requirements on the reaction time of the systems: for small computer configurations, by means of assembler processors and within the scope of a standard intermediate-level language for different types of computers; for medium and large configurations, by means of macroextensions, and intermediate-level operators. The analysis of the possibility of the efficient execution of a high-level CAMAC-language should be continued, and the means for operating with CAMAC should be switched into the structure of operational real-time systems, providing a CAMAC-apparatus status of the standard facilities. It will be necessary to investigate the possibilities of using microprocessors and instrument means for effecting algorithms of control with CAMAC systems and the unification of their programming. It will be necessary to construct syntactically oriented translators, providing the possibility of extending the programming language to new operators and language facilities.

The theme of the second Symposium, which took place in June 1978 in Dubna, was functional and system electronic CAMAC modules. More than 140 people participated in its work. Of the papers presented, 55 were selected, devoted to the urgent developments of equipment functional and system CAMAC modules and automation systems constructed on their basis for scientific research in nuclear physics, general physics, and astronomy, and in other fields of science. A comparative analysis of the characteristics and possibilities of program-controlled modular systems, organized on the basis of different international interfaces, showed that CAMAC standards (section, parallel branch, sequential main line, etc.) are efficient for solving the extensive problems of automation in scientific research. Reports were presented at the Symposium containing examples of foreign and Soviet experience in the application of CAMAC equipment in industry for monitoring and controlling technological processes. The examples showed that on the basis of CAMAC standards, an electronic commercial equipment can be constructed, taking into consideration the specific properties of utilization.

In the course of the discussion of the reports, the high level and the large number of developments in standard CAMAC, achieved in many organizations, were noted (Joint Institute of Nuclear Research; Institute of Nuclear Research of the Academy of Sciences of the USSR; Leningrad Institute of Nuclear Physics, Academy of Sciences of the USSR; Special Design Bureau of the Institute of Radio-Electronics, Academy of Sciences of the USSR; Special Design Bureau of Scientific Planning, Siberian Branch of the Academy of Sciences of the USSR, and the I. V. Kurchatov Institute of Atomic Energy). The characteristic tendencies of recent time are the development of complex systems of controllers with microprocessor functions, which permit equipment to be constructed with distributed data processing, with a large volume of interchange equipment with external facilities, memory equipment and data presentation, the construction of large-scale control systems with an accelerator, and also the successful utilization of units in the nonosecond range. The transfer of documentation and laboratory CAMAC units from organizations of the Academy of Sciences of the USSR to the corresponding Design Bureau of industrial departments for their subsequent further development and utilization of commercial manufacture was considered. The use of the many developments considered achieved in CAMAC standard, is advantageous in commercial and research organizations, and also for monitoring and controlling production processes. In this case, attention is being paid to the fact that the industrial utilization of the CAMAC standard sharply reduces the price of equipment of this type and, in its turn, provides the possibility for the national economy to realize the achievements gained by the use of CAMAC in the field of scientific research.

For the successful solution of the existing problems, the organization in the country of the commercial manufacture of sections and power packs of connections in CAMAC standard

are advantageous, and also the obtaining of a decision on the use of complexing products, ensuring high functional capabilities of the CAMAC equipment. The results of the symposia have shown the high efficiency of conducting conferences in the same mode on the specific problems originating when solving the present day problems in science and technology, with the inclusion of specialists in the trends being considered.

The proceedings of the symposia have been issued.

NEW BOOKS

R. G. Bogoyavlenskii

HYDRODYNAMICS AND HEAT EXCHANGE IN HIGH-TEMPERATURE PEBBLE-BED NUCLEAR REACTORS*

Reviewed by V. P. Smetannikov

The book contains 5 chapters, an introduction, and conclusion, and is devoted to the hydrodynamics and heat exchange of the cores of thermal-and fast-neutron, high-temperature reactors with helium cooling. The data given are mainly numerous investigations of the average and local values of the heat-transfer coefficients in the case of a gas flow through the channelless core with spherical fuel elements of a gas-cooled thermal-neutron reactor, and also investigations of the thermodynamics of the coolant flow for different packings of the spheres.

The data are interesting, conveniently processed, and can be recommended for use when planning. The results of similar investigations carried out by other authors are analyzed in the book, which adds sufficient fullness and finish to the data. Although the author also proposes to use the data given in the book for planning thermal- and fast-neutron reactors, there are no recent relations for calculating hydrodynamic and heat-exchange processes, and only a few considerations of an extremely general nature are devoted to this question. At the same time, the solution of collecting problems is of great importance in the calculation of the hydrodynamic and thermal characteristics of cassettes with microfuel, in that flow hydrodynamics are determined not so much by the sphere filling, as by the system for organizing the flow of helium through the cassette and the core as a whole. These problems are not reflected in the book to their proper degree.

The main chapters of the book (1-4) are devoted to the structural features of pebble-bed nuclear reactors, the physical model, gas flow, structure of the fuel-element charging cells, and experimental investigations of the hydrodynamics and heat exchange in spherical fillings.

The logical completion of the first four chapters is the fifth chapter, concerning the optimization of the coolant parameters and the geometrical characteristics of a pebble-bed reactor. The author considers the effect of the thermophysical properties of the coolant, heating up of the gas, average temperature of the coolant and the gas pressure on the expenditure of energy in pumping the coolant during heat removal, paying special attention to the heating up of the gas in the reactor. In fact, the heating up of the gas and the temperature at the reactor inlet are of great importance. In the opinion of the author, the effect of these factors does not receive due attention when planning reactors, which does not correspond to reality. This problem is considered, e.g., in: "Problems of Science and Technology" [Series "Nuclear-Hydrogen Power Generation," No. 2(3) (1977)]. It should be mentioned also that the procedure given for comparing the principal characteristics of the core of pebble-bed reactors does not take account of the effect of the parameters of the secondary circuit on the principle design characteristics of the reactor.

The deficiencies mentioned do not reduce the timeliness and usefulness of the book as a whole and it is of undoubted practical interest for specialists working in the field of planning gas-cooled reactors.

*Atomizdat, Moscow (1978), 112 pp., 1 Ruble, 10 Kopecks.

Translated from Atomnaya Énergiya, Vol. 46, No. 2, p. 136, February, 1979.

0038-531X/79/4602-0159$07.50

CHANGING YOUR ADDRESS?

In order to receive your journal without interruption, please complete this change of address notice and forward to the Publisher, 60 days in advance, if possible.

(Please Print)

Old Address:

name

address

city

state (or country) zip code

New Address

name

address

city

state (or country) zip code

date new address effective

name of journal

Plenum Publishing Corporation
227 West 17 Street, New York, New York 10011

Declassified and Approved For Release 2013/02/12 : CIA-RDP10-02196R000800010002-4

Lithuanian Mathematical Journal

A cover-to-cover translation of *Litovskii Matematicheskii Sbornik*

An international medium for the rapid publication of the latest developments in mathematics, this new quarterly keeps western scientists abreast of both practical and theoretical configurations. Among the many areas reported on in depth are the generalized Green's function, the Monte Carlo method, the "innovation theorem," and the Martingale problem.

This journal focuses on a number of fundamental problems, including:

- weak convergence of sums of a random number of step processes
- asymptotic expansions of large deviations
- concentration functions of finite and infinite random vectors
- linear incorrect problems in Hilbert space

Subscription: Volume 18, 1978 (4 issues) $150.00

Random Titles from this Journal

Limiting Poisson Processes in Schemes for Summation of Independent Integer-Valued Processes—R. Banys
Formal Differentiation in Spaces of Geometric Objects—R. V. Vosylius
Scalar Products of Hecek L-Series of Quadratic Fields—É. Gaigalas
Characterization of Stochastic Processes with Conditionally Independent Increments—B. Grigelionis
Limit Theorems for Products of Random Linear Transformations on the Line—A. K. Grincevicius
One Limit Distribution for a Random Walk on the Line—A. K. Grincevicius
Estimate of Remainder Term in Local Limit Theorems for Number of Renewals in the Multidimensional Case—L. Griniumiene
Solvability of a Differential Equation in a Subspace—B. Kvedaras
Modelling of a Nonlinearity by a Sequence of Markov Chains—V. V. Kleiza
Density Theorems for Sectors and Progressions—F. B. Koval'chik
Mathematical Modelling of the Combustion Process in the Chamber of a Liquid Propellant Rocket Engine—J. Kolesovas and D. Svitra

NEW RUSSIAN JOURNALS

IN ENGLISH TRANSLATION

BIOLOGY BULLETIN

Izvestiya Akademii Nauk SSSR, Seriya Biologicheskaya

The biological proceedings of the Academy of Sciences of the USSR, this prestigious new bimonthly presents the work of the leading academicians on every aspect of the life sciences—from micro- and molecular biology to zoology, physiology, and space medicine.

Volume 5, 1978 (6 issues) $175.00

SOVIET JOURNAL OF MARINE BIOLOGY

Biologiya Morya

Devoted solely to research on marine organisms and their activity, practical considerations for their preservation, and reproduction of the biological resources of the seas and oceans.

Volume 4, 1978 (6 issues) $95.00

WATER RESOURCES

Vodnye Resursy

Evaluates the water resources of specific geographical areas throughout the world and reviews regularities of water resources formation as well as scientific principles of their optimal use.

Volume 5, 1978 (6 issues) $190.00

HUMAN PHYSIOLOGY

Fiziologiya Cheloveka

A new, innovative journal concerned *exclusively* with theoretical and applied aspects of the expanding field of human physiology.

Volume 4, 1978 (6 issues) $175.00

SOVIET JOURNAL OF BIOORGANIC CHEMISTRY

Bioorganicheskaya Khimiya

Features articles on isolation and purification of naturally occurring, biologically active compounds; the establishment of their structure, methods of synthesis, and determination of the relation between structure and biological function.

Volume 4, 1978 (12 issues) $225.00

SOVIET JOURNAL OF COORDINATION CHEMISTRY

Koordinatsionnaya Khimiya

Describes the achievements of modern theoretical and applied coordination chemistry. Topics include the synthesis and properties of new coordination compounds; reactions involving intraspheral substitution and transformation of ligands; complexes with polyfunctional and macromolecular ligands; complexing in solutions; and kinetics and mechanisms of reactions involving the participation of coordination compounds.

Volume 4, 1978 (12 issues) $235.00

THE SOVIET JOURNAL OF GLASS PHYSICS AND CHEMISTRY

Fizika i Khimiya Stekla

Devoted to current theoretical and applied research on three interlinked problems in glass technology; the nature of the chemical bonds in a vitrifying melt and in glass; the structure-statistical principle; and the macroscopic properties of glass.

Volume 4, 1978 (6 issues) $125.00

LITHUANIAN MATHEMATICAL JOURNAL

Litovskii Matematicheskii Sbornik

An international medium for the rapid publication of the latest developments in mathematics, this quarterly keeps western scientists abreast of both practical and theoretical configurations. Among the many areas reported on in depth are the generalized Green's function, the Monte Carlo method, the "innovation theorem," and the Martingale problem.

Volume 18, 1978 (4 issues) $150.00

PROGRAMMING AND COMPUTER SOFTWARE

Programmirovanie

Reports on current progress in programming and the use of computers. Topics covered include logical problems of programming; applied theory of algorithms; control of computational processes; program organization; programming methods connected with the idiosyncracies of input languages, hardware, and problem classes; parallel programming; operating systems; programming systems; programmer aids; software systems; data-control systems; IO systems; and subroutine libraries.

Volume 4, 1978 (6 issues) $95.00

SOVIET MICROELECTRONICS

Mikroelektronika

Reports on the latest advances in solutions of fundamental problems of microelectronics. Discusses new physical principles, materials, and methods for creating components, especially in large systems.

Volume 7, 1978 (6 issues) $135.00

Send for Your Free Examination Copy

PLENUM PUBLISHING CORPORATION, 227 West 17th Street, New York, N.Y. 10011
In United Kingdom: Black Arrow House, 2 Chandos Road, London NW10 6NR, England
Prices slightly higher outside the U.S. Prices subject to change without notice.